UNIVERSIDADE FEDERAL DE SANTA CATARINA
CENTRO DE CIÊNCIAS FÍSICAS E MATEMÁTICAS
PROGRAMA DE PÓS-GRADUAÇÃO EM OCEANOGRAFIA

WILSON FABIANO LEITE GALVÃO

EVOLUÇÃO GEOLÓGICA DA BAÍA DA BABITONGA, SANTA CATARINA, DURANTE O QUATERNÁRIO TARDIO.

FLORIANÓPOLIS
2022

Wilson Fabiano Leite Galvão

Evolução geológica da Baía da Babitonga, Santa Catarina, durante o Quaternário Tardio.

Dissertação submetida ao Programa de Pós-Graduação em Oceanografia da Universidade Federal de Santa Catarina

Orientador: Prof. Dr. Antonio Henrique da Fontoura Klein

Coorientador: Prof. Dr. Michel Michaelovitch de Mahiques

Florianópolis

2022

Ficha de identificação da obra elaborada pelo autor,
através do Programa de Geração Automática da Biblioteca Universitária da UFSC.

Galvão, Wilson Fabiano Leite
Evolução geológica da Baía da Babitonga, Santa Catarina, durante o Quaternário Tardio / Wilson Fabiano Leite Galvão ; orientador, Antonio Henrique da Fontoura Klein, coorientador, Michel Michaelovitch de Mahiques, 2022.
150 p.

Dissertação (mestrado) - Universidade Federal de Santa Catarina, Centro de Ciências Físicas e Matemáticas, Programa de Pós-Graduação em Oceanografia, Florianópolis, 2022.

Inclui referências.

1. Oceanografia. 2. Evolução costeira. 3. Transposição de barreira e translação estuarina. 4. Vale inciso estrutural . 5. Baía da Babitonga. I. Klein, Antonio Henrique da Fontoura. II. Mahiques, Michel Michaelovitch de. III. Universidade Federal de Santa Catarina. Programa de Pós Graduação em Oceanografia. IV. Título.

Wilson Fabiano Leite Galvão

Evolução geológica da Baía da Babitonga, Santa Catarina, durante o Quaternário Tardio.

O presente trabalho em nível de mestrado foi avaliado e aprovado por banca examinadora composta pelos seguintes membros:

Prof. Dr. Christopher J. Hein
Instituição Virginia Institute of Marine Science - VIMS

Prof. Dr. Guilherme Camargo Lessa
Instituição Universidade Federal da Bahia - UFBA

Profª. Drª Carla Van Der Haagen Custódio Bonetti
Instituição Universidade Federal de Santa Catarina - UFSC

Certificamos que esta é a **versão original e final** do trabalho de conclusão que foi julgado adequado para obtenção do título de mestre em Oceanografia.

Documento assinado digitalmente
Paulo Roberto Pagliosa Alves
Data: 26/08/2022 08:25:30-0300
CPF: 805.160.419-91
Verifique as assinaturas em https://v.ufsc.br

Coordenação do Programa de Pós-Graduação

Documento assinado digitalmente
Antonio Henrique da Fontoura Klein
Data: 29/08/2022 12:39:40-0300
CPF: 696.210.710-20
Verifique as assinaturas em https://v.ufsc.br

Prof. Dr. Antonio Henrique da Fontoura Klein
Orientador

Florianópolis, 2022.

Mais um trabalho dedicado aos meus queridos amigos, à minha família e, ainda em especial, às Marias que me criaram e apoiam sempre que possível.
Que eu possa retribuir.

AGRADECIMENTOS

Agradeço ao CNPQ pelo apoio ao projeto *Subida do nível do mar e a Baía da Babitonga: uma abordagem eco-morfodinâmica para prever e mitigar impactos*, incluído no projeto *Outras Baías do Brasil*, de numeração 441545/2017-3, dentro do qual esta dissertação foi desenvolvida.

Agradeço à CAPES pelo auxilio em forma de bolsa, que recebo através do Programa de Pós-Graduação em Oceanografia (PPGO).

Agradeço ao Professor Dr. Antônio Henrique da Fontoura Klein por me guiar durante todo o desenvolvimento deste projeto e demais atividades extracurriculares que participei. Certamente foi uma jornada de oportunidades únicas.

Agradeço ao Professor Dr. Michel Michaelovitch de Mahiques pelas cruciais contribuições a este projeto no papel de coorientador, sempre com seu jeito descontraído de ser. Um grande prazer foi desenvolvermos este projeto.

Agradeço aos Professores Dr. Christopher Hein (Virginia Institute of Marine Science), Dr. Andrew Green (University of KwaZulu-Natal) e Dr. Andrew Cooper (Ulster University) e ao Dr. Luiz Antonio P. de Souza (Instituto de Pesquisas Tecnológicas) pelas discussões sobre a identificação de estruturas sedimentares nos registros sísmicos e sobre os processos sedimentares da evolução geológica.

Agradeço aos Professores Dr. Cláudio Rudolfo Tureck (Univille) e Dr. Luciano Lorenzi (Univille) pela identificação das conchas de moluscos enviados para datação por 14C.

Agradeço aos colegas do Laboratório de Oceanografia Costeira, do Laboratório de Dinâmica dos Oceanos e do projeto BaySqueeze: o Professor Dr. Pedro de Souza Pereira, , Prof Jarbas Bonetti, Professor Dr. Luis Pedro Melo de Almeida, Professor Dr. Luiz Augusto dos Santos Madureira, Professor Dr. Marcelo Accioly Teixeira de Oliveira, Professor Dr. Christopher Hein, BSc. Jennifer Connell, BSc. Sarah Grace Lott, MSc Rodolfo Jasão Soares Dias, MSc. Bruna Teixeira Pandolpho, BSc. Giuliana Dionisio, MSc. Maiara Werner Pinto, MSc. Michel Franco Prado, BSc. Yasmim Mourad Oshiro, MSc. Luana Borato, BSc. Bianca Filippi, BSc. Fábio Fleury, BSc Isadora Dutra da Silva, Letícia Volcov, BSc Mariane Couceiro Pullig, Gabriela Freire, Khauany Paola Poleza, Pedro Alípio, BSc Ligia Freitas Tebechrani, BSc Julia Miola de Castro, BSc. Patricia Tortora, BSc. Marcelo Pellicano Falleiros, Dr. Francisco Carlos Lajús Junior, BSc Pedro Lins de Souza, MSc Micael Fernando Broggi, pela disposição em contribuir com discussões desta pesquisa.

Também sou grato por suas contribuições nas jornadas para coleta de dados usados nesta pesquisa, junto do Thiago Losso, Caiçara e Bili, os simpáticos marinheiros da embarcação *Marinheiro William II*, que deram todo o suporte na coleta dos dados.

Agradeço aos colegas BSc. Agno Rubim de Assis, BSc. Felipe Cassilhas Dias, Leandro Xavier Maia e BSc. Moisés Nascimento pela disponibilidade e ajuda com dificuldades encontradas durante o processamento dos dados.

Agradeço a todas as pessoas que não estão listadas aqui, mas muito me ajudaram durante o desenvolvimento deste trabalho, que não seria o mesmo sem elas.

Por fim, e não menos importante, a maior gratidão à minha família que me fez e apoia ser quem sou.

RESUMO

O presente trabalho apresenta a análise dos depósitos sedimentares presentes na Baía da Babitonga/SC, com foco no Pleistoceno Superior e Holoceno para propor um modelo para a evolução geológica da baía. Para isso, 283 km de dados sísmicos rasos (CHIRP, faixa espectral de 0.7-12.0 kHz) foram analisados, com dez vibracores obtidos na baía. Quatro unidades estratigráficas principais foram encontradas, incluindo todos os domínios de um estuário clássico dominado por ondas: barreira, lagoa, deltas de maré, bacia central, barras de maré e deltas de cabeça de baía. A geocronologia construída através da datação por radiocarbono e revisão de literatura, e as análises petrofísicas de velocidade, densidade, radiação, suscetibilidade magnética e resistividade foram usadas para correlacionar dados sísmicos e de testemunhos sedimentares. Três das quatro unidades sismoestratigráficas são observáveis nos dados de vibracore, relacionando-se aos Trato de Sistema Transgressivo (TST) e Trato de Sistema de Mar Alto (HST), do Pleistoceno Superior e Holoceno, com depósitos do HST apresentando gás trapeado em si. O embasamento dentro da baía indica que o interior da Baía da Babitonga esteve exposto antes da fase de mar alto, de forma que este separava a baía em dois vales incisos. O primeiro deles esteve estabelecido sobre a Zona de Cisalhamento Palmital, enquanto o segundo encontrava-se sobre o atual Canal Principal. Com a elevação do nível do mar, os sistemas costeiros migraram para terra. Neste momento, o sistema laguna-barreira foi trasposto (*overstepping*) devido à alta taxa de subida do nível do mar, soldando as barreiras em transgressão na costa. Ao mesmo tempo, ocorreu a translação (*rollover*) estuarina dentro dos vales incisos até que houvesse a unificação dos vales, criando o sistema estuarino Baía da Babitonga, com drenagem unificada. Por fim, o nível do mar desceu para a sua posição atual, permitindo o desenvolvimento da costa através do preenchimento lagunar das lagoas pós-barreira, da progradação das barreiras e da formação de cordões arenosos nas desembocaduras estuarinas.

Palavras-chave: Transposição de barreira, translação estuarina, evolução costeira, vale inciso estrutural, gás raso, Baía da Babitonga.

ABSTRACT

This study presents the analysis of sedimentary deposits present in Babitonga Bay/SC, focusing on the Holocene, to propose a model for the geological evolution of the bay. For this, 283 km of shallow seismic data (CHIRP, frequency between 0.7 – 12.0 kHz) were analyzed, complimented and ground-truthed with ten vibracores obtained in the bay. Four main stratigraphic units were found, including all the domains of a classic wave-dominated estuary: barrier, lagoon, tidal deltas, central basin, tidal bars, and bay-head deltas. Geochronology was provided by radiocarbon dating and a literature review. Petrophysical analyses of velocity, density, radiation, magnetic susceptibility, and resistivity were used to correlate seismic and core data. Three of four seismo-stratigraphic units are observable in vibracore data. The observed units are related to the Upper Pleistocene and Holocene Transgressive System Tract (TST) and Highstand System Tract (HST). Highstand and regressive deposits commonly present shallow, trapped gas. The basement inside the bay shows that the interior of the Babitonga Bay was exposed before the highstand phase, separating the bay into two different structural incised valleys. The first was established over the Palmital Shear Zone, while the second was over the present Main Channel. Sea-level rise promoted the landward migration of coastal systems, in which a coastal lagoon-barrier system was overstepped, with recycled sediment welding as a transgressive barrier to the mainland. At the same time, sea-level rise causes estuarine rollover until the unification of the drainage systems of the valleys, creating a single drainage system and unique estuarine body (Babitonga Bay). Lastly, sea level dropped to its current position during the Late Holocene, during which time the coast developed through back-barrier lagoon infill, barrier progradation and sand spit development into estuarine mouths.

Keywords: barrier overstepping, estuarine rollover, coastal evolution, structural incised valley, shallow gas, Babitonga Bay

LISTA DE FIGURAS

LISTA DE TABELAS

LISTA DE ABREVIATURAS E SIGLAS

AMS – Accelerator mass spectrometry (Espectrometria de massa do acelerador)

ASR - *Average Sedimentation Rate* (Taxa Média de Sedimentação)

CHM – Centro de Hidrografia da Marinha

cps – *counts per second* (contagens por segundo)

CPRM - Companhia de Pesquisa de Recursos Minerais

GD – *Gamma density* (Densidade gama)

IBGE – Instituto Brasileiro de Geografia e Estatística

LGM – Last Glacial Maximum (Último Máximo Glacial)

Marine20 – Marine Radiocarbon Age Calibration Curve (Curva de Calibração da Idade do Radiocarbono Marinho)

MS – *Magnetic susceptibility* (Suscetibilidade magnética)

MSCL – *Multi Sensor Core Logger* (Perfilador multisensor de testemunhos)

NGR – *Natural gamma ray* (Raio Gamma Natural)

NOSAMS – National Ocean Sciences Accelerator Mass Spectrometry (Espectrometria de Massa do Acelerador Nacional de Ciências Oceânicas)

OSL – Optically Stimulated Luminescence (Luminescência Opticamente Estimulada)

SFSI – São Francisco do Sul Island

SHCal 20 – Southern Hemisphere Calibration (Calibração do Hemisfério Sul)

SIG – Sistema de Informações Geográficas

Vp – *Sound velocity* (Velocidade do som)

ZCP – Zona de Cisalhamento do Palmital

ΔR – *Reservoir correction* (Correção de reservatório)

SUMÁRIO

1 INTRODUÇÃO

Um sistema de vale inciso consiste basicamente em um vale escavado e seu preenchimento sedimentar, o qual evidencia mudanças no padrão deposicional ao longo do espaço de acomodação (DALRYMPLE et al. 1994). Incluídos neste sistema, os estuários são a porção distal de transição entre os ambientes marinho e fluvial (DALRYMPLE et al. 1992). Fácies marinhas, fluviais e de transição ocorrem em estuários e são formadas ou preenchidas de acordo com peculiaridades de seu espaço de acomodação (BOYD et al. 1992; DALRYMPLE et al. 1992; ZAITLIN et al. 1994). A partir desta tripartição faciológica, um estuário ideal apresentará depósitos aluviais, deltas de cabeceira, depósitos de bacia central, depósitos de barreiras e/ou praias e deltas de maré, se houver aporte sedimentar suficiente (DALRYMPLE et al. 1992).

Além da herança geológica, as variações do nível do mar e o aporte sedimentar proveniente através da bacia hidrográfica influenciam o processo de preenchimento do espaço de acomodação (BOYD et al. 1992; SHANLEY e MCCABE 1994). As oscilações do nível do mar afetam os sistemas deposicionais costeiros, incluindo estuários (SCAVIA et al. 2002; RASMUSSEN et al. 2018), sendo estes importantes para a compreensão do processo evolutivo das regiões costeiras (BORTOLIN et al. 2018; RONCHI et al. 2018; SIMMS et al. 2018, RONCHI et al. 2019; YOO et al. 2020; WANG et al. 2020; BABOSA et al. 2021).

Nos últimos 20 mil anos B.P., o aquecimento climático causou a subida do nível do mar até sua posição atual (COOPER et al. 2018). Durante uma transgressão, os sistemas costeiros migram por toda a plataforma, deixando algumas pistas da evolução morfológica (e.g. superfícies de inconformidades, paleocanais preenchidos, transposição e/ou translação costeira, etc.) preservadas em depósitos de Trato de Sistema Transgressivo (TST) (COLMAN e MIXON, 1988; DALRYMPLE e ZAITILIN, 1994; CHAUMILLON et al. 2010; TESSON et al., 2015; SILVA et al. 2016; ZAREMBA et al. 2016). Com a estabilização, ou momento próximo, do nível do mar inicia-se a formação do Trato de Sistema de Mar Alto (TSMA), e o espaço de acomodação sobre a plataforma criado durante a transgressão começa a ser preenchido por depósitos progradacionais e posteriormente regressivos, também deixando pistas (e.g., progradação de deltas ou bancos, incisões de paleocanais, lagoas preenchidas, progradação de cordões arenosos, etc.) da evolução geológica (WOODROFFE et al., 1992 ; KENCH, 1999;

LESSA et al., 2000; COHEN et al., 2005; ALLARD et al., 2010; HEIN et al., 2012; OLIVER et al., 2020).

A evolução estuarina pode ser decifrada através da investigação do processo de preenchimento do espaço de acomodação. Esta investigação pode ser feita usando métodos de reflexão acústica (AYRES NETO, 2000), a qual permite a observação de pacotes de sedimentos subsuperficiais (e.g. MITCHUM et al. al., 1977; SOUZA, 2006; SOUZA, 2011) e até mesmo, no caso da sísmica de alta resolução, a identificação de feições deposicionais em escala local e regional (e.g. LESSA et al. 1998; SLOSS et al. 2006; GIAGANTE et al. 2011; BASTOS et al. 2010; MARINO et al. 2013; SILVA et al. 2016; ZAREMBA et al. 2016; MARTÍNEZ-CARREÑO e GARCÍA-GIL, 2017; COOPER et al. 2018; GREEN et al. 2022).

Os estuários da costa sudeste e sul do Brasil estabeleceram-se sobre vales incisos altamente influenciados por lineamentos estruturais (PASSARELLI et al. 2011; LESSA et al. 2018)., como zonas de cisalhamento (CURY, 2009; PASSARELLI et al. 2011; BRUNO et al. 2018). Incluída no Terreno Paraná, a Baía da Babitonga é um exemplo destes estuários, onde um vale inciso se desenvolveu sobre a Zona de Cisalhamento Palmital, com forte controle tectônico (GIMENEZ et al, 2022). Embora estudos anteriores descrevam os principais padrões morfológicos e sedimentares na Baía da Babitonga (VIEIRA et al. 2008; MAZZER e GONÇALVES, 2011; VIEIRA e HORN FILHO, 2012; HORN et al. 2014; BOGO et al., 2015; VIEIRA e HORN FILHO, 2017), existe carência de investigações estratigráficas que permitam abordar a evolução da baía e sua integração com o desenvolvimento da planície costeira. Nestas circunstâncias, o objetivo deste trabalho é descrever e apresentar a arquitetura estratigráfica do estuário da Baía da Babitonga ao longo do Pleistoceno Superior e Holoceno, bem como propor um modelo evolutivo para a área de estudo, através da análise de dados sísmicos de alta resolução e testemunhos sedimentares.

1.1 PERGUNTAS DE PESQUISA

- Como o estuário tectônico da Babitonga se comportou durante a transgressão e regressão marinha no Pleistoceno Superior e Holoceno?
- Quais os processos de evolução morfodinâmica atuaram no preenchimento do espaço de acomodação da Baía da Babitonga?

1.2 OBJETIVOS

1.2.1 Objetivo Geral

Estabelecer um modelo evolutivo do Pleistoceno Superior e Holoceno para a Baía da Babitonga, através da descrição de sua estrutura e composição observada em dados sísmicos, sedimentares e petrofísicos.

1.2.2 Objetivos Específicos

- Correlacionar unidades sísmicas e sedimentares para estabelecer a estratigrafia da baía.
- Descrever a extensão e morfologia dos depósitos transgressivos e regressivos do Pleistoceno Superior e Holoceno;
- Reconstruir o preenchimento do espaço de acomodação disponível no estuário tectônico chamado Baía da Babitonga;

1.2.3 Formato da Dissertação

Esta dissertação apresenta os resultados, discussões e conclusões em forma de artigo, intitulado "*Holocene barrier overstepping, estuarine rollover and drainage merging in a sub-tropical bay*", desenvolvido e submetido à revista Marine Geology (Qualis A2 CAPES/ Area Geociências). Previamente apresenta-se a introdução, as perguntas de pesquisa, os objetivos e a revisão bibliográfica da pesquisa. Ao final, são apresentadas considerações finais e considerações para futuros trabalhos, as referências utilizadas e apêndices.

Wilson Fabiano Leite Galvão

2 HOLOCENE BARRIER OVERSTEPPING, ESTUARINE ROLLOVER AND DRAINAGE MERGING IN A SUB-TROPICAL BAY

Esta seção é destinada a apresentação do artigo científico desenvolvido e submetido para a revista Marine Geology, como parte dos requisitos para a obtenção do grau de mestre em Oceanografia pela Universidade Federal de Santa Catarina.

Florianópolis
2022

Holocene barrier overstepping, estuarine rollover and drainage merging in a sub-tropical bay

Wilson Fabiano Leite Galvão[1], Antonio Henrique da Fontoura Klein[2*], Michel Michaelovitch de Mahiques[3], Christopher J. Hein[4], Luiz Antonio Pereira de Sousa[5], Andrew Cooper[6,7], Andrew Green[6,7]

Affiliations

* Corresponding author.

1 Laboratory of Coastal Oceanography, Universidade Federal de Santa Catarina, University Campus - Trindade, Florianópolis, Santa Catarina, Brazil. - galvao.wilson.1@gmail.com

2 Laboratory of Coastal Oceanography, Universidade Federal de Santa Catarina, University Campus - Trindade, Florianópolis, Santa Catarina, Brazil. - antonio.klein@ufsc.br

3 Institute of Oceanography, University of São Paulo, São Paulo, Brazil - mahiques@usp.br

4 Virginia Institute of Marine Science, William & Mary, P.O. Box 1346, Gloucester Point, VA 23062-1346, USA - hein@vims.edu

5 Institute of Technological Research of São Paulo, Av. Almeida Prado. 532, Butantã University City, São Paulo, São Paulo, Brazil - luizlaps@gmail.com

6 School of Geography and Environmental Sciences, University of Ulster, Coleraine, Northern Ireland, United Kingdom - jag.cooper@ulster.ac.uk

7 Geological Sciences School of Agricultural, Earth and Environmental Sciences, University of KwaZulu-Natal, Westville Campus, Durban, South Africa - greena1@ukzn.ac.za

2.1 ABSTRACT

Seismic-stratigraphic and vibrocoring investigations in Babitonga Bay, Santa Catarina, Brazil reveals four main stratigraphic units related to the Upper Pleistocene and Holocene Transgressive System Tract (TST) and Highstand System Tract (HST). The interior of the Babitonga Bay was subaerially exposed during lower sea levels, and comprised two distinct incised valleys. The first was established over the Palmital Shear Zone, while the second was over the present main channel. During Holocene sea-level rise a coastal lagoon-barrier system was formed and overstepped. Estuarine facies migrated landward until the drainage systems of the valleys were unified into the single estuarine basin of Babitonga Bay. During late Holocene sea-level fall the back-barrier lagoon was infilled and, prograding barriers and sandspits developed in estuarine mouths.

Keywords: barrier overstepping, coastal evolution, structural incised valley, Babitonga Bay

2.2 INTRODUCTION

Incised valley systems comprise an excavated valley and its sedimentary filling, which evince the record changes in depositional pattern within the accommodation space (DALRYMPLE et al., 1994). Included in the incised valley system, estuaries are the transitional portion between marine and river environments (DALRYMPLE et al., 1992). Marine, fluvial, and transition facies occur in estuaries and they are formed or filled according to the peculiarities of their accommodation space (BOYD et al., 1992; DALRYMPLE et al., 1992; ZAITLIN et al., 1994). An ideal microtidal estuary will contain alluvial deposits, bay-head deltas, central basin deposits, barriers and beach deposits, and tidal deltas if there is sufficient sedimentary input (DALRYMPLE et al., 1992).

Besides the geological heritage, variations in sea level and sedimentary supply through the hydrographic basin influence the infill process of the accommodation space (BOYD et al., 1992; SHANLEY and MCCABE, 1994). These sea-level oscillations may affect coastal systems, as well as estuaries (ROY, 1994; SCAVIA et al., 2002; RASMUSSEN et al., 2018), which highlights the importance of knowing the evolutionary process of these depositional environments (BORTOLIN et a., 2018; RONCHI et al., 2018; SIMMS et al., 2018, RONCHI et al., 2019; YOO et al., 2020; WANG et al., 2020; BABOSA et al., 2021). Over the last 20 kyr B.P., climate changes led to the rise and fall of the sea level until its current level (COOPER et al., 2018). During transgression, estuaries migrate throughout the shelf, leaving various indicators (e.g., unconformities, infilled paleochannels, drowned inlet/barrier units, etc) about their position and evolution buried in transgressive system tracts (TST) (COLMAN and MIXON, 1988; DALRYMPLE and ZAITILIN, 1994; CHAUMILLON et al., 2010; TESSON et al., 2015; SILVA et al., 2016; ZAREMBA et al., 2016; RONCHI et al., 2019). The highstand system tract (HST) starts when accommodation space stops to be created by sea-level rising and it begins to be filled by regressive deposits, that also leave indications (e.g. progradational deltas, paleochannel incisions, infilled lagoons, strandplains, etc.) of geological evolution

(WOODROFFE et al., 1992; KENCH, 1999; LESSA et al., 2000; COHEN et al., 2005; ALLARD et al., 2010; HEIN et al., 2013; OLIVER et al., 2020)

Estuarine development can be deciphered by investigating the accommodation space infill using acoustic reflection methods (AYRES NETO, 2000) and recovered core samples (e.g., LESSA et al., 1998; WESCHENFELDER et al., 2014; FERNÁNDEZ et al., 2020), allowing the observation of subsurface sediment (e.g., MITCHUM et al. al., 1977; SOUZA, 2006, 2011).

The southeast and south Brazilian coast estuaries are established over incised valleys strongly influenced by adjacent mountain ranges (PASSARELLI et al., 2011; LESSA et al., 2018). while some, including Babitonga Bay exhibit strong tectonic control (GIMENEZ et al., 2022). Although previous studies have described morphological and sedimentary patterns in Babitonga Bay (VIEIRA et al., 2008; MAZZER e GONÇALVES, 2011; VIEIRA e HORN FILHO, 2012; HORN et al., 2014; BOGO et al., 2015; VIEIRA e HORN FILHO, 2017), the bay stratigraphy and evolution has not been investigated. This paper aims to describe and interpret the stratigraphic architecture of Babitonga Bay and propose an evolutionary model for the study site, through high resolution seismic data supported by sedimentary cores.

2.3 REGIONAL SETTING

Babitonga Bay is on the north coast of Santa Catarina, in southern Brazil (Figure 1). The southern and southeastern Brazilian estuaries are related to alongshore-oriented grabens (LESSA et al., 2018), developing itself over the Palmital Shear Zone due to neotectonic activities (GIMENEZ et al., 2022) on the southern border of Paranaguá Tectonostratigraphic Terrane, which is the rocky formation that abuts the coastal plain (CURY, 2009). Babitonga Bay is composed of three large segments: the Palmital Channel in the north; the Linguado Channel in the south; and the Main Channel in the northeast. Together these form an estuarine complex of approximately 160 km², with a maximum width and length of 5 km and 20 km, respectively (CREMER et al., 2006). The Linguado Channel was closed artificially by a railway

embankment in 1935, leaving only the central body connecting the bay to the sea (CREMER et al., 2016).

Babitonga Bay reaches its greatest depth in the Main Channel, (27 meters at the mouth) (MAZZER and GONÇALVES, 2011), hower, 75% of the geomorphological features (Channels, tidal flats, banks, shallow plains, rocky outcrops, and rocky islands) occur in water < 5m deep (MAZZER and GONÇALVES, 2011).

The wave climate has an average wave height of 1.0 – 1.5 m and a peak period of 12 s (KLEIN et al., 2016b). 60% of the ocean swell comes from the east, 20% from the southeast, 7% from the east-northeast, and 5% from the south-southeast (ALVES, 1996; RODRIGUES et al., 2004). The coast is microtidal; average height in São Francisco Harbor is around 85 cm, with a maximum of 125 cm (TRUCCOLO and SCHETTINI, 1999). The hydrodynamics in the bay are dominated by the tide, and seasonal variations in the fluvial input do not cause variations in the salinity inside the bay (NOERBERG et al., 2020)

In structural terms, the bay is located in the Serrinha-Palmital River suture system, specifically on the Palmital River Shear Zone (ZCP). Such a shear zone (Figure 1) is characterized as the transcurrent type, being part of a fault system at the limits of the Paranaguá (CURY, 2009). Gimenez et al. (2022) described Babitonga Bay as a true example of a tectonic estuarine valley shaped by neotectonic activities.

The Paranaguá coastal plain is composed of deposits from the landward migration and welding of Holocene barriers into Paranaguá coast, preserving some portion of back-barrier lagoons (LESSA et al., 2000; SOUZA, 2001; ANGULO et al., 2009). Guaratuba Bay and Paranaguá Bay are also located within this coastal plain, presenting low available accommodation space (LESSA 1998; BARBOSA and SUGUIO, 1999), with Guaratuba Bay having the smaller accommodation of the group (CASTRO et al., 2008). The drainage over the Paranaguá does not have a dominant direction, but a pattern can be observed. From Babitonga Bay until Paranaguá Bay, the drainage seems to run over the granitic suites until the paleo-estuarine plains developed over the troughs in the Pleistocene/Holocene strand plain (LESSA et al., 2000; SOUZA, 2001; ANGULO et al., 2009)

Regressive foredune ridge barriers and estuaries compose the regional shore (KLEIN et al. 2016b), and Quaternary deposits surround the bay (SOUZA et al., 2001; ANGULO and SOUZA, 2004; ANGULO et al., 2009) adjacent to rocky outcrops of different ages (CURY, 2009; IGLESIAS et al., 2011). Holocene regressive deposits in the strand plain seem to be eroded at the southern part of the Paranaguá and feed the northern region through alongshore transport (LESSA et al., 2000), as the Holocene barriers are larger in the north portion of the Terrane, as well as the adjacent shelf slope. Corroborating this, Souza et al. (2001) describe sandspits northward growing along the coast of the Itapoá strand plain. Vieira et al. (2008) describe the sedimentation in the bay as shallow marine, with typically sandy sediments and higher concentrations of biodetritic carbonate; estuarine sedimentation, composed of muddy sediments with a high concentration of organic matter; and mixed sedimentation, which would be the transition zone between the first two.

Regarding sea level variations, the region was in transgression between the last 20 kyr B.P. and 5-6 kyr B.P., leaving a position of 120 m below the current level (ANGULO et al., 2006; COOPER et al., 2016). In this interval, occasional meltwater events accelerated this process, enabling the preservation of coastal sedimentary features, such as the sandy barriers preserved in the sedimentary deposits of Tijucas Bay – SC (about 120 km southwest of study area), described by Cooper et al. (2016). The rising sea-level reach present sea-level about 7 kyr B.P (ANGULO et al., 2006). At the same time, phreatic-level sandstones were described around ~60 km northeast of Babitonga Bay in the shelf, at depths between 18-29 m by Simioni et al. (2018). During the end of the transgression, the base level was about 2 to 4 meters above the present, between 6,000 and 5,000 years ago (Angulo et al., 2006), where valleys and bays were flooded by the sea (e.g., LESSA et al., 2000; HEIN et al., 2014; COOPER et al., 2019). Since then, the sea level has dropped to current levels, causing the coast to advance towards the sea (e.g., ÂNGULO et al., 2008; HEIN et al., 2012; HEIN et al, 2016; COOPER et al., 2019).

In summary, Babitonga Bay developed over a shallow coastal plain controlled by neotectonics events, with wave dominated coast and mixed energy inside its estuarine body.

The estuary body is mainly composed by a main channel, submarine plains and some tidal banks.

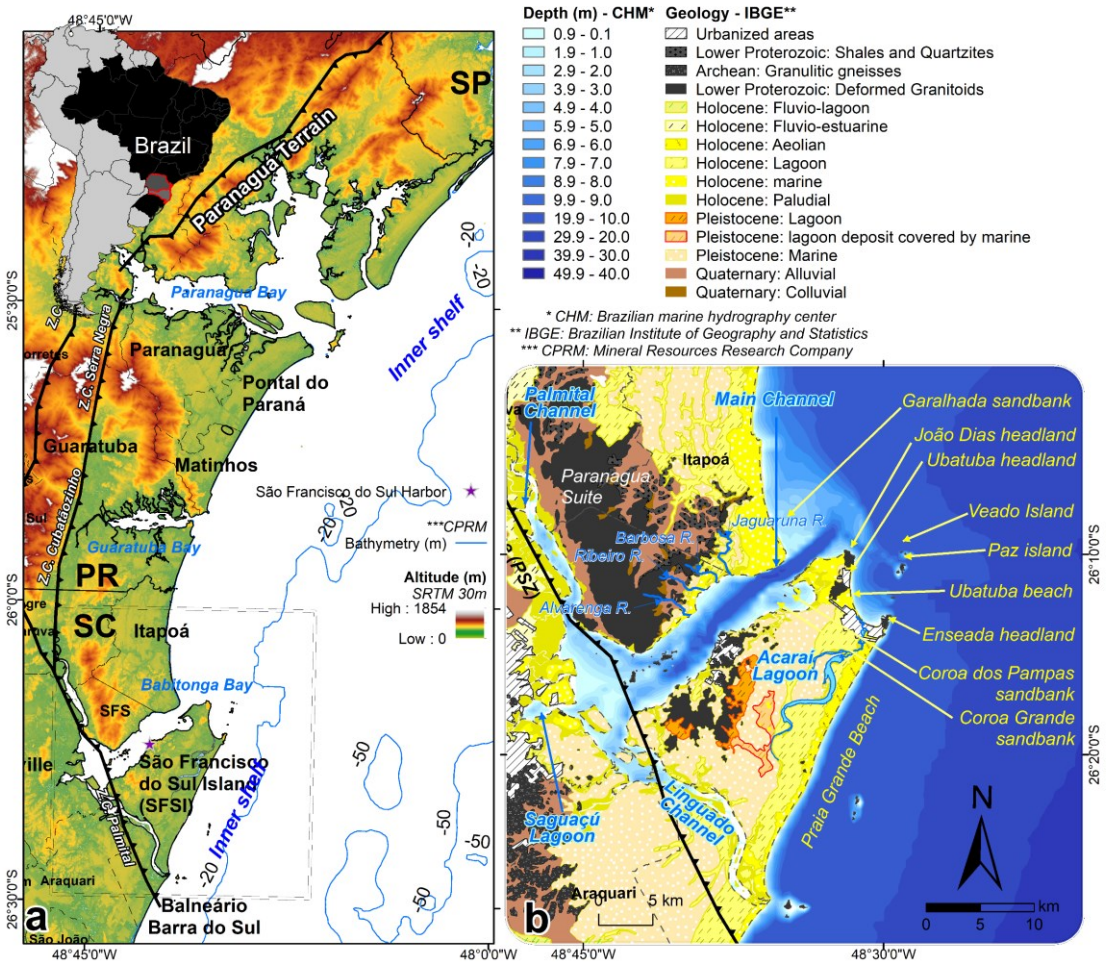

Figure 1. A. Location map of study area. B. Detail of Babitonga Bay.

2.4 MATERIALS AND METHODS

Over 283-line km of high-resolution seismic data were collected at the Babitonga Bay and adjacent coastal compartments, between depths of ~1 and ~18 m (Figure 2) using an

EdgeTech® CHIRP profiler of model SB-512i, operating with a frequency range of 0.7 – 12 kHz. Navigation was recorded using a DGPS antenna, with a vertical and horizontal accuracy of 0.5 and 0.25, respectively axes.

Data processing and interpretation were conducted using SonarWiz®. A two-way travel time of 1600 m/s was applied for sediment and 1500 m/s for water. For the frequency filtering, a band-pass filter was applied with a frequency window of 0,7-12 kHz. The main unconformities were analyzed (2D and 3D view) and seismic units were defined and exported for their geographic distribution in ArcGIS®. Internal reflectors and lateral contacts as (Mitchum and Vail, 1977), were used for stratigraphical interpretation of units.

Vibracores were collected in pairs at five sites inside Babitonga Bay (Figure 2). Core length ranges from 160 cm to 300 cm. The longer of each core pair from each site was used for sedimentary facies description, granulometric analysis, and radiocarbon dating. The shorter of each core pair was used to analyze sediment geophysical properties. Grain-size analyses were conducted using the Laser Diffraction Analyzer (LA-950). Radiocarbon ages were acquired through an accelerator mass spectrometry (AMS), using intact shells or fragments that cross the growth lines and with an unbroken hinge. The analyses were performed at National Ocean Sciences Accelerator Mass Spectrometry (NOSAMS) facility (Woods Hole, Massachusetts, USA). Calibrated ages were calculated using the SHCal20 (Hogg et al., 2020) and the Marine20 (Heaton et al., 2020) curves, using a reservoir correction (ΔR) of -150 ± 40 yrs, based on the value from Paranaguá Bay (~85 km northward of Babitonga Bay) (ANGULO et al., 2005). Geophysical properties of the cores (velocity, density, radiation, magnetic susceptibility, and resistivity) were obtained using a Geotek® Multi-Sensor Core Logger (MSCL).

Additionally, a compilation of published ages from Holocene stratigraphic units from within ~100 km of Babitonga Bay were compiled (Figure 2) to aid in analysis about geological evolution of the estuarine system.

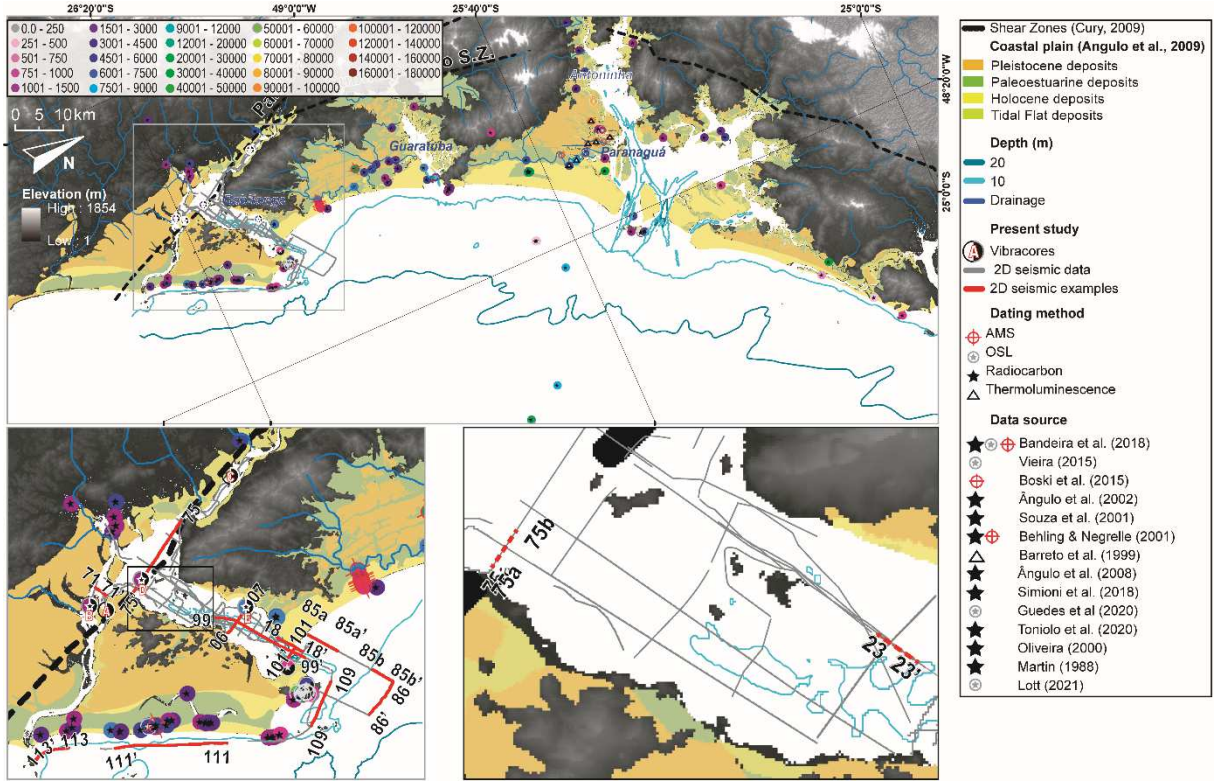

Figure 2. Field and literature collected data. Colored circles corresponds to geochronology compilation.

2.5 RESULTS

2.5.1 Seismic Unconformities and, Units and Facies

Besides the rocky basement, four main unconformities and five seismic units were found in Babitonga Bay (Figure 3). In addition, two sub-units are preserved only as paleochannel deposits. These two sub-units do not occur in the internal islands in the Main Channel region, which is an area of very low accommodation space due to the shallow rocky basement. Figure 2 shows the vertical distribution of the main unconformities and the basal reflectors of the sub-units.

2.5.2 Unconformities

The first unconformity (Figure 3 -RB) is discontinuous and irregular. A strong signal return and the absence of internal reflectors below its irregular surface identify it as the bedrock basement. It occurs in the Main Channel and near the rocky headlands and islands on the Inner Shelf (IS).

The second unconformity, R1, is present in the whole bay and at some points in the IS. Its shallowest part occurs in the Palmital Channel and deepens in the Linguado and Main channels and the IS (Figure 3 -R1). The weakening of the acoustic signal and multiple reflections do not permit the observation of R1 in some (or all) parts.

Between R1 and R2, the R1.5 unconformity incises Unit 1, creating the base of some channels near Joinville city and in front of the Ribeiro, Barbosa and Jaguaruna Rivers (Figure 3 -R1.5). It also occurson the IS as the base of channels. The deepest location of R1.5 is in the Main channel.

Present in the whole bay, the erosive unconformity R2 occurs in most of the IS. The deepest occurrences are next to the mouth of the bay, and on the IS. The shallowest parts of this unconformity are in the Main Channel (Figure 3 -R2).

Similar to R1.5, inside the bay, unconformity R2.5 appears as a channel incision at the Joinville city and in front of the Ribeiro, Barbosa, and Jaguaruna rivers (Figure 3 -R2.5). Regardless of the channel incision characteristics, R2.5 presents some regular concordant surfaces at IS outside the bay.

Unconformity R3 is a transgressive tidal ravinement surface that covers the whole bay and the nearest part of the IS, where it is flat. Across the shore, in front of the Itapoá coast, this unconformity ends (toplap) in its following unconformity at depths between 15 and 18 m. Also, at the Praia Grande, near the Acarai Lagoon, R3 has a depression. The unconformity reflects the bathymetric profile along the Main Channel, with some changes across the channel. In the innermost part of the bay, R3 reaches its shallowest depths (Figure 3 -R3).

The last prominent unconformity (R4) seems to be a regressive tidal ravinement surface and is present throughout the surveyed area. It broadly follows the morphology of the bay and seafloor but deepens seaward (Figure 3 -R4).

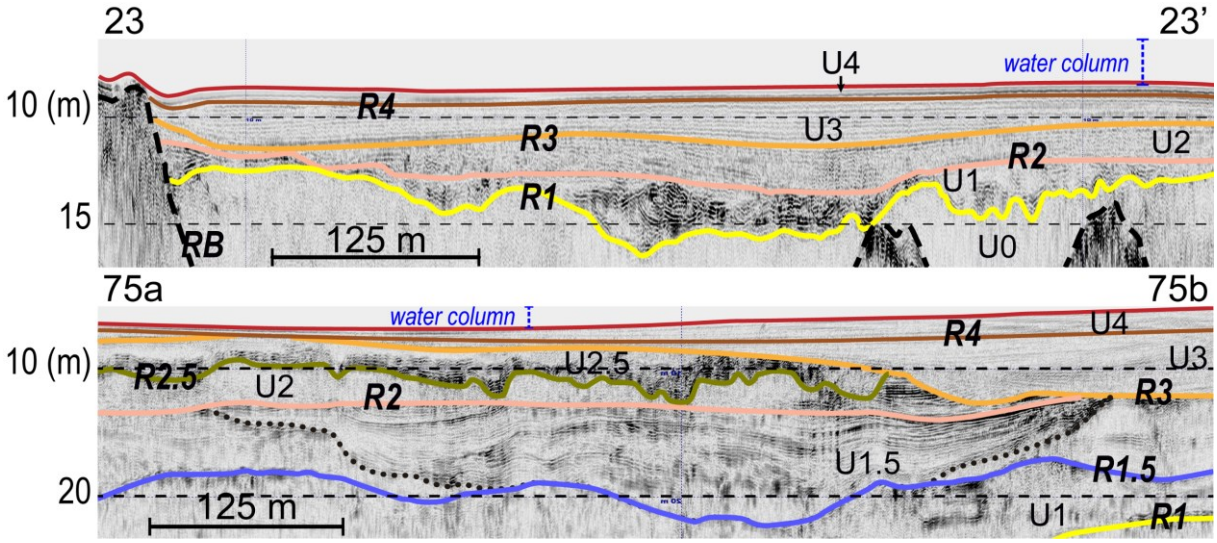

Figure 3. Seismic unconformities and units. See Figure 2 for location.

2.5.2.1 Units

Unit 0 is bounded by has the RB at base and the unconformity R1 is the its surface upper limit. This unit fills bedrock lows with distribution limited by the presence of bedrock and only occurs when there is available accommodation between RB and R1 (Figure 4 – RB).

With the unconformity R1 as its base, Unit 1 has the same geographical distribution as R1 (Figure 4 – R1), and presents 4.2 m mean of thicknesses, that ranges between 0.5 and 16 m. This unit does not have internal reflectors and is transparent. The top of this unit is eroded by the unconformity R1.5 or is capped by the unconformity R2.

At the interior of the bay, the main channel and the IS delimit the extent of unit 1.5. Unit 1.5 is the remnant portion of a unit formed by the infilling of the space created by the unconformity R1.5. Its original upper limit was reworked, and now, the unconformity R2 is the actual upper limit. This unit represents the deepest part of the deposit, which is composed of

infilled channels. Its distribution shows that this unit is related to nearby rivers since it is in the outflow region of these fluvial systems where U1.5 is located (Figure 4 – R1.5). U1.5 thicknesses ranges from 0.5 to 14 m, with a mean of 4.8 m.

Unit 2 caps both units 1 and 1.5, is observed throughout the whole bay (Figure 4 – R2), and has 1.4 m medium thickeness varying between 0.5 and 3 m. Excluding the inner shelf, this unit's maximum and minimum depth can be observed in the center of the Main Channel. Outside the bay, the most significant depth occurs near the mouth of the Linguado Channel, the Main Channel, and the Acaraí Lagoon.

Unit 2.5 is internally transparent throughout the inner region of the bay, where it is found at its shallowest depths (Figure 4 – R2.5). Its thicknesses range between 1 and 11.5 m, with a mean of 6 m. On the shelf, depths increase, and U2.5 starts to present subparallel and divergent internal reflectors, as found at the mouth of the Main Channel and Ubatuba Beach.

The thickness of Unit 3 varies with the morphology of the bay and shelf, where the margins and bay delta have the thinnest thickness. Meanwhile, the deepest parts of the bay and the shelf are the thickest. Unit U3 has an average thickness of 4 m, but varies from 1 to 18 m in thickness (Figure 4 – R3). In the innermost part of the bay U3 has medium and weak intensity reflectors, while in the Main Channel and the shelf only reflectors of low intensity are present. Unit 3 contains acoustic gas features (Figure 4 – RG).

Finally, Unit 4 is observed in the whole surveyed area (Figure 4 – R4). The high sea level deposition composes this unit. Its internal reflectors are weak in the Grande Island and Linguado Channel areas but in the rest of the bay and the Inner Shelf it exhibits medium to strong internal reflectors. The unit contains multiple horizontal subparallel reflectors. The thickness ranges from 1 to 3 m. Some shallow gas features also occur in weak intensity reflectors (especially in the Linguado channel).

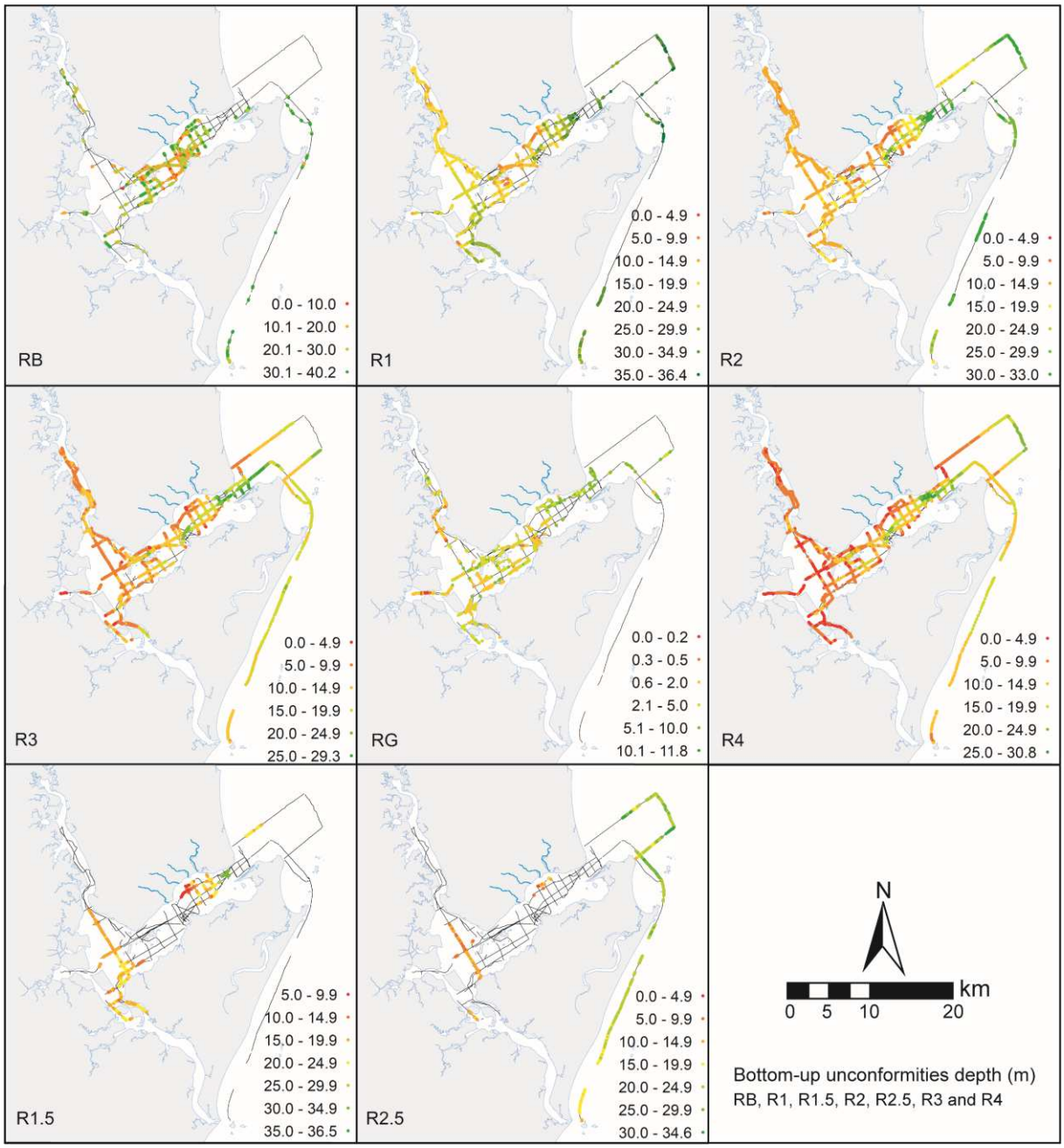

Figure 4. Geographical distribution and depth (in meters) of each unconformity as the basal reflector of subsequent sub-units (e.g., R4 is the basal surface for U4).

2.5.2.2 Facies

Twelve seismic facies (SF) types were identified (Table 1) of which one represents the rocky basement. The seismic types do not occur in the whole area or the same seismic unit. Furthermore, the seismic facies may have different spatial occurrences inside a seismic unit.

Units 3 and 4 display high amplitude and irregular reflections that mask the underlying reflectors. The extent of these facies may vary and the large ones makes local comprehension difficult (Table 1 – SFG).

SF-I is the seismic facies observed in Unit 0. This unit has no internal reflectors inside the bay and very few on the IS. When present, the internal reflectors are sparse, with low frequency and medium to low amplitude. (Table 1 – SF-I).

SF-II presents a pattern of low frequency, weak to medium amplitude. The reflections can be subparallel or chaotic. These seismic facies occur in the interior of the bay, preferentially at the greatest depths (Table 1 – SF-II).

Facies SF-III occurs in Unit 2 and Unit 3. These facies are composed of low or high amplitude and frequency reflectors with an oblique-tangential progradation pattern. The SF-III angle is usually high and occurs where the slope is high. Inside the bay, the reflectors high amplitude. Meanwhile, at IS, it occurs in front of Praia Grande beach, where the reflections have a low amplitude (Table 1 – SF-III).

Units 1.5 and 2.5 also display the seismic facies SF-IV. Here the reflectors may have low, medium, or high amplitude, always with high frequency. Near the Ribeira and Jaguaruna rivers (northern margin of the bay) and the Linguado Channel, the amplitude is medium to high. The reflections build a divergent concave-up pattern infill. In the mouth of the bay, the amplitude is low (Table 1 – SF-IV).

Units 1, 2, and 2.5 display high frequency within the SF-V outside the bay. The reflectors may present low, medium, or high amplitude. Seaward to the mouth of Babitonga Bay, the amplitude of these reflections is high, while in front of Ubatuba and Praia Grande beaches, the reflectors display low and medium values. The infill pattern is mostly subparallel, but Unit 2.5 may display concave-up reflectors in front of the Main Channel mouth. Below

these high-frequency reflections, a transparent infilling pattern may be present (Table 1 – SF-V).

Seismic facies SF-VI presents high amplitude, high frequency, and parallel reflections. The reflections build low-angle clinoforms that prograde seaward. It is found exclusively in Unit 3, at the Babitonga Bay mouth, adjacent to Itapoá City (Table 1 – SF-VI).

Seismic Facies VII displays low and medium amplitude, low frequency, and concave up divergent infill reflections. Sometimes, the infill pattern may be transparent. Units 1 and 2 present the SF-VIII at the Linguado Channel mouth region, near the northern margin (Table 1 – SF-VII).

Found within Units 1, 2, and 3, occurring in the adjacencies of the Babitonga bay mouth, facies SF-VIII presents transparent or low amplitude and frequency reflections. These reflections may be parallel or up-concave (Table 1 – SF-VIII).

The whole surveyed area presents evidence of facies SF-IX. It is characterized by high amplitude, high frequency, and continuous parallel reflections. The reflectors reproduce the bathymetrical shape. However, this facies displays asymmetrical convex-up reflections inside the Palmital Channel and at the bay mouth. Unit 4 is the only unit that contains these seismic facies. (Table 1 – SF-IX).

Facies	Unit	Internal reflectors	Interpretation	Local	System tract	Seismic example
SFRB	-	-	Rocky basement	Babitonga Bay; Adjacency of headlands	-	
SFG	U3 U4	High mplitude, hyperbolic, no visible internal reflectors.	Gas	Babitonga Bay; Inner shelf	TST	
SF-I	U0	Transparent fill pattern and no internal reflectors.	Undifferentiated deposits	Babitonga Bay; Inner shelf	?	
SF-II	U1 U2 U3	Low-frequency reflectors, with low or medium amplitude; Subparallel or chaotic reflectors.	Protected environments, bay, lagoon, central estuarine basin.	Babitonga Bay.	TST	U3 U2
SF-III	U2 U3	Low or high amplitude and frequency; High diving angle; Sigmoidal or oblique-tangential clinoforms.	Bay-head delta, prograding banks, tidal banks and tidal flats.	Babitonga Bay; Inner shelf	TST	
SF-IV	U1.5 U2.5	Medium or high amplitude and frequency; Parallel or concave upward reflectors, with an agradational filling pattern.	Low course river channels, Lateral migration, point bars, Meandering channels.	Babitonga Bay.	TST	U3
SF-V	U1 U2 U2.5	Low, medium or high amplitude; Sub-horizontal reflectors; High frequency.	Barrier	Babitonga Bay; Inner shelf	TST	U3
SF-VI	U3	High amplitude and frequency; Parallel reflectors; Clinoforms with low diving angle of the clinoforms; Seaward progradation.	Foreshore	Babitonga Bay mouth (northern shore Itapoá)	TST	U4
SF-VII	U1 U2	Low and medium amplitudes, with low frequency; Upward concavity reflections onlapping the margins; The fill pattern can be transparent.	Tide channel	Linguado Channel mouth.	TST	
SF-VIII	U1 U2 U3	Transparent fill pattern or with low amplitude and low-frequency reflectors; Parallel or up-concave reflectors that builds a divergent pattern fill.	Flood and ebb tide deltas	Babitonga Bay mouth.	TST	U3 U2
SF-IX	U4	High-amplitude and high-frequency reflectors; Parallel reflectors with high continuity.	Present sedimentation	Whole surveyed area	HST	

Table 1. Characteristics and distribution of the seismic facies found in the study area. Some facies occur more than one Seismic Unit. It also happens for the different System Tracts (TST and HTS).

2.5.3 Core petrophysical parameters and Units

Vibrocore A (Fig. 6) from the Linguado Channela predominantly is dominated by silty sand. The compressive wave velocity (Vp) ranges from 1591 and 1831 m/s, where increasing towards the surface. With the same pattern, the gamma density (GD) varies between 1.20 and 1.31 g/cm³. Opposing this pattern, natural gamma ray (NGR) values decrease closer to the surface, ranging between 61.8 and 66.4. The magnetic susceptibility (MS) is roughly consistent throughout the core, at an average value of 3.5 10^{-5} SI until 70 cm depth, when it oscillates between 3.94 and 7.94 10^{-5} SI. Resistivity values range between 0.215 and 0.382 Ohm, highest associated with mollusk shells. The petrophysical parameters present spikes near 95 cm (Figure 5). A radiocarbon age of 3204 ± 178 cal B.P. from 94.5 cm depth reveals an Average Sedimentation Rate (ASR) of 0.29 mm/year.

Vibrocore B from the Linguado channel is also dominated by sand and silty sand, with mollusk shells throughout the core. Both the Vp and GD values decrease upward. The Vp value ranges between 1708 and 1915 m/s and the GD from 12.1 to 13.6 g/cm³. The NGR drops from 63.5 to 59.5 Ohm.m and stabilizes between 58 and 60 cps downcore. The MS is stable until the 100 cm depth when its values oscillate upward. This parameter ranges from 0.89 to 7.0 10^{-5} SI. The resistivity varies between 0.27 and 0.40 Ohm.m, with its value shrinking upward. The spikes in the petrophysical parameters occur at 140 and 250 cm (Figure 5). The base of the core dates to 2306 ± 195 cal B.P., with an ASR of 1,18 mm/year

Vibrocore C is dominated by silty sand and coarse sand and some gravel. It presents a variable pattern ranging from 1709 to 1959 m/s Vp, while the GD has the exact pattern, ranging from 1.21 and 1.37 g/cm³. The NGR ranges between 60.7 and 66.6 cps, decreasing from the base until 70 cm, where the values increase towards the top. Fluctuating between 3.86 and 10.6 10^{-5} SI, the MS presents a decreasing trend, with an abrupt increase at 50 cm depth from base to top. Resistivity varies from 0.33 to 0.51 Ohm.m. The petrophysical parameters spikes do not occur like the other cores. No mollusk shell was available for radiocarbon measurements, so no dates or accretion rates are available from this core (Figure 5).

Dominated by sandy silt, vibrocore D presents Vp values ranging from 1638 to 1748 m/s. The parameters GD, NGR, and Resistivity decrease upward, varying between 1.12 to 1.23 g/cm³, 60.4 to 64.8 cps, and 0.17 to 0.30 Ohm.m, respectively. The MS values range between 4.0 and 7.39 10^{-5} SI. At the depth of 125 cm, the above described petrophysical values get out of the trend (Figure 5). Two radiocarbon ages of 213 and 1456 ± 157 cal B.P. were obtained at depths of 236.5 and 292.5 cm, respectively, indicating an ASR of 2,01 mm/year.

The predominant sediments in vibrocore E are sandy silt and silty sand. Its Vp ranges between 1669 and 1948 m/s, decreasing upward. This pattern also happens with the GD and Resistivity proprieties. GD varies from 1.14 to 1.37 g/cm³, while Resistivity ranges between 0.18 and 0.34. The NGR varies from 57.6 to 62.4 cps. The MS ranges between 0.484 to 3.90, increasing upward. The petrophysical parameters move away of the trend at the 100 cm depth (Figure 5). Radiocarbon data indicates that the deposit presents an ASR of 0.31 mm/year, with an age of 6921 ± 199 cal B.P. at 217 cm depth.

The sedimentary facies distribution observed in the cores (Figure 5) agrees with the depositional patterns of Babitonga Bay (Vieira et al., 2008). The sandy cores (core C and E) occur in river-tide-influenced and estuarine-tide-influenced areas in the Palmital Channel and the Main Channel. Near the Linguado Channel, the inner estuary presents silt or silty sand deposits with some sandy lenses (cores A, B, and D) formed during high energy events of constricted tides (Dalrymple et al., 1992).

Vigorous fluctuations in petrophysical parameters occur when trapped gas features appear in the sediment, as Delavy et al. (2015) reported. These fluctuations appear as low values for the Vp, GD, and NGD and high values for Resistivity. Along with the petrophysical parameters, the radiocarbon ages allowed the recognition of three stratigraphic units present in the cores that match with seismic units U2, U3, and U4 (Figure 5).

Unit U2 was observed only in the Main Channel, in core E. Its basal boundary was not reached in the cores, but its upper limit is identified by the sudden change in petrophysical parameters given by the occurrence of trapped gas. The sedimentary facies also change at the

boundary, changing from silty fine sand with some organic fragments and mica to poorly sorted sand with shells in unit U3.

Unit U3 is also found in the Palmital and Linguado Channels (cores C and A). The first, core C, also presents poorly sorted sand and organic fragments. Core A is composed of silty sand with the occurrence of shells at the upper part and some organic matter mixed in some peat material at the bottom. The petrophysical parameters inside the U3 vary mainly in core C. Still, none of the oscillations are as significant as those in the upper boundary in core A, where trapped gas occurs.

Lastly, Unit U4 is present in all cores with silty sand deposits, with shell and organic matter occurring in core B, which can be explained by the fact that this core was collected in front of a river mouth, near its bay-head delta. Sudden oscillations of the petrophysical parameters appear in the presence of trapped gas. Apart from that, MS values fluctuate in cores A and C, where the sediment is composed only of silty sand.

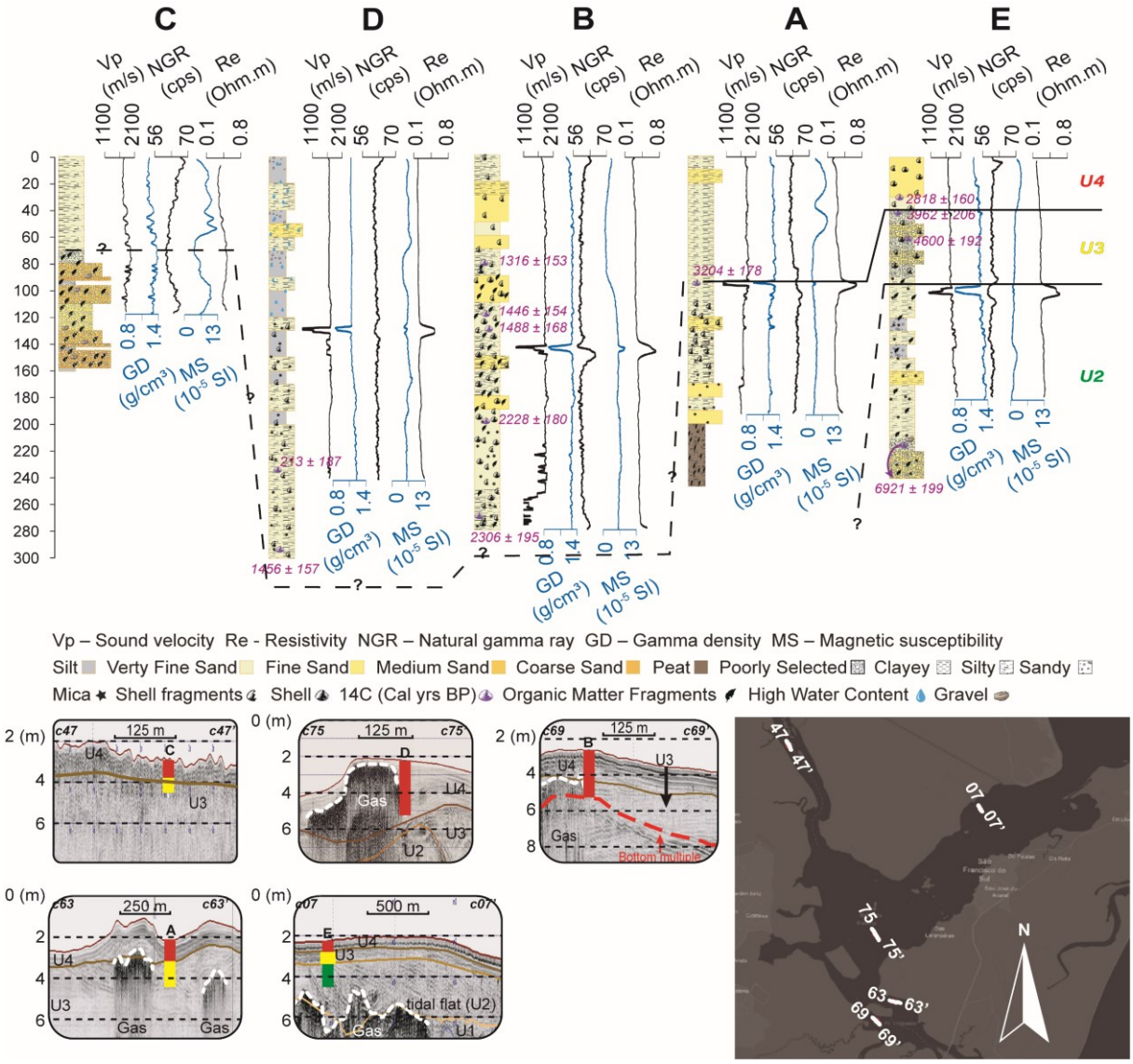

Figure 5. Stratigraphic units (U2 - green, U3 - yellow and U4 - red) of the vibrocores. Three stratigraphical units were found, with some variations in sediment. The sudden change in the petrophysical parameters is related to trapped gas in sediment layers.

The upward decrease in Vp and GD, suggest that the porosity of the sediment seems to decrease towards the surface (BLUM, 1997) and imply changes in water content (KELLER, 1969), that also lead to a decrease in Re values. As the MS values are related with magnetic materials (BLUM, 1997), the up-core increase in MS values suggests some input of ferromagnetic mineral into the last 75 cm of sediment. Finally, the correlation between NGR

and muddy sediment allows the observation in some changes in sedimentation patterns (SERRA, 1984). The tidal flat over the bay-head delta of the Saguaçu lagoon (see Figure 2, Core B) seems to increase in mud content, while it decreases in the other cores.

Differences between ASR values in Babitonga Bay cores indicate the occurrence of more than one depositional pattern, established by different estuarine sedimentary environments. The first estuarine environment is the tidal flat located near Saguaçú lagoon and the Linguado Channel (VIEIRA et al., 2017), which presents the highest ASR (Table 2 - Core D). Secondly, there is the bay-head delta in the Linguado channel (Table 2 - Core B). Lastly, the tidal bank in the main channel presents the lower ASR (Table 2 - Core E).

These three sedimentary environments are found in the estuarine conceptual models proposed by Dalrymple et al. (1992). The hydrodynamic energy in the tidal flat is low, while the energy is high in the tidal banks. The same authors also describe that, in periods of marine regression, the tidal flat deposits advance over the central basin of the estuary, occupying a larger accommodation space with respect to other sedimentary environments. On the other hand, tidal bank deposits and barriers develop on older morphostratigraphic features of the same genesis, with a smaller accommodation space. Thus, both the hydrodynamic energy and the accommodation space influenced the sedimentary accretion of the most recent unit (U4).

Table 2. Long-term average accretion of the cores distributed along Babitonga Bay.

Core	Age	Depth (cm)	Average Sedimentation Rate (mm/yr)
A	3204 ± 178	94.5	0.29
B	2306 ± 195	271	1.18
C	No Data	No Data	No Data
D	1456 ± 157	292.5	2.01
E	6921 ± 199	217	0.31

2.6 DISCUSSION

2.6.1 Stratigraphic interpretation

The interpretation of the stratigraphic units found in the study area is presented below (Figure 7). This is based on the correlation between the knowledge about estuarine and inner shelf morphostratigraphy, the seismic facies found, their geographic position and the cores collected in Babitonga Bay.

2.6.1.1 Seismic Facies RB (SFRB) – Rocky Basement

The lack of lateral continuity and the close association with outcrops supportthe interpretation of this facies as rock basement (see Table 1 and Figure 7- SFRB). The basement is relatively elevated in the center of the bay, where a rocky outcrop is exposed on its floor (see Table 1 and Figure 7 – RB). The rocky basement delimits the accommodation space and influences the evolution of the bay.

2.6.1.2 Seismic Facies G (SFG) – Gas

Acoustic features associated with gas were observed in several locations (see Table 1 – SFG, and Figure 5), detailed in Figure 6.

Gas echo-charactert	Echo-character features	Gas	Occurrence (%)
Acoustic turbidity (AT)	Reflector with an intense signal at the top, continuous and linear.	Trapped	74
Acoustic blanking (AB)	Irregular up-concave reflectors.	Migration	25
Black shadow (BS)	Strongly reflective acoustic character, with several multiples.	Trapped	0,8
Intra-sedimentary plume (ISP)	Parabolic anomalies that cross real reflectors.	Migration	0,2

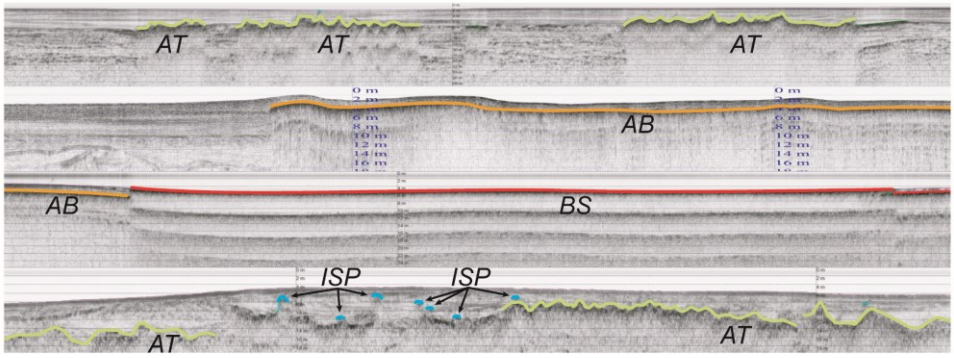

Figure 6. Echo-characters features. Source: Klein et al.(2016a).

There is no clear pattern in the distribution of gas features. however, the depths of occurrence are shallower in the main channel, suggesting a geological control in the depth of occurrence of such features. Thus, shallower depths are associated with a shallower sedimentary package, which is a result of the smaller accommodation space given by the raised basement. Such seismic features are related to change in Vp, GD and Re petrophysical parameters (Figure 5)

2.6.1.3 Seismic Facies I (SF-I) – Unknown

No sedimentary environment can be identified from the SF-I, as it does not have a well-defined basal limit and its filling pattern is transparent (Table 1 - SFI; Figure 7 - U0). Further, no cores penetrated to this unit. These facies are interpreted as undifferentiated deposits.

2.6.1.4 Seismic Facies II (SF-II) – Central Basin

The entire main channel and Linguado Channel feature subparallel reflectors with low amplitude and high continuity and frequency (Table 1 - SFII; Figure 7 - *cb*). Also, these facies have low resistance to the penetration of the acoustic signal, which is consistent with the fine material composed of silty sands or sandy muds collected from this unit in the cores E and D (Figure 5). Base on 14c ages of core E, we interpret these facies as deposits from the central basin of the bay such as described by Dalrymple et al. (1992) and presented by Nordfjord et al. (2006), Greene et al. (2007), Tesson et al. (2015).

2.6.1.5 Seismic Facies III (SF-III) – Bay-Head Deltas, Longitudinal Banks, and Tidal Flat

The high frequency, medium to high amplitude internal reflections in SF-III prograde with an oblique-tangential pattern into the bay. The clinoforms may be associated with truncated channels or not. Such facies are incised by channels, in the inner part of the estuary, indicating that the deposit is from as bay-head deltas, such as seem in previous estuarine infill studies (e.g., GREENE at al., 2007; ANDERSON et al., 2008; TESSON et al., 2015; COOPER et al., 2016; Figure 7 - line 71-71´). With their mounded external geometry, the clinoforms represent longitudinal banks, in the Main Channel. Without the mounded forms, at the margins of the bay, these facies represent the progradation of sand banks or tidal flats (Figure 7- *bhd and* tfb).

2.6.1.6 Seismic Facies IV (SF-IV) – Lower Course of Fluvial System

In the interior of the bay, near the Linguado Channel, these facies present high-amplitude and high-frequency reflectors, which show a complex filling pattern, built by convex reflectors between concave reflectors (Table 1 and Figure 7 – SFIII). This type of facies is interpreted as a point bar deposit (e.g., GHAZI and MOUNTNEY, 2009). On the other hand,

between the Alvarenga Stream and the Ribeiro River, the filling pattern of these channels is divergent.

The reflectors of this facies have their upper limit marked by the D2 unconformity. The occurrence of this facies near the rivers flowing into the bay lead us to believe that this is a lower course of a fluvial environment, which had been drowned during the rise in the base level.

2.6.1.7 Seismic Facies V (SF-V) – Barrier systems

The FS-V reflectors are typically sub-parallel in front of the Main Channel and Praia Grande. In the most distal portion of the inner shelf, some reflectors present evidence of subtle retrogradation towards the coast (Figure 7 - line 85b-85b'), interpreted as washover deposits (e.g., TILLMANN and WUNDERLICH, 2013; ZĂINESCU et al., 2019). Washovers form through wave overwash in high energy events are more significant in situations where the Relative Sea Level is rising in a transgressive environment (BUYNEVICH and DONNELLY et al., 2006). Underneath these reflectors, a transparent fill pattern is observed (Figure 7 - *bbl*). This transparent feature is interpreted as a muddy backbarrier deposit (e.g., GOFF et al., 2019) from secondary tidal channels or lagoons (GREEN et al., 2013; COOPER et al., 2018).

In addition to the parallel reflectors, some concave reflectors are found truncating the FS-V and occasionally with evidence of lateral migration in the shelf. Adjacent to Praia de Ubatuba and Praia Grande beaches, the concave reflectors that cut the transparent filling pattern are interpreted as backbarrier tidal channels (Figure 7 – lines 109-109’ and 111-111’). They are commonly associated with gas features (SFG), reaffirming the interpretation of this as a muddy lagoonal deposit.

On the adjacent inner shelf between Praia de Ubatuba and Praia Brava, SF-V features oblique prograding reflectors along the edge, which build a mounded geometry next to the rocky basement. This is indicative of a barrier anchored in a rocky promontory (e.g., COOPER et al., 2016; COOPER et al., 2018). Growth direction was toward the north, agreeing with the

dominant trend of longshore transport in this region (COSTA et al., 2019. The lack of erosive truncation features within this feature indicate that it was a local topographic high. The faciological configuration of SF-V is interpreted as drowned transgressive coastal barrier system deposits (e.g., PARHAM et al., 2007; RIEU et al., 2005; COOPER et al., 2018), which correlate with marine phreatic sandstones found by Simioni et al. (2018) in the adjacent inner shelf.

2.6.1.8 Seismic Facies VI (SF-VI) – Shoreface

In the northern part of the study area, near the Itapoá City coast, Unit 3 presents strong continuous parallel seaward dipping reflections which (Figure 7 - line 18-18'). These facies represent the shoreface (e.g., JOUET et al., 2006; LIU and GOFF, 2018; CHOI et al., 2020). Additionally, acoustic turbidity (gas) features occur at the base of the unit. The gas probably originates from the unit below (Unit 2). Its average thickness is 6 m and it varies between 1 and 15 m.

2.6.1.9 Seismic Facies VII (SF-VII) – Linguado Channel Mouth

In front of the Linguado Channel mouth, at the south of the study area, concave -up reflections compose the filling of the Units 1 and 2 (Figure 7 – line 113-113''). These facies are interpreted as paleochannels infilled by suspension settling (e.g., NORDFJORD et al., 2006; RONCHI et al., 2018) and, therefore, as past positions of the Linguado Channel and its distributaries.

2.6.1.10 Seismic Facies VIII (SF-VIII) – Tidal Delta System

The Babitonga Bay mouth region is characterized by tidal-delta system seismic features in Units 1, 2, and 3. These features have transparent to low amplitude and low to

medium frequency. The pattern infill of the flood-tidal delta body is parallel and forms a mounded shape geometry at the mouth of the main channel (Figure 7 – line 101-101'). The bottom of the mound is characterized by acoustic turbidity (Figure 7 – *at*), indicating the presence of muddy deposits that are interpreted as back-barrier deposits (e.g., DE SANTIS et al., 2020). Also, paleochannels with transparent pattern infill are observable, indicating the presence of tidal channels in the flood tidal delta (Figure 7 – line 101-101 – *ftp*) (FITZGERALD et al., 2012).

Outside the bay, in front of Itapoá Beach, the Galharadas sandbank occurs above the ebb-tidal delta. Its mounded geometry is composed of low amplitude and frequency reflectors in Unit 3. Also, mounded geometries are present seaward, indicating the limit of the ebb-tidal delta. Meanwhile, ebb-tidal channels are present in Units 1 and 2. Its morphology is characterized by up-concave reflections infill pattern of paleochannels distributed along the seismic section, indicating the main ebb channel, some distributary channels, and some distributary mouth bars (e.g., FITZGERALD et al., 2004).

2.6.1.11 Seismic Facies IX (SF-IX) – Present Sedimentation

Present in all records, SF-IX is the last facies observed. Its upper limit is the bottom of the bay, and its lower limit, in general, is U3. Therefore, Unit 4 is the only seismic unit that contains these facies. They are formed by modern sedimentation, where local hydrodynamics promotes the occurrence of bedforms in some regions, such as the mouth of the Babitonga Bay, as shown in Figure 7 (line 99-99').

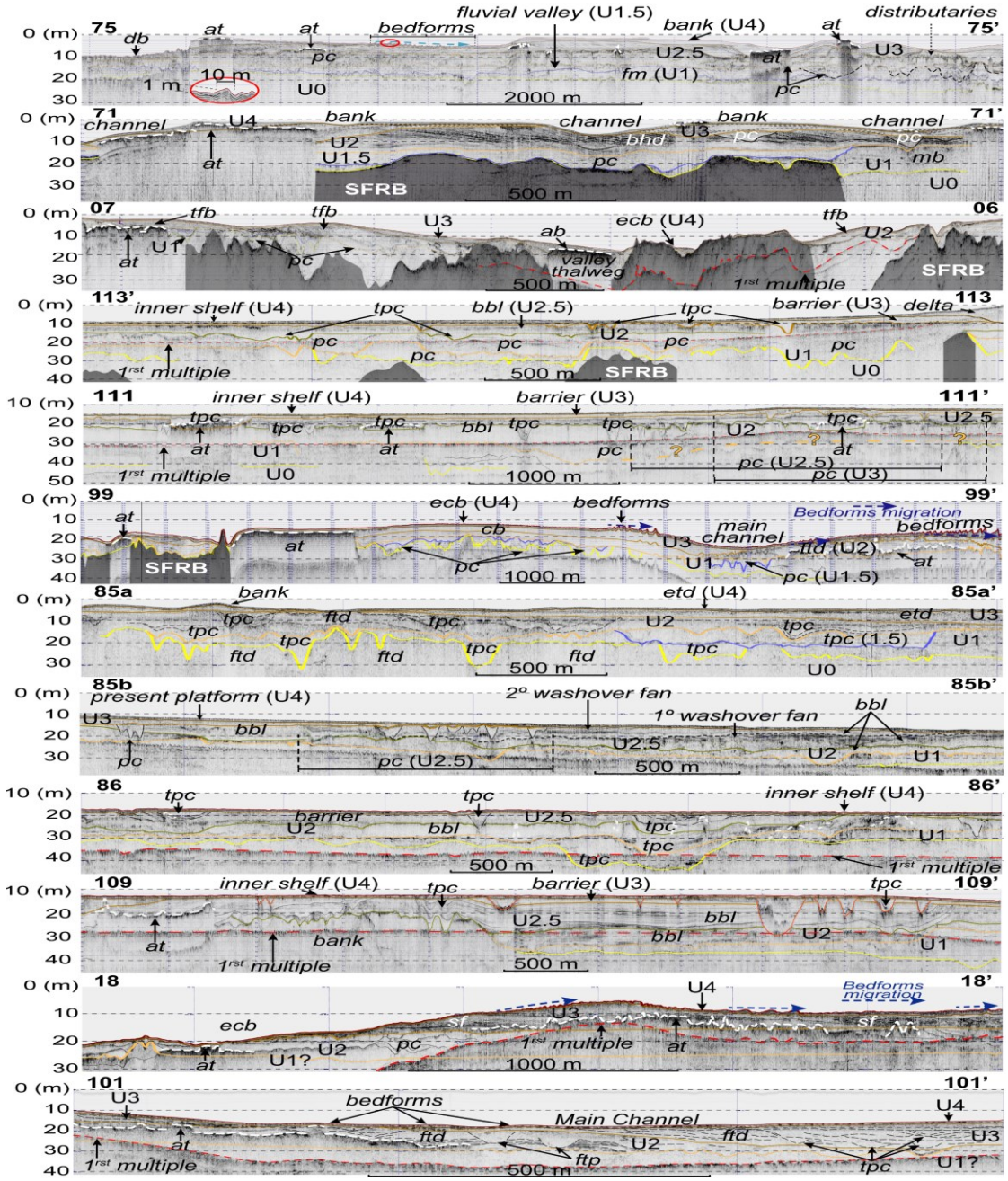

Figure 7. Seismic Unconformities, Units and, Facies interpreted. (ab) acoustic blanking, (at) acoustic turbidity, (bbl) back-barrier lagoon, (bhd) bay-head delta, (ecb) estuarine central basin, (db) dredged bottom, (etd) ebb tidal delta, (fm) fluvial margin, (ftd) flood tidal delta, (mb) marginal bank, (pc) palleochannel, (tfb) tidal flat/bank prograding towards bay depocenter, (tpc) tidal paleochannel. See Figure 2 for location. White dashed lines identify trapped gas. Red dashed line identifies multiple reflections. Other dashed lines represent the supposed position of the respective colored unconformity for locals that the reflectors are not observable. U1 and U2 are transgressive units, while U3 and U4 are highstand units.

2.6.2 Babitonga Bay stratigraphy

Babitonga Bay sedimentary infill consists of both Transgressive System Tract (TST) and Highstand System Tracts (HST), units (Figure 8). These systems tracts comprise estuarine, back-barrier lagoon, coastal barrier, tide deltas and inner shelf deposits. Both the TST and HST are observable in the whole bay, where the TST presents deposits in a retrogradation pattern, while the HST shows a depositional prograding pattern.

From bottom-up, the observable sedimentary fill starts from the Transgressive Surface (TS), where the TST is composed by estuarine channels, bay-head deltas and its channels, central basin, flood and tidal delta and its channels, back-barrier lagoon and washover fans deposits. The Maximum Flooding Surface (MFS) separates the HST from the TST. At the HST, the following facies are observable: tide banks, tide channels, bay-head deltas, estuarine central basin, ebb and flood delta and channels. Finally, at the present estuarine floor, some bedforms occurs in regions of high wave and tidal energy.

Inside the bay, the rocky basement played an important role in providing the accommodation for infill, as its presence was responsible for segmenting the estuarine system in two incised valleys until their drowning by the sea-level rise, a process that unified the valleys in an estuarine system similar to the present Babitonga Bay at 5 – 6 kyr B.P. Around 70 km northward of the study site, this estuarine infill setup occurs in the Paranaguá Bay (LESSA, 1998). Excluding the estuarine deposits, an analogous stratigraphic pattern also occurs about 110 km southward of Babitonga Bay, with a barrier-lagoon system preserved by overstepping processes in the inner shelf (COOPER et al., 2016). Babitonga Bay estuarine infill patterns, similar to that observed here for Babitonga Bay, also is observable worldwide structural incised valleys, as the French structural estuaries in Bay of Biscay (CHAUMILLON et al., 2008) and in Thau lagoon (FERRER et al., 2010). Martínez-Carreño and García-Gil (2017) also present similar estuarine infill processes in Spanish coast, at Ria de Vigo.

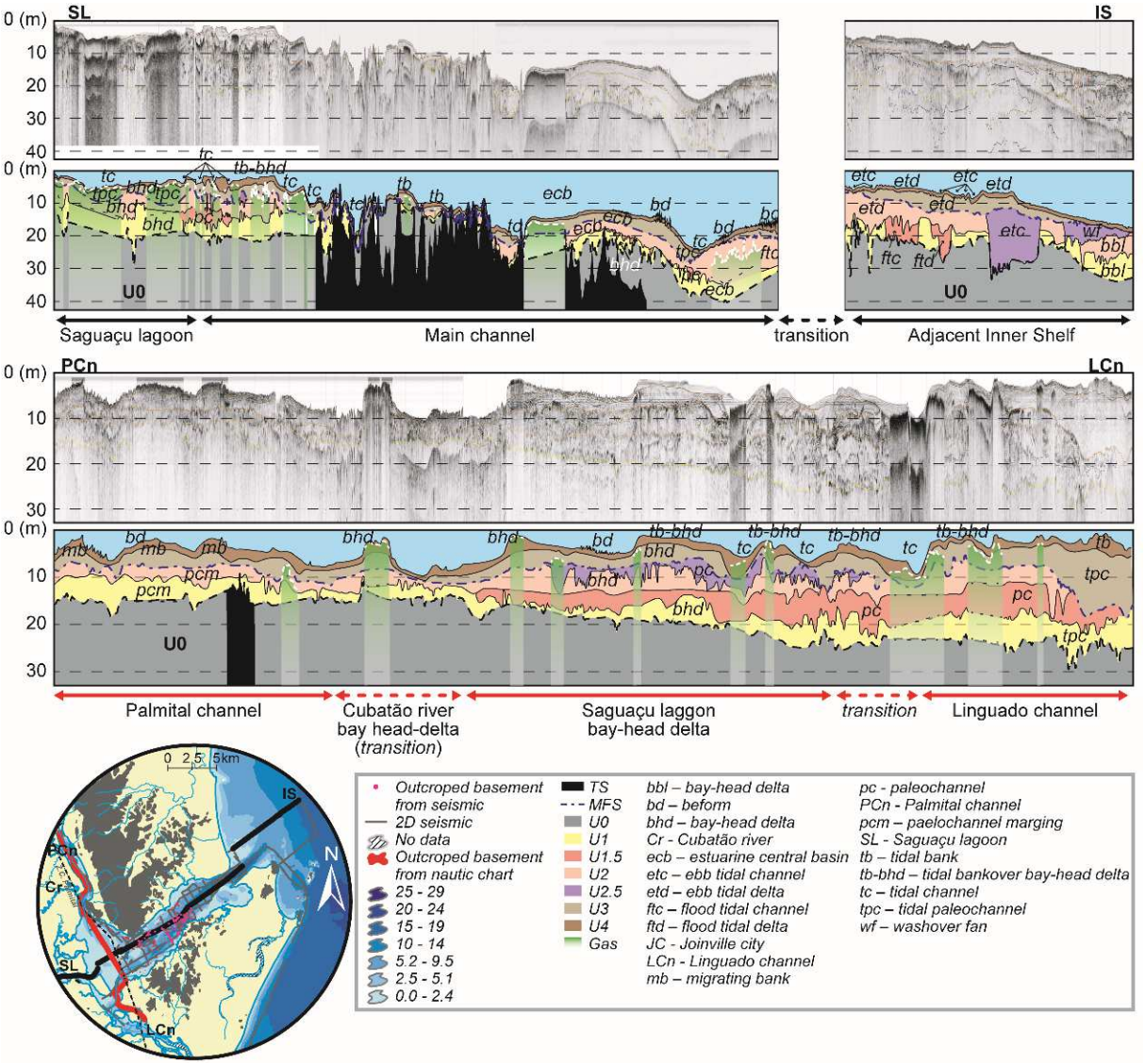

Figure 8. Composite profile through Sections I (red line) and II (black line) of the Babitonga Bay. Note the separation of systems by rocky basement. Systems I and II present cut-and-fill structures that deepen towards the sea. The greatest depths occurred in the Main Channel region, in System II.

2.6.3 Estuarine evolution

During the LGM, the study site was characterized by of two tectonic river valleys built by neotectonics activity (GIMENEZ et al., 2022). These valleys were separated by the basement outcrop inside the bay. When these valleys were re-flooded during the Holocene, two separate

fluvial systems developed (Systems I and II) alongside a constricted lagoonal system (System III) between 12 – 8 kyr. On the adjacent inner shelf, an older lagoon-barrier system is preserved (System IV) probably at 9 – 8 kyr B.P., during the last melt water pulse (Figure 9).

With the sea-level rising, marine ravinement started to rework the coastal deposits landward with different rates guided by meltwater events (COOPER et al., 2016). These different rates enabled both estuarine rollover and barrier overstep processes, preserving two transgressive sedimentary units (U1 and U2).

2.6.3.1 Rollover

Starting with the oldest transgressive unit (U1), the coast was retreating landward by a process of rollover (Figure 9), while a lagoon-barrier system sheltered the coast along the whole coast of SFSI. This coastal environment is observable by a back-barrier lagoon and tidal-delta channels preserved deposits evidencing the coastal environment (MULHERN et al., 2021). Some sandbars also occurred near the flooded tidal delta inside the back-barrier lagoon. At the same time, fluvio-tidal channels were meandering inside the incised valleys. They are the unique preserved features occurring mainly in the seaward portion of the valleys. So, the Linguado Channel and the mouth of the Main Channel are the locations where these channels are most preserved. Between the exposed basement (granitic suites inside the bay) and the gneiss in the SFSI, an enclosed lagoon environment was connected to the Palmital-Linguado estuarine system (Systems I, II and III, in Figure 9 – U1).

2.6.3.2 Overstepping

The last meltwater pulse, about 8k BP (Figure 9), led to the overstepping of the barrier-lagoon system (Figure 9 - U1). On the shelf, the lagoon-barrier system migrated landward with the width of the tidal inlet shrinking, while the flood tidal delta migrated landward in both incised valleys (Systems I and II, in Figure 9). The barriers at the SFSI coast started to open,

and tidal inlets were established. Rising sea level enabled waves to overwash the barriers (COOPER et al., 2018), suggesting higher storm wave heights (e.g., CARTER and ORFORD, 1981), forming the washover deposits observable in front of the Itapoá coast (Figure 9 - U2). Similar to what occurred at the now drowned barrier offshore of Tijucas Bay (COOPER et al., 2016), about ~120 km south of Babitonga Bay, overstepping of Babitonga's barrier may have reduced the available sand for coastal plain development. Such scenario explains the small size of the Babitonga sand barriers compared to adjacent ones in Guaratuba and Paranaguá bays pointed by Lessa et al. (2000).

At that moment, behind the back-barrier lagoon, a tidal flat probably was present as Dalrymple et al. (1992) describe estuarine systems. Similarly, at Itapoá, a tidal flat was located between the back-barrier lagoons and an estuarine system developed over the lowland caves of the Pleistocene strand plain (SOUZA, 1999). The tidal flat at SFSI was the transition between the Pleistocene strand plain and the back-barrier lagoon (Figure 9 - U2). Inside the valleys, the exposed basement starts to be flooded. The fluvio-tidal channels are now occurring in front of the rivers reaching the Linguado channel and Itapoá area. The constricted lagoon seems to maintain its morphology.

Seismic records showed that the SFSI coast transgressive barriers evolved into barrier islands, with two inlets in the east and one in the north connecting the sea and the back-barrier lagoon. The barrier migrated from the adjacent inner shelf islands and welded to the Ubatuba and João Dias headlands (Figure 9 – U2). Using ground penetration radar (GPR), Lott (2021) describes the welding and development processes of this barrier, where the coastal drift formed sand spits along the headlands and infilled the submerged adjacent inner shelf. The Itapoá coast also developed barrier islands, with the estuary reaching its maximum flood in the coastal plain (SOUZA, 1999).

2.6.3.3 Drainage unification

The sea-level reach its maximum level at 5 to 6 k.y. B.P. (ANGULO et al., 2006) in SE Brazilian coast. At this time, the Babitonga Bay is established as Systems I, II and III merged due to bay flooding (Figure 9 – U3). Most of the basement that delimited the different valley was drowned, forming the islands in the inner archipelago of Babitonga. In this context, the late Holocene drainage of Babitonga Bay was now united, linked to the sea by the Linguado and the Main Channels. Linguado channel was fronted by a tidal delta in the adjacent inner shelf, while the tidal deltas in the Main Channel migrates landwards and are now occupying the same position of the current flood and ebb deltas. Longitudinal tidal bars that migrate onto the central basin also occurs in the Main Channel.

2.6.3.4 Estuarine and coastal plain progradation

After the highstand, sea level fell to its present level and the coast prograded seaward, developing the Holocene strand plain (Figure 9 - U4). In Itapoá, the strand plain was formed after the infill of the estuary at the Pleistocene coastal plain and the barrier / back-barrier lagoon (SOUZA, 1999). The same process occurred on the SFSI coast, though with the Acaraí lagoon formed between the Pleistocene strand plain and the Holocene welded barrier. This lagoon is connected to the sea by the Ubatuba beach, which now extends around the Ubatuba Headland and feeds downdrift sand spits by wave-driven headland bypassing (LOTT, 2021). Also, the SFSI coastal barrier was worked by wind, providing dunes development above the welded barrier (ZULAR et al., 2013).

Inside Babitonga Bay, the tidal delta developed in the same place as it was at the highstand, expanding its lateral ranges as the accommodation space on the shelf and inside the Main Channel was filled. Additionally, some marginal banks developed in both deltas (Galharadas, Coroa Grande and Coroa dos Pampas sandbanks). Channel margins developed as the tidal plains prograded onto the estuary, along Palmital and Linguado Channels, simultaneously with their tributary rivers. Such sedimentation promotes the occurrence of

shallow gas trapped in the sediment, similar to what was observed in Paranaguá Bay (ANDRADE et al., 2021).

During this period, increasing MS values inside the Main Channel and a trend of decreasing MS values in Palmital Channel (Figure 5) reveal changes in sediment source to these sites. Also in the bay, in the upper portion of the deposits, another change in sediment sauce is revealed by NGR values (see Figure 5). This proxy values growth shows that the muddy content has increased in the latter moments of sedimentary deposition.

Recently (1935) the Linguado Channel totaly lost its connection to the sea due to a bridge built across the channel. This anthropic intervention changed the hydrological pattern, leading to a new one in which the mouths of both channels changed, in particular through the development of a sandspit barrier in front of the mouth of the Linguado Channel (SOUZA 1999; SILVEIRA et al., 2012). Such sandspit may have disturbed alongshore transport, fomenting Itapoá coast erosion, along the local channel dredging and maintenance practice.

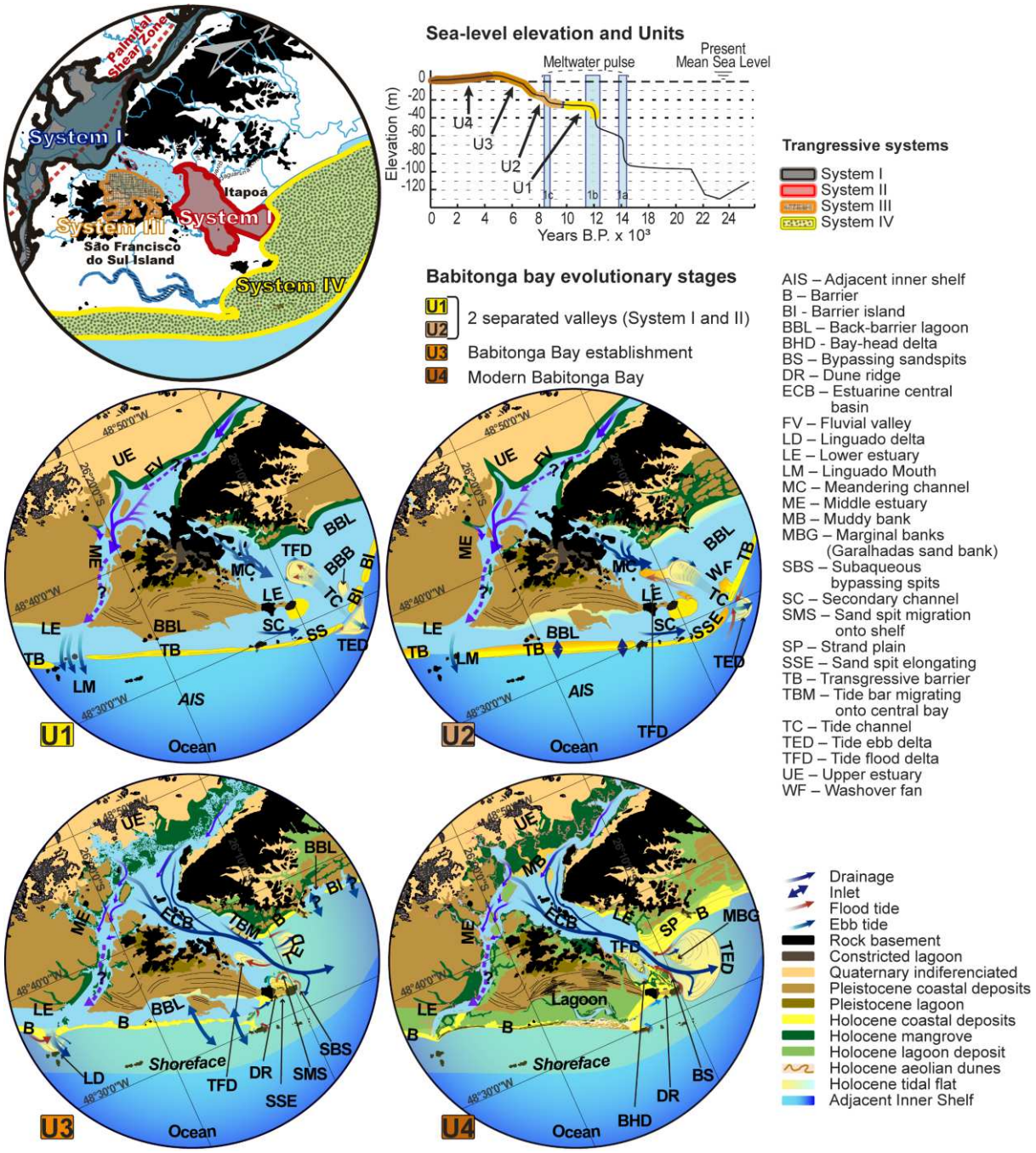

Figure 9. Holocene evolution of Babitonga Bay along sea-level rising and fall. Here the most significant change was the drowning of the rocky basement that separated Systems I, II, and III ("Stage 1" and "Stage 2"). At the high sea-level Stage 3, the lagoon system protected by barriers was strangled and barriers welded on the coast. The marine regression starts, and the welded barriers form aeolian dunes and the Holocene coastal plain ("Stage 4").

2.7 CONCLUSION

Seismic, sedimentary and petrophysical data enlightened the infill processes of Babitonga Bay and the evolution of its adjacent coastal systems. Such data displayed both transgressive and highstand system tracts (TST and HST), which includes fluvial, estuarine and coastal depositional systems.

Stratigraphic interpretations give insights into the processes responsible for forming the paleo lagoon-barrier system along the São Francisco do Sul Island (SFSI) and Itapoá coast, preserved by rollover and overstepping processes. These processes are related to rapid sea-level rise driven by meltwater pulses between 8000 – 12000 years B.P. Such interpretations also shed light upon the evolution of estuarine systems inside Babitonga Bay, where two tectonic valleys and one constricted lagoon occurred before the sea-level highstand.

During the TST, barrier-lagoon overstepping process may have promoted differences in sand availability in Babitonga Bay adjacent coastal plain (São Francisco do Sul Island and Itapoá), resulting in a strandplain smaller than Guaratuba and Paranaguá bays. Rising sea level also led to an estuarine retraction by a rollover process, advancing landward over the exposed rocky basement and Pleistocene terraces, flooding the structural incised valleys.

Reaching the sea-level highstand, in the HST, the flooding of tectonic valleys and a constricted lagoon created a single drainage system and estuarine body (Babitonga Bay). This new estuary was connected to the sea by two entrances separated by a bedrock-cored island (SFSI) characterized by a Pleistocene strand plain and coastal lagoon-barrier system.

Finally, the present Babitonga Bay was established with sea level falling to modern elevation, developing along the Itapoá and northern SFSI coasts a strand plain with back-barrier lagoons which were filled and associated barriers welding onto the mainland. Longshore transport and headland bypassing built sandspits along the coast, such as the ones at Linguado and Main channels.

2.8 ACKNOWLEDGEMENTS

We thank Professors Dr. Cláudio Rudolfo Tureck (Univille) and Dr. Luciano Lorenzi (Univille) for the identification of mollusc shells sent for 14C dating. Also, we thank all colleagues involved in some part of this work.

Funding: This work was supported by the Conselho Nacional de Desenvolvimento Científico e Tecnológico (CNPq) througth the project *Subida do nível do mar e a Baía da Babitonga: uma abordagem eco-morfodinâmica para prever e mitigar impactos*, included in the *Outras Baías do Brasil* [grant: 441545/2017-3].

REFERENCES

ALLARD, J., CHAUMILLON, E., BERTIN, X., POIRIER, C., & GANTHY, F. 2010. **Sedimentary record of environmental changes and human interferences in a macrotidal bay for the last millenaries: the Marennes-Oléron Bay (SW France)**. Bulletin de la Société Géologique de France, v. 181, n. 2, p. 151-169.

ALVES, J. H. G. D. M**. Refração do espectro de ondas oceânicas em águas rasas: Aplicações à região costeira de São Francisco do Sul, SC**. 1996. Tese (Dissertação em Engenharia Ambiental) - Programa de Pós-Graduação em Engenharia Ambiental. Universidade Federal de Santa Catarina, Florianópolis. 107p.

ANDRADE, J.F.P.; NOERNBERG, M. A.; NAGAI, R. H. 2021. **Shallow gas high-resolution seismic signatures in a subtropical estuary**. Geo-Marine Letters, v. 41, n. 3, p. 1-14.

ANGULO, R. J., DE SOUZA, M. C., ASSINE, M. L., PESSENDA, L. C. R., & DISARÓ, S. T. 2008. **Chronostratigraphy and radiocarbon age inversion in the Holocene regressive barrier of Paraná, southern Brazil**. Marine Geology, v. 252, n. 3-4, p. 111-119.

ANGULO, R. J., PESSENDA, L. C. R., & SOUZA, M. D. 2002**. O significado das datações ao 14C na reconstrução de paleoníveis marinhos e na evolução das barreiras quaternárias do litoral paranaense**. Revista Brasileira de Geociências, v. 32, n. 1, p. 95-106.

ANGULO, R. J.; LESSA, G. C.; DE SOUZA, M. C. 2006**. A critical review of mid- to late-Holocene sea-level fluctuations on the eastern Brazilian coastline**. Quaternary science reviews, v. 25, n. 5-6, p. 486-506.

ANGULO, R.J.; SOUZA, M.C. 2004. **Mapa Geológico da planície costeira entre o rio Saí-Guaçu e a Baía de São Francisco, litoral norte do estado de Santa Catarina**. Boletim Paranaense de Geociências, v. 55.

ANGULO, R.J.; SOUZA, M.C.; LESSA, G.C. 2009. **The Holocene barrier systems of Paranaguá and northern Santa Catarina coasts, southern Brazil**. In: Geology and geomorphology of Holocene coastal barriers of Brazil. Springer, Berlin, Heidelberg. p. 135-176.

AYRES NETO, A. 2000. **Uso da sísmica de reflexão de alta resolução e da sonografia na exploração mineral submarina**. Brazilian Journal of Geophysics, v. 18, n. 3, 2000.

BALTZER, A., TESSIER, B., NOUZE, H., BATES, R., MOORE, C., & MENIER, D. 2005. **Seistec seismic profiles: a tool to differentiate gas signatures**. Marine Geophysical Researches, v. 26, n. 2, p. 235-245.

BARBOSA, C F.; SUGUIO, K. 1999. **Biosedimentary facies of a subtropical microtidal estuary; an example from southern Brazil**. Journal of sedimentary research, v. 69, n. 3, p. 576-587.

BARBOZA, E. G., DILLENBURG, S. R., LOPES, R. P., ROSA, M. L. C., CARON, F., ABREU, V., ... & TOMAZELLI, L. J. 2021. **Geomorphological and stratigraphic evolution of a fluvial incision in the coastal plain and inner continental shelf in southern Brazil**. Marine Geology, v. 437, p. 106514.

BASTOS, A. C., VILELA, C. G., QUARESMA, V. S., & ALMEIDA, F. K. 2010. **Mid-to Late-Holocene estuarine infilling processes studied by radiocarbon dates, high**

resolution seismic and biofacies at Vitoria Bay, Espírito Santo, Southeastern Brazil. Anais da Academia Brasileira de Ciências, v. 82, n. 3, p. 761-770.

BLUM, P., 1997, **Physical properties handbook: a guide to the shipboard measurement of physical properties of deep-sea cores**. Available from: http://www-odp.tamu.edu/publications/tnotes/tn26/CHAP6.PDF.HTM. Acessado em 07 de julho de 2022.

BOGO, M., SOUZA, M.C., ANGULO, R.J.L BARBOSA, E.G. & ROSA, M.L.C.C. 2015. **Arquitetura deposicional da barreira holocênica na porção meridional da Ilha de São Francisco do Sul, SC, Brasil**. Pesquisas em Geociências, v. 42, n. 3, p. 281-295.

BORTOLIN, E. C., WESCHENFELDER, J., & COOPER, A. 2018. **Incised valley paleoenvironments interpreted by seismic stratigraphic approach in Patos Lagoon, Southern Brazil**. Brazilian Journal of Geology, v. 48, p. 533-551.

BOYD, R.; DALRYMPLE, R.; ZAITLIN, B. A. 1992. **Classification of clastic coastal depositional environments**. Sedimentary Geology, v. 80, n. 3-4, p. 139-150.

BRUNO, H., ALMEIDA, J., HEILBRON, M., SALOMÃO, M., & CURY, L. 2018. **Architecture of major precambrian tectonic boundaries in the northern part of the Dom Feliciano Orogen, southern Brazil: Implications for the West Gondwana amalgamation**. Journal of South American Earth Sciences, v. 86, p. 301-317.

CARTELLE, V., GARCÍA-MOREIRAS, I., MARTÍNEZ-CARREÑO, N., SOBRINO, C. M., GARCÍA-GIL, S. 2022. **The role of antecedent morphology and changing sediment sources in the postglacial palaeogeographical evolution of an incised valley: The sedimentary record of the Ría de Arousa (NW Iberia)**. Global and Planetary Change, v. 208, p. 103727.

CARTER, R. W. G.; ORFORD, J. D. 1981. **Overwash processes along a gravel beach in south-east Ireland**. Earth Surface Processes and Landforms, v. 6, n. 5, p. 413-426.

CASTRO, L.G.; FERREIRA, J.F.; ANGULO, R.J. 2008. **Modelo gravimétrico-magnético do gráben de Paranaguá-PR, Brasil**. Revista Brasileira de Geofísica, v. 26, p. 273-292.

CHAUMILLON, E., BERTIN, X., FALCHETTO, H., ALLARD, J., WEBER, N., WALKER, P., POUVREAU, N., WOPPELMANN, G. **2008. Multi time-scale evolution of a wide estuary linear sandbank, the Longe de Boyard, on the French Atlantic coast**. Marine Geology, v. 251, n. 3-4, p. 209-223.

CHAUMILLON, E.; TESSIER, B.; REYNAUD, J.Y. 2010. **Stratigraphic records and variability of incised valleys and estuaries along French coasts**. Bulletin de la Société géologique de France, v. 181, n. 2, p. 75-85.

CHOI, D. L., Shin, D. H., Jin, J. Y., Lee, Y. K., & Kum, B. C. 2020 **High-resolution seismic stratigraphy offshore Haeundae beach in Busan, South Korea**. Journal of Coastal Research, v. 102, n. SI, p. 187-193.

COHEN, M. C., LARA, R. J., BEHLING, H., & ANGULO, R. J**.** 2005. **A model of Holocene mangrove development and relative sea-level changes on the Bragança Peninsula (northern Brazil)**. Wetlands Ecology and Management, v. 13, n. 4, p. 433-443.

COLMAN, S. M.; MIXON, R. B. 1988. **The record of major Quaternary sea-level changes in a large coastal plain estuary, Chesapeake Bay, eastern United States. Palaeogeography, Palaeoclimatology**, Palaeoecology, v. 68, n. 2-4, p. 99-116.

COOPER, J. A. G., GREEN, A. N., MEIRELES, R. P., KLEIN, A. H., SOUZA, J., & TOLDO, E. E. 2016. **Sandy barrier overstepping and preservation linked to rapid sea level rise and geological setting**. Marine Geology, v. 382, p. 80-91.

COOPER, J. A. G., GREEN, A. N., MEIRELES, R., KLEIN, A. H. F., DE ABREU, J. G. N., & TOLDO, E. E. 2019. **Tidal strait to embayment: Seismic stratigraphy and evolution of a rock-bounded embayment in the context of Holocene sea level change**. Marine Geology, v. 415, p. 105972.

COOPER, J. A. G., MEIRELES, R. P., GREEN, A. N., KLEIN, A. H. F., & TOLDO, E. E. 2018. **Late Quaternary stratigraphic evolution of the inner continental shelf in response to sea-level change, Santa Catarina, Brazil**. Marine Geology, v. 397, p. 1-14.

COSTA, W. L.L., SILVEIRA, L. F., KLEIN, A. H.F. 2019. **Influence Of Wave Climate And Tidal Regime On Headland Bypassing-Study Case: Northern São Francisco Do Sul Island, Sc, Brazil**. In: Coastal Sediments 2019: Proceedings of the 9th International Conference. p. 488-501.

CREMER, M. J 2006. O estuário da Baía da Babitonga.In: CREMER, M. J, MORALES, P. R. D., OLIVEIRA, T M. N. **Diagnóstico ambiental da Baía da Babitonga**. Joinville, Editora Univille, p. 15-19

CURY, L. F. 2009. **Geologia do Terreno Paranaguá**. Tese (Doutorado em Geociências) – Curso de Pós-Graduação em Geoquímica e Geotectônica. Universidade de São Paulo, São Paulo. 202p. Available in: https://www.teses.usp.br/teses/disponiveis/44/44141/tde-06072009-113335/publico/LFC.pdf. Acessado em 09 de junho de 2022

DALRYMPLE, R. W.; BOYD, R.; ZAITLIN, B. 1994. A**. History of research, types and internal organisation of incised-valley systems: introduction to the volume**. Society for Sedimentary Geology. Special Publication No. 51, 9 p.

DALRYMPLE, R. W.; ZAITLIN, B. 1994. **A. High-resolution sequence stratigraphy of a complex, incised valley succession, Cobequid Bay—Salmon River estuary, Bay of Fundy, Canada**. Sedimentology, v. 41, n. 6, p. 1069-1091.

DALRYMPLE, R. W.; ZAITLIN, B. A.; BOYD, R. 1992. **Estuarine facies models; conceptual basis and stratigraphic implications.** Journal of Sedimentary Research, v. 62, n. 6, p. 1130-1146.

DE SANTIS, V., CALDARA, M., PENNETTA, L. 2020. "**Continuous" Backstepping of Holocene Coastal Barrier Systems into Incised Valleys: Insights from the Ofanto and Carapelle-Cervaro Valleys**. Water, v. 12, n. 6, p. 1799.

EDGETECH. 2019. **EdgeTech 3200: Portable sub-bottom profiler, EdgeTech**, West Wareham, MA, USA. Available in: https://www.edgetech.com/products/sub-bottom-profiling/3200-high-penetr ation-sub-bottom-profiler/. Accessed: 16, abril de 2022.

FÉLIX, C. A.; MAHIQUES, M. M. 2013. **Late quaternary evolution and shallow gas formation in a tropical estuarine environment: the case of the Bertioga channel, Brazil**. In: 2013 IEEE/OES Acoustics in Underwater Geosciences Symposium. IEEE, p. 1-8.

FERNÁNDEZ, E. A. P., GINSBERG, S. S., ALIOTTA, S**.** 2020. **Seismic stratigraphy of late Neogene-Quaternary units and evolutionary model in the inner sector of Bahia Blanca estuary (Argentina)**. Journal of South American Earth Sciences, v. 104, p. 102793.

FERRER, P., BENABDELLOUAHED, M., CERTAIN, R., TESSIER, B., BARUSSEAU, J. P., & BOUCHETTE, F. 2010. **The Late Holocene sediment infilling and beach barrier dynamics of the Thau lagoon (Gulf of Lions, Mediterranean sea, SE France)**. Bulletin de la Société Géologique de France, v. 181, n. 2, p. 197-209

FITZGERALD, D. M., KULP, M., PENLAND, S., FLOCKS, J., & KINDINGER, J. 2004. **Morphologic and stratigraphic evolution of muddy ebb-tidal deltas along a subsiding coast: Barataria Bay, Mississippi River Delta**. Sedimentology, v. 51, n. 6, p. 1157-1178.

FITZGERALD, D., BUYNEVICH, I.., HEIN, C. 2012. **Morphodynamics and facies architecture of tidal inlets and tidal deltas. In: Principles of tidal sedimentology**. Springer, Dordrecht. p. 301-333.

GHAZI, S., MOUNTNEY, N. P. 2009. **Facies and architectural element analysis of a meandering fluvial succession: The Permian Warchha Sandstone, Salt Range, Pakistan**. Sedimentary Geology, v. 221, n. 1-4, p. 99-126.

GIAGANTE, D. A., ALIOTTA, S., GINSBERG, S. S., VECCHI, L. G., & SPAGNUOLO, J. O. 2011. **Evolution of a coastal alluvial deposit in response to the last Quaternary marine transgression, Bahía Blanca estuary, Argentina**. Quaternary research, v. 75, n. 3, p. 614-623.

GIMENEZ, V. B., SALAMUNI, E., DOS SANTOS, J. M., PEYERL, W. R. L., FARIAS, T. F., & SANCHES, E. 2022. **The role of fault reactivation in the geomorphological evolution of coastal landforms on passive continental margins: Evidence from a tectonic estuary in southern Brazil**. Geomorphology, p. 10813.

GOFF, J. A., REED, A. H., GAWARKIEWICZ, G., WILSON, P. S., & KNOBLES, D. P. 2019. **Stratigraphic analysis of a sediment pond within the New England Mud Patch: New constraints from high-resolution chirp acoustic reflection data**. Marine Geology, v. 412, p. 81-94.

GREEN, A. N., COOPER, J. A. G., LEUCI, R., & THACKERAY, Z. 2013. **Formation and preservation of an overstepped segmented lagoon complex on a high-energy continental shelf**. Sedimentology, v. 60, n. 7, p. 1755-1768.

GREEN, A. N., HUMPHRIES, M. S., COOPER, J. A. G., STRACHAN, K. L., GOMES, M., & DLADLA, N. N. 2022. **The Holocene evolution of Lake St Lucia, Africa's largest estuary: Geological implications for contemporary management**. Estuarine, Coastal and Shelf Science, p. 107745.

HEIN, C. J., FITZGERALD, D. M., CLEARY, W. J., ALBERNAZ, M. B., DE MENEZES, J. T., KLEIN, A. H. D. F. 2013. **Evidence for a transgressive barrier within a regressive strand plain system: Implications for complex coastal response to environmental change**. Sedimentology, v. 60, n. 2, p. 469-502.

HEIN, C. J., FITZGERALD, D. M., DE MENEZES, J. T., CLEARY, W. J., KLEIN, A. H., & ALBERNAZ, M. B. 2014. **Coastal response to late-stage transgression and sea-level highstand**. GSA Bulletin, v. 126, n. 3-4, p. 459-480.

HEIN, C. J., FITZGERALD, D. M., DE SOUZA, L. H., GEORGIOU, I. Y., BUYNEVICH, I. V., KLEIN, A. H. D. F., MENEZES, J.T., CLEARY, W.J. & SCOLARO, T. L. 2016. **Complex coastal change in response to autogenic basin infilling: An example from a sub-tropical Holocene strand plain**. Sedimentology, v. 63, n. 6, p. 1362-1395.

HORN FILHO, N. O., SCHMIDT, A. D., BENEDET, C., NEVES, J., PIMENTA, L. H. F., PAQUETTE, M., ... & SANTOS, C. G. 2014. **Estudo geológico dos depósitos clásticos quaternários superficiais da planície costeira de Santa Catarina, Brasil**. Gravel, v. 12, n. 1, p. 41-107.

IGLESIAS, C. M. D. F., ZERFASS, H., SILVA, M. A. S. D., & KLEIN, C. 2011. **Geologia e recursos minerais da folha Joinville-SG**. 22-ZB: estado de Santa Catarina. CPRM.

JOUET, G., BERNÉ, S., RABINEAU, M., BASSETTI, M. A., BERNIER, P., DENNIELOU, B., ... & TAVIANI, M. 2006. **Shoreface migrations at the shelf edge and sea-level changes around the Last Glacial Maximum (Gulf of Lions, NW Mediterranean).** Marine Geology, v. 234, n. 1-4, p. 21-42.

KELLER, G. V. 1969. **Electrical resistivity measurements, Midway and Kure atolls**. US Govt. Print. Off..

KENCH, P.S. 1990. **Geomorphology of Australian estuaries: review and prospect**. Australian Journal of Ecology, v. 24, n. 4, p. 367-380.

KLEIN, A. H. D. F., SHORT, A. D., & BONETTI, J. 2016b Santa Catarina beach systems. In: **Brazilian Beach Systems**. Springer, Cham, p. 465-506.

KLEIN, A. H. F., DEMARCO, L. F. W., GUESSER, V., FLEMMING, G. R., BONETTI, J., PORPILHO, D., AYRES NETO, A. SOUZA, J. A. G., FÉLIX, C. A. 2016a. **Shallow gas seismic structures: forms and distribution on Santa Catarina Island, Southern Brazil.** Brazilian Journal of Oceanography, v. 64, n. 4, p. 325-338.

LESSA, G. C., ANGULO, R. J., GIANNINI, P. C., & ARAÚJO, A. D. 2000. **Stratigraphy and Holocene evolution of a regressive barrier in south Brazil**. Marine Geology, v. 165, n. 1-4, p. 87-108.

LESSA, G. C., MEYERS, S. R., & MARONE, E. 1998.**Holocene stratigraphy in the Paranagua Bay estuary, southern Brazil.** Journal of Sedimentary Research, v. 68, n. 6, p. 1060-1076.

LESSA, G. C., SANTOS, F. M., SOUZA FILHO, P. W., & CORRÊA-GOMES, L. C. 2018. Brazilian estuaries: a geomorphologic and oceanographic perspective. In: **Brazilian Estuaries**. Springer, Cham, p. 1-37.

LIU, S.; GOFF, J.A. 2018. . **Lower shoreface seismic stratigraphy and morphology off Fire Island, New York: Evidence for lobate progradation and linear erosion**. Continental Shelf Research, v. 163, p. 23-34.

LOTT, S. G., HEIN, C. J., KLEIN, A. H. F., CONNELL, J. E., OLIVEIRA, M. A. T., PINTO, M. W., GALVÃO, W. F. L., **Centennial-scale coastal landform development associated with longshore transport and headland bypassing: São Francisco do Sul Island, Brazil. EP22A**. Online presentation. AGU Fall Meeting, New Orleans, LA. 2021.

MARINO, I. K., SANTOS, M. A. C., & SILVA, C. G. 2013. **Processing of high-resolution, shallow seismic profiles, Guanabara Bay–Rio de Janeiro State, Brazil.** Brazilian Journal of Geophysics, v. 31, n. 4, p. 579-594.

MARTÍNEZ-CARREÑO, N.; GARCÍA-GIL, S. 2017. **Reinterpretation of the Quaternary sedimentary infill of the Ría de Vigo, NW Iberian Peninsula, as a compound incised valley**. Quaternary Science Reviews, v. 173, p. 124-144.

MAZZER, A. M., & GONÇALVES, M. L. 2012. **Aspectos geomorfológicos da baía da Babitonga, Santa Catarina, Brasil: caracterização morfométrica**. Revista Brasileira de Geomorfologia, v. 12.

MITCHUM JR, R. M.; VAIL, P. R.; SANGREE, J. B. 1977. Seismic stratigraphy and global changes of sea level: Part 6. **Stratigraphic interpretation of seismic reflection patterns in depositional sequences: Section 2**. Application of seismic reflection configuration to stratigraphic interpretation.

MULHERN, J S.; JOHNSON, C. L.; GREEN, A. N. 2021. **When is a barrier island not an island? When it is preserved in the rock record**. Frontiers in Earth Science, v. 8, p. 634.

NOERNBERG, M.A.; RODRIGO, P.A.; LUERSEN, D.M. 2020. **Seasonal and fortnightly variability of the hydrodynamic regime at Babitonga Bay, Southern of Brazil**. Regional Studies in Marine Science, v. 40, p. 101518.

NORDFJORD, S., GOFF, J. A., AUSTIN JR, J. A., & GULICK, S. P. S. 2006. **Seismic facies of incised-valley fills, New Jersey continental shelf: implications for erosion and preservation processes acting during latest Pleistocene–Holocene transgression**. Journal of Sedimentary Research, v. 76, n. 12, p. 1284-1303.

OLIVEIRA, T. M. N. de; RIBEIRO, J. M. G.; BARROS, V. G.; SIMM, M.; MELLO, Y. R. de; ZEH, 2017. K. K. **Bacias hidrográficas da região de Joinville: Gestão e dados**. Joinville, Editora Univille, 94 p.

OLIVER, T. S., TAMURA, T., BROOKE, B. P., SHORT, A. D., KINSELA, M. A., WOODROFFE, C. D., THOM, B. G. 2020. **Holocene evolution of the wave-dominated embayed Moruya coastline, southeastern Australia: Sediment sources, transport rates and alongshore interconnectivity**. Quaternary Science Reviews, v. 247, p. 106566.

PARHAM, P. R., RIGGS, S. R., CULVER, S. J., MALLINSON, D. J., & WEHMILLER, J. F. 2007. **Quaternary depositional patterns and sea-level fluctuations, northeastern North Carolina.** Quaternary Research, v. 67, n. 1, p. 83-99.

PASSARELLI, C. R., MCREATH, I., BASEI, M. Â. S., SIGA JR, O., & NETO, M. D. C. C. 2011. **Heterogeneity in syntectonic granitoids emplaced in a major shear zone, southern Brazil**. Journal of South American Earth Sciences, v. 32, n. 4, p. 369-378.

PLETS, R., DIX, J., BASTOS, A., & BEST, A. 2007. **Characterization of buried inundated peat on seismic (Chirp) data, inferred from core information**. Archaeological Prospection, v. 14, n. 4, p. 261-272.

RASMUSSEN, D. J., BITTERMANN, K., BUCHANAN, M. K., KULP, S., STRAUSS, B. H., KOPP, R. E., & OPPENHEIMER, M. 2018. **Extreme sea level implications of 1.5 C, 2.0 C, and 2.5 C temperature stabilization targets in the 21st and 22nd centuries**. Environmental Research Letters, v. 13, n. 3, p. 034040.

RIEU, R., VAN HETEREN, S., VAN DER SPEK, A. J., & DE BOER, P. L. 2005. **Development and preservation of a mid-Holocene tidal-channel network offshore the western Netherlands**. Journal of Sedimentary Research, v. 75, n. 3, p. 409-419.

RODRIGUES, M. L. G., FRANCO, D., & SUGAHARA, S. 2004.**Climatologia de frentes frias no litoral de Santa Catarina**. Revista Brasileira de Geofísica, v. 22, n. 2, p. 135-151.

RONCHI, L., FONTANA, A., CORREGGIARI, A., & ASIOLI, A. 2018. L**ate Quaternary incised and infilled landforms in the shelf of the northern Adriatic Sea (Italy)**. Marine Geology, v. 405, p. 47-67.

RONCHI, L., FONTANA, A., CORREGGIARI, A., & REMIA, A. 2019. **Anatomy of a transgressive tidal inlet reconstructed through high-resolution seismic profiling**. Geomorphology, v. 343, p. 65-80.

ROY, P S. 1994. **Holocene estuary evolution - stratigraphic studies from southeastern Australia**.

SCAVIA, D., FIELD, J. C., BOESCH, D. F., BUDDEMEIER, R. W., BURKETT, V., CAYAN, D. R., ... & TITUS, J. G. 2002. **Climate change impacts on US coastal and marine ecosystems**. Estuaries, v. 25, n. 2, p. 149-164.

SERRA, O. E. 1983. **Fundamentals of well-log interpretation**. Developments in Petroleum Science, 15A.

SHANLEY, K. W.; MCCABE, P. J. 1994. **Perspectives on the sequence stratigraphy of continental strata**. AAPG bulletin, v. 78, n. 4, p. 544-568.

SILVA, A. G. A., STATTEGGER, K., SCHWARZER, K., & VITAL, H. 2016. **Seismic stratigraphy as indicator of late Pleistocene and Holocene sea level changes on the NE Brazilian continental shelf**. Journal of South American Earth Sciences, v. 70, p. 188-197.

SILVEIRA, L., BENEDET, L., SIGNORIN, M., & BONANATA, R; 2012. **Evaluation of the relationships between navigation channel dredging and erosion of adjacent beaches in southern Brazil**. In: Proceedings of the Coastal Engineering Conference. p. 1-15.

SIMIONI, B. I., ANGULO, R. J., VEIGA, F. A., OLIVEIRA, L. H. S., & SOUZA, M. C. D. 2018. **Genesis of submerged sandstones in Paraná State continental shelf, Southern Brazil, based on cementation patterns, ages and stable isotopes**. Brazilian Journal of Oceanography, v. 66, p. 267-282.

SIMMS, A. R., RODRIGUEZ, A. B., & ANDERSON, J. B. 2018. **Bayhead deltas and shorelines: Insights from modern and ancient examples**. Sedimentary Geology, v. 374, p. 17-35.

SLOSS, C. R., JONES, B. G., MCCLENNEN, C. E., CARLI, J., & PRICE, D. M. 2006. **The geomorphological evolution of a wave-dominated barrier estuary: Burrill Lake, New South Wales, Australia**. Sedimentary Geology, v. 187, n. 3-4, p. 229-249.

SOUZA, L. A. P. SBP 3.5, 7, 10 2011. **kHz, Chirp (0.5-2.0 kHz), Chirp (2-12kHz), Chirp (10-18 kHz), Boomer (0.5-2 kHz) e Sparker (0.1-1.0 kHz): Quando Decidir Por Uma Ou Por Outra Fonte Acústica?** In: 12th International Congress of the Brazilian Geophysical Society. 6 p.

SOUZA, L.A.P. 2006. **Revisão Crítica da Aplicabilidade dos Métodos Geofísicos na Investigação de Áreas Submersas Rasas**. Tese (Doutorado em Ciências) – Curso de Pós-Graduação em Ciências, área de Oceanografia Química e Geológica. Universidade de São Paulo, São Paulo. 311p. Available in: https://teses.usp.br/teses/disponiveis/21/21133/tde-30102006-171206/publico/TESE_Laps_2006.pdf. Accessed: 07 de junho de 2022. Unpublished results.

SOUZA, M. C.. 1999. **Mapeamento da planície costeira e morfologia e dinâmica das praias do Município de Itapoá, Estado de Santa Catarina: subsídios à ocupação**. MSc dissertation, Curso de Pós-Graduação em Geologia Ambiental, Departamento de Geologia, Universidade Federal do Paraná, Curitiba. Available in: https://www.acervodigital.ufpr.br/handle/1884/6581. Accessed 09 de julho de 2022. Unpublished results.

SOUZA, M.C.; ANGULO, R.J.; PESSENDA, L.C.R. 2001. **Evolução paleogeográfica da planície costeira de Itapoá, litoral norte de Santa Catarina**. Revista Brasileira de Geociências, v. 31, n. 2, p. 223-230.

TESSON, M. POSAMENTIER, H. GENSOUS, B. 2015. **Compound incised-valley characterization by high-resolution seismics in a wave-dominated setting: example of the Aude and Orb rivers, Languedoc inner shelf, Gulf of Lion, France**. Marine Geology, v. 367, p. 1-21.

TILLMANN, T.; WUNDERLICH, J. 2013. **Barrier rollover and spit accretion due to the combined action of storm surge induced washover events and progradation: Insights from ground-penetrating radar surveys and sedimentological data**. Journal of Coastal Research, n. 65 (10065), p. 600-605.

TRUCCOLO, E. C.; SCHETTINI, C. A. 1999. **Marés astronômicas na baía da Babitonga, SC.** Brazilian Journal of Aquatic Science and Technology, v. 3, n. 1, p. 57-66.

VIEIRA, C. V. 2015. **Evolução paleogeográfica da planície costeira do extremo norte da ilha de São Francisco do Sul, Santa Catarina, Brasil**. 322 p. Tese (Doutorado em Geografia) Universidade Federal de Santa Catarina, Florianópolis. Available in: https://repositorio.ufsc.br/xmlui/handle/123456789/169570. Accessed: 01 de junho de 2022. Unpublished results.

VIEIRA, C. V., & HORN FILHO, N. O. 2012. **Mapeamento geológico costeiro do canal do Palmital, litoral Norte de Santa Catarina**. Geosul, 27(54), 33-54.

VIEIRA, C. V., HORN FILHO, N. O. 2017. **Paisagem marinha da baía da Babitonga, nordeste do Estado de Santa Catarina**. Revista Brasileira de Geografia Física, v. 10, n. 05, p. 1677-1689.

VIEIRA, C. V., HORN FILHO, N. O., BONETTI, C. V. D. H. C., & BONETTI, J. 2008. **Caracterização morfosedimentar e setorização do complexo estuarino da Baía da Babitonga/SC**. Boletim Paranaense de Geociências, v. 62.

WANG, R., COLOMBERA, L., & MOUNTNEY, N. P. 2020. **Quantitative analysis of the stratigraphic architecture of incised-valley fills: a global comparison of Quaternary systems**. Earth-Science Reviews, v. 200, p. 102988.

WEBER, N., CHAUMILLON, E., TESSON, M., & GARLAN, T. 2004. **Architecture and morphology of the outer segment of a mixed tide and wave-dominated-incised valley, revealed by HR seismic reflection profiling: the paleo-Charente River, France**. Marine Geology, v. 207, n. 1-4, p. 17-38.

WESCHENFELDER, J., BAITELLI, R., CORRÊA, I. C., BORTOLIN, E. C., & SANTOS, C. B. 2014. **Quaternary incised valleys in southern Brazil coastal zone**. Journal of South American Earth Sciences, v. 55, p. 83-93.

WOODROFFE, C. D.; MULRENNAN, M. E.; CHAPPELL, J. 1993. **Estuarine infill and coastal progradation, southern van Diemen Gulf, northern Australia**. Sedimentary Geology, v. 83, n. 3-4, p. 257-275.

YOO, D. G., HONG, S. H., LEE, G. S., KIM, J. C., YOON, H. H., & CHEONG, D. 2020. **Stratigraphic evolution of the Nakdong River valley in response to late Quaternary sea-level changes**. Marine Geology, v. 427, p. 106243.

ZĂINESCU, F. I., VESPREMEANU-STROE, A., TĂTUI, F. 2019. **The formation and closure of the Big Breach of Sacalin spit associated with extreme shoreline retreat and shoreface erosion**. Earth Surface Processes and Landforms, v. 44, n. 11, p. 2268-2284.

ZAITLIN, B. A.; DALRYMPLE, R. W.; BOYD, R. O. N. 1994. **The stratigraphic organization of incised-valley systems associated with relative sea-level change**. Society for Sedimentary Geology. Special Publication, No. 51, 16 p.

ZAREMBA, N., MALLINSON, D. J., LEORRI, E., CULVER, S., RIGGS, S., MULLIGAN, R., HORSMAN, E., MITRA, S. 2016. **Controls on the stratigraphic framework and paleoenvironmental change within a Holocene estuarine system: Pamlico Sound, North Carolina, USA**. Marine Geology, v. 379, p. 109-123.

ZULAR, A., SAWAKUCHI, A. O., GUEDES, C. C., MENDES, V. R., NASCIMENTO JR, D. R., GIANNINI, P. C., GIANINI, V. A. P. & DeWitt, R. 2013. **Late**

Holocene intensification of colds fronts in southern Brazil as indicated by dune development and provenance changes in the São Francisco do Sul coastal barrier. Marine Geology, v. 335, p. 64-77.

3 CONSIDERAÇÕES FINAIS E RECOMENDAÇÕES PARA FUTUROS TRABALHOS

O presente trabalho aborda a evolução geológica da Baía da Babitonga através de dados de sísmica 2D de ultra alta resolução (CHIRP), descrevendo os detalhes dos depósitos da última transgressão marinha até presente. As peculiaridades do pacote sedimentar anterior a esse período é desconhecido, por limitações do método. Para essa investigação, dados de sísmica 2D de alta resolução (BOOMER), seriam necessários.

Para complementar a análise apresentada, o Canal do Linguado e sua foz poderiam ser investigados. Assim, a evolução nessa região pode ser mais detalhada. Com o fechamento do Canal do Linguado em 1935, o padrão sedimentar entre o fechamento e o mar se alterou, causando mudanças morfológicas na região. Tais mudanças poderiam ser investigadas para estudo de evolução costeira mediante intervenção humana.

O modelo geológico proposto pode ser ampliado para a plataforma interna adjacente com dados sísmicos que permitam a observação dos paleocanais que ali percorriam durante o Último Máximo Glacial. Caso tais dados se estendam sobre a planície costeira da região, um modelo evolutivo regional também pode ser desenvolvido.

4 CONTRIBUIÇÕES CIENTÍFICAS

As principais contribuições científicas durante o desenvolvimento deste trabalho são:

(1) O estuário tectônico denominado Baía da Babitonga se encontra sobre dois vales tectônicos. Essa configuração geológica ocorria quando o nível do mar estava cerca de 10m abaixo do atual, durante o fim da transgressão pleistocênica;

(2) Durante a última transgressão marinha, sistemas de barreiras costeiras foram transpostas (*overstepping*), os estuários transladaram (*rollover*) em direção ao continente e os vales tectônicos se uniram, formando a Baía da Babitonga;

(3) A composição sedimentar na Baía da Babitonga foi alterada durante a regressão marinha, conforme as assinaturas de susceptibilidade magnética e radiação natural dos sedimentos mostram.

(4) Os depósitos sedimentares regressivos na Baía da Babitonga obstruem a passagem de gás formado em camadas sedimentares mais antigas, formando bolsões de gás na Baía da Babitonga.

REFERÊNCIAS

ALLARD, J., CHAUMILLON, E., BERTIN, X., POIRIER, C., & GANTHY, F. **Sedimentary record of environmental changes and human interferences in a macrotidal bay for the last millenaries: the Marennes-Oléron Bay (SW France)**. Bulletin de la Société Géologique de France, v. 181, n. 2, p. 151-169, 2010.

ALVES, J. H. G. D. M**. Refração do espectro de ondas oceânicas em águas rasas: Aplicações à região costeira de São Francisco do Sul, SC**. Tese (Dissertação em Engenharia Ambiental) - Programa de Pós-Graduação em Engenharia Ambiental. Universidade Federal de Santa Catarina, Florianópolis. 107p, 1996.

ANDRADE, J.F.P.; NOERNBERG, M. A.; NAGAI, R. H. **Shallow gas high-resolution seismic signatures in a subtropical estuary**. Geo-Marine Letters, v. 41, n. 3, p. 1-14, 2021.

ANGULO, R. J., PESSENDA, L. C. R., & SOUZA, M. D.. **O significado das datações ao 14C na reconstrução de paleoníveis marinhos e na evolução das barreiras quaternárias do litoral paranaense**. Revista Brasileira de Geociências, v. 32, n. 1, p. 95-106, 2002.

ANGULO, R.J.; SOUZA, M.C. **Mapa Geológico da planície costeira entre o rio Saí-Guaçu e a Baía de São Francisco, litoral norte do estado de Santa Catarina**. Boletim Paranaense de Geociências, v. 55, 2004.

ANGULO, R. J., DE SOUZA, M. C., ASSINE, M. L., PESSENDA, L. C. R., & DISARÓ, S. T. **Chronostratigraphy and radiocarbon age inversion in the Holocene regressive barrier of Paraná, southern Brazil**. Marine Geology, v. 252, n. 3-4, p. 111-119, 2008.

ANGULO, R.J.; SOUZA, M.C.; LESSA, G.C. **The Holocene barrier systems of Paranaguá and northern Santa Catarina coasts, southern Brazil**. In: Geology and geomorphology of Holocene coastal barriers of Brazil. Springer, Berlin, Heidelberg, 2009. p. 135-176.

AYRES NETO, A. **Uso da sísmica de reflexão de alta resolução e da sonografia na exploração mineral submarina**. Brazilian Journal of Geophysics, v. 18, n. 3, 2000.

BALTZER, A., TESSIER, B., NOUZE, H., BATES, R., MOORE, C., & MENIER, D. **Seistec seismic profiles: a tool to differentiate gas signatures**. Marine Geophysical Researches, v. 26, n. 2, p. 235-245, 2005.

BARBOSA, C F.; SUGUIO, K. **Biosedimentary facies of a subtropical microtidal estuary; an example from southern Brazil**. Journal of sedimentary research, v. 69, n. 3, p. 576-587, 1999.

BARBOZA, E. G., DILLENBURG, S. R., LOPES, R. P., ROSA, M. L. C., CARON, F., ABREU, V., ... & TOMAZELLI, L. J. **Geomorphological and stratigraphic evolution of a fluvial incision in the coastal plain and inner continental shelf in southern Brazil**. Marine Geology, v. 437, p. 106514, 2021.

BASTOS, A. C., VILELA, C. G., QUARESMA, V. S., & ALMEIDA, F. K. **Mid-to Late-Holocene estuarine infilling processes studied by radiocarbon dates, high resolution seismic and biofacies at Vitoria Bay, Espírito Santo, Southeastern Brazil**. Anais da Academia Brasileira de Ciências, v. 82, n. 3, p. 761-770, 2010.

BLUM, P., 1997, **Physical properties handbook: a guide to the shipboard measurement of physical properties of deep-sea cores**. Available from: http://www-odp.tamu.edu/publications/tnotes/tn26/CHAP6.PDF.HTM. Acessado em 07 de julho de 2022.

BOGO, M., SOUZA, M.C., ANGULO, R.J.L BARBOSA, E.G. & ROSA, M.L.C.C. **Arquitetura deposicional da barreira holocênica na porção meridional da Ilha de São Francisco do Sul, SC, Brasil**. Pesquisas em Geociências, v. 42, n. 3, p. 281-295, 2015.

BORTOLIN, E. C., WESCHENFELDER, J., & COOPER, A. **Incised valley paleoenvironments interpreted by seismic stratigraphic approach in Patos Lagoon, Southern Brazil**. Brazilian Journal of Geology, v. 48, p. 533-551, 2018.

BOYD, R.; DALRYMPLE, R.; ZAITLIN, B. A. **Classification of clastic coastal depositional environments**. Sedimentary Geology, v. 80, n. 3-4, p. 139-150, 1992.

BRUNO, H., ALMEIDA, J., HEILBRON, M., SALOMÃO, M., & CURY, L. **Architecture of major precambrian tectonic boundaries in the northern part of the Dom Feliciano Orogen, southern Brazil: Implications for the West Gondwana amalgamation**. Journal of South American Earth Sciences, v. 86, p. 301-317, 2018.

CARTELLE, V., GARCÍA-MOREIRAS, I., MARTÍNEZ-CARREÑO, N., SOBRINO, C. M., GARCÍA-GIL, S. **The role of antecedent morphology and changing sediment sources in the postglacial palaeogeographical evolution of an incised valley: The sedimentary record of the Ría de Arousa (NW Iberia)**. Global and Planetary Change, v. 208, p. 103727, 2022.

CARTER, R. W. G.; ORFORD, J. D. **Overwash processes along a gravel beach in south-east Ireland**. Earth Surface Processes and Landforms, v. 6, n. 5, p. 413-426, 1981.

CASTRO, L.G.; FERREIRA, J.F.; ANGULO, R.J. **Modelo gravimétrico-magnético do gráben de Paranaguá-PR, Brasil**. Revista Brasileira de Geofísica, v. 26, p. 273-292, 2008.

CHAUMILLON, E., BERTIN, X., FALCHETTO, H., ALLARD, J., WEBER, N., WALKER, P., POUVREAU, N., WOPPELMANN, G. **Multi time-scale evolution of a wide estuary linear sandbank, the Longe de Boyard, on the French Atlantic coast**. Marine Geology, v. 251, n. 3-4, p. 209-223, 2008.

CHAUMILLON, E.; TESSIER, B.; REYNAUD, J.Y. **Stratigraphic records and variability of incised valleys and estuaries along French coasts**. Bulletin de la Société géologique de France, v. 181, n. 2, p. 75-85, 2010.

CHOI, D. L., Shin, D. H., Jin, J. Y., Lee, Y. K., & Kum, B. C.. **High-resolution seismic stratigraphy offshore Haeundae beach in Busan, South Korea**. Journal of Coastal Research, v. 102, n. SI, p. 187-193, 2020.

COHEN, M. C., LARA, R. J., BEHLING, H., & ANGULO, R. J**. A model of Holocene mangrove development and relative sea-level changes on the Bragança Peninsula (northern Brazil)**. Wetlands Ecology and Management, v. 13, n. 4, p. 433-443, 2005.

COLMAN, S. M.; MIXON, R. B. **The record of major Quaternary sea-level changes in a large coastal plain estuary, Chesapeake Bay, eastern United States**. Palaeogeography, Palaeoclimatology, Palaeoecology, v. 68, n. 2-4, p. 99-116, 1988.

COOPER, J. A. G., GREEN, A. N., MEIRELES, R. P., KLEIN, A. H., SOUZA, J., & TOLDO, E. E. **Sandy barrier overstepping and preservation linked to rapid sea level rise and geological setting**. Marine Geology, v. 382, p. 80-91, 2016.

COOPER, J. A. G., MEIRELES, R. P., GREEN, A. N., KLEIN, A. H. F., & TOLDO, E. E. **Late Quaternary stratigraphic evolution of the inner continental shelf in response to sea-level change, Santa Catarina, Brazil**. Marine Geology, v. 397, p. 1-14, 2018.

COOPER, J. A. G., GREEN, A. N., MEIRELES, R., KLEIN, A. H. F., DE ABREU, J. G. N., & TOLDO, E. E. **Tidal strait to embayment: Seismic stratigraphy and evolution of a rock-bounded embayment in the context of Holocene sea level change**. Marine Geology, v. 415, p. 105972, 2019.

CREMER, M. J. O estuário da Baía da Babitonga.In: CREMER, M. J, MORALES, P. R. D., OLIVEIRA, T M. N. **Diagnóstico ambiental da Baía da Babitonga**. Joinville, Editora Univille, p. 15-19, 2006.

COSTA, W.L.L.; SILVEIRA, L. F.; KLEIN, A.H.F. **Influence of wave climate and tidal regime on headland bypassing-study case: northern São Francisco do Sul Island**, SC, Brazil. 2019

CURY, L. F. **Geologia do Terreno Paranaguá**. Tese (Doutorado em Geociências) – Curso de Pós-Graduação em Geoquímica e Geotectônica. Universidade de São Paulo, São Paulo. 202p, 2009. Disponível em: https://www.teses.usp.br/teses/disponiveis/44/44141/tde-06072009-113335/publico/LFC.pdf. Acessado em 09 de junho de 2022

DALRYMPLE, R. W.; BOYD, R.; ZAITLIN, B. A**. History of research, types and internal organisation of incised-valley systems: introduction to the volume**. Society for Sedimentary Geology. Special Publication No. 51, 9 p., 1994.

DALRYMPLE, R. W.; ZAITLIN, B. A. **High-resolution sequence stratigraphy of a complex, incised valley succession, Cobequid Bay—Salmon River estuary, Bay of Fundy, Canada**. Sedimentology, v. 41, n. 6, p. 1069-1091, 1994.

DALRYMPLE, R. W.; ZAITLIN, B. A.; BOYD, R. **Estuarine facies models; conceptual basis and stratigraphic implications.** Journal of Sedimentary Research, v. 62, n. 6, p. 1130-1146, 1992.

DE SANTIS, V., CALDARA, M., PENNETTA, L. **"Continuous" Backstepping of Holocene Coastal Barrier Systems into Incised Valleys: Insights from the Ofanto and Carapelle-Cervaro Valleys**. Water, v. 12, n. 6, p. 1799, 2020.

EDGETECH. **EdgeTech 3200: Portable sub-bottom profiler, EdgeTech**, West Wareham, MA, USA, 2019. Disponível em: https://www.edgetech.com/products/sub-bottom-profiling/3200-high-penetr ation-sub-bottom-profiler/. Acesso em: 16, abril de 2022.

FÉLIX, C. A.; MAHIQUES, M. M. **Late quaternary evolution and shallow gas formation in a tropical estuarine environment: the case of the Bertioga channel, Brazil**. In: 2013 IEEE/OES Acoustics in Underwater Geosciences Symposium. IEEE, 2013. p. 1-8.

FERNÁNDEZ, E. A. P., GINSBERG, S. S., ALIOTTA, S. **Seismic stratigraphy of late Neogene-Quaternary units and evolutionary model in the inner sector of Bahia Blanca estuary (Argentina)**. Journal of South American Earth Sciences, v. 104, p. 102793, 2020.

FERRER, P., BENABDELLOUAHED, M., CERTAIN, R., TESSIER, B., BARUSSEAU, J. P., & BOUCHETTE, F. **The Late Holocene sediment infilling and beach barrier dynamics of the Thau lagoon (Gulf of Lions, Mediterranean sea, SE France)**. Bulletin de la Société Géologique de France, v. 181, n. 2, p. 197-209, 2010.

FITZGERALD, D. M., KULP, M., PENLAND, S., FLOCKS, J., & KINDINGER, J. **Morphologic and stratigraphic evolution of muddy ebb-tidal deltas along a subsiding**

coast: Barataria Bay, Mississippi River Delta. Sedimentology, v. 51, n. 6, p. 1157-1178, 2004.

FITZGERALD, D., BUYNEVICH, I.., HEIN, C**. Morphodynamics and facies architecture of tidal inlets and tidal deltas. In: Principles of tidal sedimentology**. Springer, Dordrecht, 2012. p. 301-333.

GHAZI, S., MOUNTNEY, N. P. **Facies and architectural element analysis of a meandering fluvial succession: The Permian Warchha Sandstone, Salt Range, Pakistan**. Sedimentary Geology, v. 221, n. 1-4, p. 99-126, 2009.

GIAGANTE, D. A., ALIOTTA, S., GINSBERG, S. S., VECCHI, L. G., & SPAGNUOLO, J. O. **Evolution of a coastal alluvial deposit in response to the last Quaternary marine transgression, Bahía Blanca estuary, Argentina**. Quaternary research, v. 75, n. 3, p. 614-623, 2011.

GIMENEZ, V. B., SALAMUNI, E., DOS SANTOS, J. M., PEYERL, W. R. L., FARIAS, T. F., & SANCHES, E. **The role of fault reactivation in the geomorphological evolution of coastal landforms on passive continental margins: Evidence from a tectonic estuary in southern Brazil**. Geomorphology, p. 108132, 2022.

GREEN, A. N., COOPER, J. A. G., LEUCI, R., & THACKERAY, Z.. **Formation and preservation of an overstepped segmented lagoon complex on a high-energy continental shelf**. Sedimentology, v. 60, n. 7, p. 1755-1768, 2013.

PARHAM, P. R., RIGGS, S. R., CULVER, S. J., MALLINSON, D. J., & WEHMILLER, J. F. **Quaternary depositional patterns and sea-level fluctuations, northeastern North Carolina.** Quaternary Research, v. 67, n. 1, p. 83-99, 2007.

GREEN, A. N., HUMPHRIES, M. S., COOPER, J. A. G., STRACHAN, K. L., GOMES, M., & DLADLA, N. N. **The Holocene evolution of Lake St Lucia, Africa's largest estuary: Geological implications for contemporary management**. Estuarine, Coastal and Shelf Science, p. 107745, 2022.

GOFF, J. A., REED, A. H., GAWARKIEWICZ, G., WILSON, P. S., & KNOBLES, D. P. **Stratigraphic analysis of a sediment pond within the New England Mud Patch: New constraints from high-resolution chirp acoustic reflection data**. Marine Geology, v. 412, p. 81-94, 2019.

HEIN, C. J., FITZGERALD, D. M., CLEARY, W. J., ALBERNAZ, M. B., DE MENEZES, J. T., KLEIN, A. H. D. F. **Evidence for a transgressive barrier within a regressive strand plain system: Implications for complex coastal response to environmental change**. Sedimentology, v. 60, n. 2, p. 469-502, 2013.

HEIN, C. J., FITZGERALD, D. M., DE SOUZA, L. H., GEORGIOU, I. Y., BUYNEVICH, I. V., KLEIN, A. H. D. F., MENEZES, J.T., CLEARY, W.J. & SCOLARO, T. L. **Complex coastal change in response to autogenic basin infilling: An example from a sub-tropical Holocene strand plain**. Sedimentology, v. 63, n. 6, p. 1362-1395, 2016.

HORN FILHO, N. O., SCHMIDT, A. D., BENEDET, C., NEVES, J., PIMENTA, L. H. F., PAQUETTE, M., ... & SANTOS, C. G. **Estudo geológico dos depósitos clásticos quaternários superficiais da planície costeira de Santa Catarina, Brasil**. Gravel, v. 12, n. 1, p. 41-107, 2014.

IGLESIAS, C. M. D. F., ZERFASS, H., SILVA, M. A. S. D., & KLEIN, C. **Geologia e recursos minerais da folha Joinville-SG. 22-ZB: estado de Santa Catarina**. CPRM, 2011.

JOUET, G., BERNÉ, S., RABINEAU, M., BASSETTI, M. A., BERNIER, P., DENNIELOU, B., ... & TAVIANI, M. **Shoreface migrations at the shelf edge and sea-level changes around the Last Glacial Maximum (Gulf of Lions, NW Mediterranean).** Marine Geology, v. 234, n. 1-4, p. 21-42, 2006.

KELLER, G. V. **Electrical resistivity measurements, Midway and Kure atolls**. US Govt. Print. Off. 1969.

KENCH, P.S. **Geomorphology of Australian estuaries: review and prospect**. Australian Journal of Ecology, v. 24, n. 4, p. 367-380, 1999.

KLEIN, A. H. F., DEMARCO, L. F. W., GUESSER, V., FLEMMING, G. R., BONETTI, J., PORPILHO, D., AYRES NETO, A. SOUZA, J. A. G., FÉLIX, C. A. **Shallow gas seismic structures: forms and distribution on Santa Catarina Island, Southern Brazil.** Brazilian Journal of Oceanography, v. 64, n. 4, p. 325-338, 2016a.

KLEIN, A. H. D. F., SHORT, A. D., & BONETTI, J. Santa Catarina beach systems. In: **Brazilian Beach Systems**. Springer, Cham, p. 465-506 2016b.

LESSA, G. C., MEYERS, S. R., & MARONE, E.**Holocene stratigraphy in the Paranagua Bay estuary, southern Brazil.** Journal of Sedimentary Research, v. 68, n. 6, p. 1060-1076, 1998.

LESSA, G. C., SANTOS, F. M., SOUZA FILHO, P. W., & CORRÊA-GOMES, L. C. Brazilian estuaries: a geomorphologic and oceanographic perspective. In: **Brazilian Estuaries**. Springer, Cham, p. 1-37. 2018

LESSA, G. C., ANGULO, R. J., GIANNINI, P. C., & ARAÚJO, A. D. **Stratigraphy and Holocene evolution of a regressive barrier in south Brazil**. Marine Geology, v. 165, n. 1-4, p. 87-108, 2000.

LIU, S.; GOFF, J.A. **Lower shoreface seismic stratigraphy and morphology off Fire Island, New York: Evidence for lobate progradation and linear erosion**. Continental Shelf Research, v. 163, p. 23-34, 2018.

LOTT, S. G., HEIN, C. J., KLEIN, A. H. F., CONNELL, J. E., OLIVEIRA, M. A. T., PINTO, M. W., GALVÃO, W. F. L., **Centennial-scale coastal landform development associated with longshore transport and headland bypassing: São Francisco do Sul Island, Brazil**. EP22A. AGU Fall Meeting, New Orleans, LA. 2021.

MARINO, I. K., SANTOS, M. A. C., & SILVA, C. G. **Processing of high-resolution, shallow seismic profiles, Guanabara Bay–Rio de Janeiro State, Brazil.** Brazilian Journal of Geophysics, v. 31, n. 4, p. 579-594, 2013.

MARTÍNEZ-CARREÑO, N.; GARCÍA-GIL, S. **Reinterpretation of the Quaternary sedimentary infill of the Ría de Vigo, NW Iberian Peninsula, as a compound incised valley**. Quaternary Science Reviews, v. 173, p. 124-144, 2017.

MAZZER, A. M., & GONÇALVES, M. L. **Aspectos geomorfológicos da baía da Babitonga, Santa Catarina, Brasil: caracterização morfométrica**. Revista Brasileira de Geomorfologia, v. 12, 2012.

MITCHUM JR, R. M.; VAIL, P. R.; SANGREE, J. B. **Seismic stratigraphy and global changes of sea level: Part 6. Stratigraphic interpretation of seismic reflection patterns in depositional sequences: Section 2**. Application of seismic reflection configuration to stratigraphic interpretation. 1977.

MULHERN, J S.; JOHNSON, C. L.; GREEN, A. N. **When is a barrier island not an island? When it is preserved in the rock record**. Frontiers in Earth Science, v. 8, p. 634, 2021.

NOERNBERG, M.A.; RODRIGO, P.A.; LUERSEN, D.M. **Seasonal and fortnightly variability of the hydrodynamic regime at Babitonga Bay, Southern of Brazil**. Regional Studies in Marine Science, v. 40, p. 101518, 2020.

NORDFJORD, S., GOFF, J. A., AUSTIN JR, J. A., & GULICK, S. P. S. **Seismic facies of incised-valley fills, New Jersey continental shelf: implications for erosion and preservation processes acting during latest Pleistocene–Holocene transgression**. Journal of Sedimentary Research, v. 76, n. 12, p. 1284-1303, 2006.

OLIVEIRA, T. M. N. de; RIBEIRO, J. M. G.; BARROS, V. G.; SIMM, M.; MELLO, Y. R. de; ZEH, K. K. **Bacias hidrográficas da região de Joinville: Gestão e dados**. Joinville, Editora Univille, 94 p. 2017.

OLIVER, T. S., TAMURA, T., BROOKE, B. P., SHORT, A. D., KINSELA, M. A., WOODROFFE, C. D., THOM, B. G. **Holocene evolution of the wave-dominated embayed Moruya coastline, southeastern Australia: Sediment sources, transport rates and alongshore interconnectivity**. Quaternary Science Reviews, v. 247, p. 106566, 2020.

PASSARELLI, C. R., MCREATH, I., BASEI, M. Â. S., SIGA JR, O., & NETO, M. D. C. C. **Heterogeneity in syntectonic granitoids emplaced in a major shear zone, southern Brazil**. Journal of South American Earth Sciences, v. 32, n. 4, p. 369-378, 2011.

PLETS, R., DIX, J., BASTOS, A., & BEST, A. **Characterization of buried inundated peat on seismic (Chirp) data, inferred from core information**. Archaeological Prospection, v. 14, n. 4, p. 261-272, 2007.

RASMUSSEN, D. J., BITTERMANN, K., BUCHANAN, M. K., KULP, S., STRAUSS, B. H., KOPP, R. E., & OPPENHEIMER, M. **Extreme sea level implications of 1.5 C, 2.0 C, and 2.5 C temperature stabilization targets in the 21st and 22nd centuries**. Environmental Research Letters, v. 13, n. 3, p. 034040, 2018.

RIEU, R., VAN HETEREN, S., VAN DER SPEK, A. J., & DE BOER, P. L. **Development and preservation of a mid-Holocene tidal-channel network offshore the western Netherlands**. Journal of Sedimentary Research, v. 75, n. 3, p. 409-419, 2005.

RODRIGUES, M. L. G., FRANCO, D., & SUGAHARA, S. **Climatologia de frentes frias no litoral de Santa Catarina**. Revista Brasileira de Geofísica, v. 22, n. 2, p. 135-151, 2004.

RONCHI, L., FONTANA, A., CORREGGIARI, A., & ASIOLI, A. L**ate Quaternary incised and infilled landforms in the shelf of the northern Adriatic Sea (Italy)**. Marine Geology, v. 405, p. 47-67, 2018.

RONCHI, L., FONTANA, A., CORREGGIARI, A., & REMIA, A. **Anatomy of a transgressive tidal inlet reconstructed through high-resolution seismic profiling**. Geomorphology, v. 343, p. 65-80, 2019.

ROY, Peter S. **Holocene estuary evolution - stratigraphic studies from southeastern Australia**. 1994.

SERRA, O. E. **Fundamentals of well-log interpretation**. Developments in Petroleum Science, 15A. 1983.

SCAVIA, D., FIELD, J. C., BOESCH, D. F., BUDDEMEIER, R. W., BURKETT, V., CAYAN, D. R., ... & TITUS, J. G. **Climate change impacts on US coastal and marine ecosystems**. Estuaries, v. 25, n. 2, p. 149-164, 2002.

SHANLEY, K. W.; MCCABE, P. J. **Perspectives on the sequence stratigraphy of continental strata**. AAPG bulletin, v. 78, n. 4, p. 544-568, 1994.

SILVEIRA, L., BENEDET, L., SIGNORIN, M., & BONANATA, R. **Evaluation of the relationships between navigation channel dredging and erosion of adjacent beaches in southern Brazil**. In: Proceedings of the Coastal Engineering Conference. 2012. p. 1-15.

SILVA, A. G. A., STATTEGGER, K., SCHWARZER, K., & VITAL, H. **Seismic stratigraphy as indicator of late Pleistocene and Holocene sea level changes on the NE Brazilian continental shelf**. Journal of South American Earth Sciences, v. 70, p. 188-197, 2016.

SIMIONI, B. I., ANGULO, R. J., VEIGA, F. A., OLIVEIRA, L. H. S., & SOUZA, M. C. D. **Genesis of submerged sandstones in Paraná State continental shelf, Southern Brazil, based on cementation patterns, ages and stable isotopes**. Brazilian Journal of Oceanography, v. 66, p. 267-282, 2018.

SIMMS, A. R., RODRIGUEZ, A. B., & ANDERSON, J. B. **Bayhead deltas and shorelines: Insights from modern and ancient examples**. Sedimentary Geology, v. 374, p. 17-35, 2018.

SLOSS, C. R., JONES, B. G., MCCLENNEN, C. E., CARLI, J., & PRICE, D. M. **The geomorphological evolution of a wave-dominated barrier estuary: Burrill Lake, New South Wales, Australia**. Sedimentary Geology, v. 187, n. 3-4, p. 229-249, 2006.

SOUZA, M. C.**. Mapeamento da planície costeira e morfologia e dinâmica das praias do Município de Itapoá, Estado de Santa Catarina: subsídios à ocupação**. Unpublished MSc dissertation, Curso de Pós-Graduação em Geologia Ambiental, Departamento de Geologia, Universidade Federal do Paraná, Curitiba, 1999. Disponível em: https://www.acervodigital.ufpr.br/handle/1884/6581. Acesso em 09 de julho de 2022.

SOUZA, L. A. P. **SBP 3.5, 7, 10kHz, Chirp (0.5-2.0 kHz), Chirp (2-12kHz), Chirp (10-18 kHz), Boomer (0.5-2 kHz) e Sparker (0.1-1.0 kHz): Quando Decidir Por Uma Ou Por Outra Fonte Acústica?** In: 12th International Congress of the Brazilian Geophysical Society. 6 p, 2011.

SOUZA, L.A.P. **Revisão Crítica da Aplicabilidade dos Métodos Geofísicos na Investigação de Áreas Submersas Rasas**. Tese (Doutorado em Ciências) – Curso de Pós-Graduação em Ciências, área de Oceanografia Química e Geológica. Universidade de São Paulo, São Paulo. 311p, 2006. Disponível em: https://teses.usp.br/teses/disponiveis/21/21133/tde-30102006-171206/publico/TESE_Laps_2006.pdf. Acesso em: 07 de junho de 2022.

SOUZA, M.C.; ANGULO, R.J.; PESSENDA, L.C.R. **Evolução paleogeográfica da planície costeira de Itapoá, litoral norte de Santa Catarina**. Revista Brasileira de Geociências, v. 31, n. 2, p. 223-230, 2001.

TILLMANN, T.; WUNDERLICH, J. **Barrier rollover and spit accretion due to the combined action of storm surge induced washover events and progradation: Insights from ground-penetrating radar surveys and sedimentological data**. Journal of Coastal Research, n. 65 (10065), p. 600-605, 2013.

TRUCCOLO, E. C.; SCHETTINI, C. A. **Marés astronômicas na baía da Babitonga, SC.** Brazilian Journal of Aquatic Science and Technology, v. 3, n. 1, p. 57-66, 1999.

TESSON, M. POSAMENTIER, H. GENSOUS, B. **Compound incised-valley characterization by high-resolution seismics in a wave-dominated setting: example of the Aude and Orb rivers**, Languedoc inner shelf, Gulf of Lion, France. Marine Geology, v. 367, p. 1-21, 2015.

VIEIRA, C. V. **Evolução paleogeográfica da planície costeira do extremo norte da ilha de São Francisco do Sul, Santa Catarina, Brasil**. 322 f. 2015. Tese (Doutorado em Geografia) Universidade Federal de Santa Catarina, Florianópolis. Disponível em: https://repositorio.ufsc.br/xmlui/handle/123456789/169570. Acesso em: 01 de junho de 2022.

VIEIRA, C. V., & HORN FILHO, N. O. **Mapeamento geológico costeiro do canal do Palmital, litoral Norte de Santa Catarina**. Geosul, 27(54), 33-54. 2012.

VIEIRA, C. V., HORN FILHO, N. O., BONETTI, C. V. D. H. C., & BONETTI, J. **Caracterização morfosedimentar e setorização do complexo estuarino da Baía da Babitonga/SC**. Boletim Paranaense de Geociências, v. 62, 2008.

VIEIRA, C. V., HORN FILHO, N. **O. Paisagem marinha da baía da Babitonga, nordeste do Estado de Santa Catarina**. Revista Brasileira de Geografia Física, v. 10, n. 05, p. 1677-1689, 2017.

WANG, R., COLOMBERA, L., & MOUNTNEY, N. P. **Quantitative analysis of the stratigraphic architecture of incised-valley fills: a global comparison of Quaternary systems**. Earth-Science Reviews, v. 200, p. 102988, 2020.

WEBER, N., CHAUMILLON, E., TESSON, M., & GARLAN, T. **Architecture and morphology of the outer segment of a mixed tide and wave-dominated-incised valley, revealed by HR seismic reflection profiling: the paleo-Charente River, France**. Marine Geology, v. 207, n. 1-4, p. 17-38, 2004.

WESCHENFELDER, J., BAITELLI, R., CORRÊA, I. C., BORTOLIN, E. C., & SANTOS, C. B**. Quaternary incised valleys in southern Brazil coastal zone**. Journal of South American Earth Sciences, v. 55, p. 83-93, 2014.

WOODROFFE, C. D.; MULRENNAN, M. E.; CHAPPELL, J. **Estuarine infill and coastal progradation, southern van Diemen Gulf, northern Australia**. Sedimentary Geology, v. 83, n. 3-4, p. 257-275, 1993.

YOO, D. G., HONG, S. H., LEE, G. S., KIM, J. C., YOON, H. H., & CHEONG, D. **Stratigraphic evolution of the Nakdong River valley in response to late Quaternary sea-level changes**. Marine Geology, v. 427, p. 106243, 2020.

ZĂINESCU, F. I., VESPREMEANU-STROE, A., TĂTUI, F. **The formation and closure of the Big Breach of Sacalin spit associated with extreme shoreline retreat and shoreface erosion**. Earth Surface Processes and Landforms, v. 44, n. 11, p. 2268-2284, 2019.

ZAITLIN, B. A.; DALRYMPLE, R. W.; BOYD, R. O. N. **The stratigraphic organization of incised-valley systems associated with relative sea-level change**. Society for Sedimentary Geology. Special Publication, No. 51, 16 p., 1994.

ZAREMBA, N., MALLINSON, D. J., LEORRI, E., CULVER, S., RIGGS, S., MULLIGAN, R., HORSMAN, E., MITRA, S. **Controls on the stratigraphic framework and paleoenvironmental change within a Holocene estuarine system: Pamlico Sound, North Carolina, USA**. Marine Geology, v. 379, p. 109-123, 2016.

ZULAR, A., SAWAKUCHI, A. O., GUEDES, C. C., MENDES, V. R., NASCIMENTO JR, D. R., GIANNINI, P. C., GIANINI, V. A. P. & DeWitt, R. **Late Holocene intensification of colds fronts in southern Brazil as indicated by dune development and provenance changes in the São Francisco do Sul coastal barrier**. Marine Geology, v. 335, p. 64-77, 2013.

APÊNDICE A - VIBROCORES PETROPHYSICAL PROPERTIES

The petrophysical parameters of velocity (Vp), gamma density (GD), natural gamma ray (NGR), magnetic susceptibility (MS) and resistivity, as well as the radiocarbon (14C) ages, and granulometry of sampled vibrocores in Babitonga Bay are presented in Figure 10.

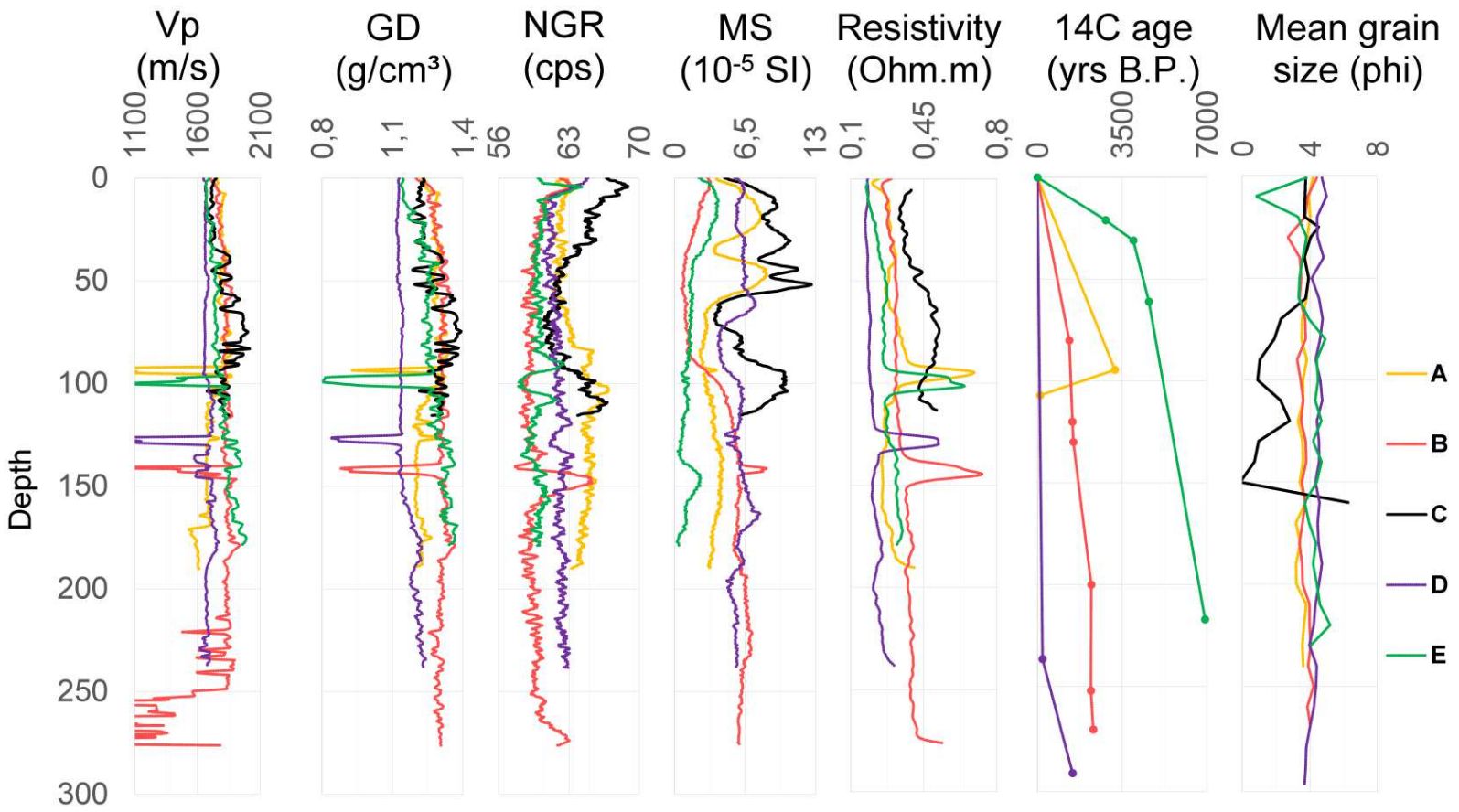

Figure 10. MSCL petrophysical parameters, age and granulometry for the vibrocores sampled inside Babitonga Bay. Note that core A presents its deepest radiocarbon sample contaminated, as its age decreased downward the core.

APÊNDICE B - PARANAGUÁ TECTONOSTRATIGRAPHIC TERRANE GEOCHRONOLOGY

Age data compilation is presented in the following Table 3.

Table 3. Compilation of geological ages along the Paranaguá Tectonostratigraphic Terrane.

Laboratory ID	Method	S	W	Elevation (m)	Material	Environment	Age	Source
	Radiometric Plus	-26,338309	-48,565777	0,5	Bone fragment	Marine	4460 ± 30	2018 Bandeira et al
	Radiometric Plus	-26,338309	-48,565777	0,55	Shell	Marine	5470 ± 30	2018 Bandeira et al
	Optically stimulated luminescence (OSL)	-26,338309	-48,565777	0,6	Sediment	Marine	4330 ± 700	2018 Bandeira et al
	Optically stimulated	-26,33830	-48,56577	0,3	Sediment	Marine	5670 ± 850	2018 Bandeir

Laboratory ID	Method	S	W	Elevation (m)	Material	Environment	Age	Source
	luminescence (OSL)	9	7					a et al
Beta N. 452919	Radiometric Plus	-26,4401483	-48,6052109	0	Shell of *A. flexuosa*	Marine	3045 ± 115	2018 Bandeira et al
Beta N. 452916	Radiometric Plus	-26,4401022	-48,6051517	0	Shell of *A. flexuosa*	Marine	3215 ± 110	2018 Bandeira et al
Beta N. 446685	Radiometric Plus	-26,2894049	-48,5466764	85	Shell of *ostreídeos*	Lagoon deposit	1697,5 ± 117,5	2018 Bandeira et al
Beta N. 446689	Radiometric Plus	-26,2813907	-48,5413793	0	Shell of *A. flexuosa*	Lagoon deposit	3200 ± 100	2018 Bandeira et al
Beta N. 418382	Radiometric Plus	-26,2795072	-48,540478	60	Shell of *A. flexuosa*	Lagoon deposit	3115 ± 110	2018 Bandeira et al

Laboratory ID	Method	S	W	Elevation (m)	Material	Environment	Age	Source
Beta N. 418383	Radiometric Plus	-26,2795072	-48,540478	320	Shell of *A. flexuosa*	Lagoon deposit	3072,5 ± 117,5	2018 Bandeira et al
Beta N. 452918	Radiometric Plus	-26,2791006	-48,5404466	68	Shell of *A. flexuosa*	Lagoon deposit	2935 ± 135	2018 Bandeira et al
Beta N. 446686	Radiometric Plus	-26,2834006	-48,5428085	25	Shell of Anomalocardia sp.	Lagoon deposit	4010 ± 135	2018 Bandeira et al
Beta N. 446688	Radiometric Plus	-26,2851051	-48,5427425	136,5	Shell of *A. flexuosa*	Lagoon deposit	2805 ± 135	2018 Bandeira et al
Beta N. 446691	Radiometric Plus	-26,4147305	-48,5973977	38,5	Shell of *A. flexuosa*	Marine	2632,5 ± 97,5	2018 Bandeira et al
Beta N. 452914	Radiometric Plus	-26,40819	-48,59818	57,5	Shell of *A. flexuosa*	Lagoon deposit	3260 ± 120	2018 Bandeir

Laboratory ID	Method	S	W	Elevation (m)	Material	Environment	Age	Source
Beta N. 452920	Radiometric Plus	19 - 26,4081085	47 - 48,5980561	45	Shell of *A. flexuosa*	Lagoon deposit	3270 ± 120	a et al 2018 Bandeira et al 2018
Beta N. 452910	Radiometric Plus	- 26,374047	- 48,5786034	0	Shell of *A. flexuosa*	Marine	6170 ± 85	
Beta N. 452909	Radiometric Plus	- 26,3663045	- 48,572774	62,5	Shell of *A. flexuosa*	Marine	4695 ± 140	
Beta N. 452915	Radiometric Plus	- 26,3665714	- 48,573079	67,5	Shell of *A. flexuosa*	Marine	4697,5 ± 107,5	
Beta N. 452912	Radiometric Plus	- 26,3660072	- 48,5722693	65	Shell of *A. flexuosa*	Marine	3540 ± 125	
Beta N.	Radiometric Plus	-	-	0	Shell of *A.*	Marine	3685 ± 130	2018

Laboratory ID	Method	S	W	Elevation (m)	Material	Environment	Age	Source
446684		26,3336113	48,5617589		*flexuosa*			Bandeira et al 2018
Beta N. 453208	Radiometric Plus	-26,3318692	-48,5612045	50	Shell of *A. flexuosa*	Marine	3585 ± 130	Bandeira et al 2018
Beta N. 418381	Radiometric Plus	-26,3469668	-48,5649044	35	Shell of *A. flexuosa*	Rocky cave	4695 ± 90	Bandeira et al 2018
Beta N. 418379	Accelerator mass spectrometry (AMS)	-26,3306076	-48,5629035	35	Human bone (tíbia?)	Lagoon deposit	5282 ± 41	Bandeira et al 2018
Beta N. 418380	Radiometric Plus	-26,3306076	-48,5629035	95	Shell of *A. flexuosa*	Lagoon deposit	5417,5 ± 92,5	Bandeira et al 2018
Beta N. 452917	Radiometric Plus	-26,3305987	-48,5629137	195	Shell of *A. flexuosa*	Lagoon deposit	5600 ± 105	Bandeira et al

Laboratory ID	Method	S	W	Elevation (m)	Material	Environment	Age	Source
Beta N. 452913	Radiometric Plus	-26,3141964	-48,5605034	50	Shell of *A. flexuosa*	Lagoon deposit	2875 ± 145	2018 Bandeira et al
Beta N. 452911	Radiometric Plus	-26,3140394	-48,5602964	40	Shell of *A. flexuosa*	Lagoon deposit	2855 ± 135	2018 Bandeira et al
Beta N. 446683	Radiometric Plus	-26,3178008	-48,5623105	92,5	Shell of *A. flexuosa*	Lagoon deposit	2632,5 ± 102,5	2018 Bandeira et al
Beta N. 446690	Radiometric Plus	-26,3213411	-48,5582307	15,5	Shell of *P. pectinatus*	Lagoon deposit	5587,5 ± 107,5	2018 Bandeira et al
Beta N. 446687	Radiometric Plus	-26,4034513	-48,6066307	267,5	Shell of *A. flexuosa*	Paludial deposit	2477,5 ± 92,5	2018 Bandeira et al
4099	Optically stimulated	-26,18786	-48,53359	12,3	Sediment	Aeolian deposit	13325 ± 2200	2015 Tese C.

Laboratory ID	Method	S	W	Elevation (m)	Material	Environment	Age	Source
	luminescence (OSL)	32	4					V. Vieira 2015
4316	Optically stimulated luminescence (OSL)	-26,1878632	-48,533594	6	Sediment	Aeolian deposit	47550 ± 7900	Tese C. V. Vieira 2015
4100	Optically stimulated luminescence (OSL)	-26,1787226	-48,527356	5,32	Sediment	Aeolian deposit	11650 ± 1250	Tese C. V. Vieira 2015
4101	Optically stimulated luminescence (OSL)	-26,1795011	-48,53012	11,77	Sediment	Aeolian deposit	13750 ± 2140	Tese C. V. Vieira 2015
4315	Optically stimulated luminescence	-26,1795011	-48,53012	3,77	Sediment	Aeolian deposit	37600 ± 5200	Tese C. V.

Laboratory ID	Method	S	W	Elevation (m)	Material	Environment	Age	Source
4102	(OSL) Optically stimulated luminescence (OSL)	-26,1840838	-48,531073	10,23	Sediment	Aeolian deposit	8070 ± 2470	Vieira 2015 Tese C. V. Vieira 2015
4314	Optically stimulated luminescence (OSL)	-26,1840838	-48,531073	7,13	Sediment	Aeolian deposit	24630 ± 8120	Tese C. V. Vieira 2015
CNA862	Accelerator mass spectrometry (AMS)	-26,08341	-48,62916	3,7	Espodossoil	Sand barrier	5870 ± 35	Boski et al 2015
b-256340	Accelerator mass spectrometry (AMS)	-26,08341	-48,62916	3,7	Espodossoil	Sand barrier	5980 ± 40	Boski et al 2015
b-256341	Accelerator mass spectrometry	-26,08401	-48,61925	2,3	Espodossoil	Sand barrier	2450 ± 0	Boski

Laboratory ID	Method	S	W	Elevation (m)	Material	Environment	Age	Source
	(AMS)	1	8					et al
	Accelerator mass	-						2015
b-277301	spectrometry	26,08379	-48,62069	2,4	Espodossoil	Sand barrier	2840 ± 40	Boski
	(AMS)	6						et al
	Accelerator mass	-	-					2015
b-277302	spectrometry	26,08415	48,61645	2,2	Espodossoil	Sand barrier	2310 ± 40	Boski
	(AMS)	6	2					et al
	Accelerator mass	-	-					2015
CNA863	spectrometry	26,08443	48,61316	2,6	Espodossoil	Sand barrier	1450 ± 40	Boski
	(AMS)	6	8					et al
	Accelerator mass	-	-					2015
b-277303	spectrometry	26,08463	48,61078	2,4	Espodossoil	Sand barrier	1300 ± 40	Boski
	(AMS)	5	4					et al
		-	-			Coastal Plains		2002
I-695	Radiocarbon	25,43722	48,45388	-1,5	Wood	(Marines	2675 ± 150	Angulo
		2	9			terraces)		et al
SI-431	Radiocarbon	-	-48,5275	-1,2	Shells	Fluviomarine	5690 ± 200	2002

Laboratory ID	Method	S	W	Elevation (m)	Material	Environment	Age	Source
		25,691389				Plains (mangroves and swamps)		Angulo et al
SI-327	Radiocarbon	-25,848611	-48,538611	0	Shells	Coastal plain (Beach)	3830 ± 120	2002 Angulo et al
SPS-0012	Radiocarbon	-25,93	-48,641667	-1,2	Shells	Fluviomarine Plains (mangroves and swamps)	4390 ± 300	2002 Angulo et al
SPS-0022	Radiocarbon	-25,878333	-48,574167	0	Shells	Coastal Plains (Marine terraces and sandy ridges)	5770 ± 150	2002 Angulo et al
Bah-1279	Radiocarbon	-25,966111	-48,640556	0	Shells	Fluviomarine Plains (mangroves	5820 ± 220	2002 Angulo et al

Laboratory ID	Method	S	W	Elevation (m)	Material	Environment	Age	Source
						and swamps)		
Bah-1271	Radiocarbon	-25,582222	-48,491111	-1,5	Shells	Planície costeira (Cordões arenosos)	5040 ± 230	2002 Angulo et al
Bah-1277	Radiocarbon	-25,948611	-48,603056	-1	Shells	Fluviomarine Plains (mangroves and swamps)	3160 ± 170	2002 Angulo et al
Bah-1278	Radiocarbon	-25,948611	-48,603056	-1	Shells	Fluviomarine Plains (mangroves and swamps)	2970 ± 150	2002 Angulo et al
Bah-1270	Radiocarbon	-25,553889	-48,463333	-0,9	Shells	Fluviomarine Plains (mangroves and swamps)	2680 ± 240	2002 Angulo et al

Laboratory ID	Method	S	W	Elevation (m)	Material	Environment	Age	Source
Bah-1269	Radiocarbon	-25,5425	-48,525278	-1	Shells	Lagoon Terraces (flood plains on the edge of coastal lagoons)	2650 ± 170	2002 Angulo et al
Bah-1388	Radiocarbon	-25,373056	-48,314444	0	Wood	Fluviomarine Plains (mangroves and swamps)	1100 ± 150	2002 Angulo et al
GSC-5243	Radiocarbon	-25,874444	-48,599722	-1,6	Wood	Coastal Plains (Marines terraces)	6140 ± 80	2002 Angulo et al
GSC-4678	Radiocarbon	-25,329167	-48,403056	-2	Wood	Coastal Plains (Marines terraces)	5380 ± 60	2002 Angulo et al
CENA-121	Radiocarbon	-25,245	-	-4	Wood	Fluviomarine	40000	2002

Laboratory ID	Method	S	W	Elevation (m)	Material	Environment	Age	Source
			48,078333			Plains (mangroves and swamps)		Angulo et al
GSC-5255	Radiocarbon	-25,538889	-48,290556	-2,9	Worm	Rocky coast - Island	3500 ± 60	2002 Angulo et al
GSC-5251	Radiocarbon	-25,538889	-48,290556	-0,4	Worm	Rocky coast - Island	790 ± 80	2002 Angulo et al
CENA-120	Radiocarbon	-25,563333	-48,44	-2,2	Wood	Coastal Plains (Marine terraces and sandy ridges)	4310 ± 70	2002 Angulo et al
CENA-143	Radiocarbon	-25,548333	-48,291667	-2,1	Worm	Rocky coast - Island	3300 ± 60	2002 Angulo et al
CENA-135	Radiocarbon	-	-	-1,3	Worm	Coastal Plains	1890 ± 60	2002

Laboratory ID	Method	S	W	Elevation (m)	Material	Environment	Age	Source
		25,193333	47,971667			(Marine terraces and sandy ridges)		Angulo et al
CENA-136	Radiocarbon	-25,193333	-47,971667	-0,3	Worm	Coastal Plains (Marine terraces and sandy ridges)	500 ± 60	2002 Angulo et al
CENA-138	Radiocarbon	-25,735278	-48,364167	-1,2	Worm	Rocky coast - Island	1280 ± 60	2002 Angulo et al
CENA-137	Radiocarbon	-25,735278	-48,364167	-0,2	Worm	Rocky coast - Island	490 ± 60	2002 Angulo et al
CENA-140	Radiocarbon	-25,851667	-48,534444	-3,6	Worm	Rocky coast	4750 ± 70	2002 Angulo et al
CENA-141	Radiocarbon	-	-	-3,5	Worm	Rocky coast	5300 ± 70	2002

Laboratory ID	Method	S	W	Elevation (m)	Material	Environment	Age	Source
		25,851667 - 25,851667	48,534444 - 48,534444					Angulo et al 2002
CENA-142	Radiocarbon			-1,1	Worm	Rocky coast	2470 ± 70	Angulo et al 2002
GSC-5246	Radiocarbon	-25,955	-48,646944	-0,6	Shells	Coastal plain (Marine terrain)	3480 ± 60	Angulo et al 2002
CENA-t22	Radiocarbon	-25,563333	-48,44	-0,9	Shells	Fluviomarine Plains (mangroves and swamps)	3480 ± 70	Angulo et al 2002
CENA-200	Radiocarbon	-25,563333	-48,44	-2,1	Wood	Fluviomarine Plains (mangroves and swamps)	37200 ± 1450	Angulo et al 2002
CENA-207	Radiocarbon	-	-	0	Shell	Planície	560 ± 85	2002

Laboratory ID	Method	S	W	Elevation (m)	Material	Environment	Age	Source
		25,266667	48,058333			costeira (Esporão arenoso)		Angulo et al
CENA-300	Radiocarbon	-25,698056	-48,501944	-4,2	Shell	Lagoon Terraces (flood plains on the edge of coastal lagoons)	3250 ± 70	2002 Angulo et al
CENA-301	Radiocarbon	-25,698056	-48,501667	-2,7	Wood and vegetable debris	Lagoon Terraces (flood plains on the edge of coastal lagoons)	6090 ± 80	2002 Angulo et al
CENA-1274	Radiocarbon	-25,73166	-48,61	0	Wood	Dúvida	1310 ± 60	2002 Angulo

Laboratory ID	Method	S	W	Elevation (m)	Material	Environment	Age	Source
		7						et al
		-	-					2001
CENA-204	Radiocarbon	26,073333	48,603333	0,2	Worm tubes	Rocky coast	2130 ± 60	Souza
		3	3					et al
		-	-					2001
CENA-206	Radiocarbon	26,073333	48,603333	2,1	Worm tubes	Rocky coast	3530 ± 70	Souza
		3	3					et al
		-	-					2001
CENA-205	Radiocarbon	26,073333	48,603333	2,5	Worm tubes	Rocky coast	4200 ± 70	Souza
		3	3					et al
		-	-		Wood frangments	Planície paleoestuarina		2001
CENA-275	Radiocarbon	26,010278	48,622778	-0,4			6480 ± 90	Souza
		8	8					et al
		-	-		Shell of A. brasiliana	Planície paleoestuarina		2001
CENA-276	Radiocarbon	26,176944	48,619444	2			5510 ± 70	Souza
		4	4					et al
GX-14060	Radiocarbon	-	-	0	Worm	Rocky coast	6080 ± 250	2001

Laboratory ID	Method	S	W	Elevation (m)	Material	Environment	Age	Source
		26,176667	48,618333					Souza et al 2001
Bah-1280	Radiocarbon	-26,966667	-48,641667	0	Shells	Planície paleoestuarina	5820 ± 220	Souza et al 2001
GSC-5246	Radiocarbon	-26,228333	-48,498056	3,05	Shell of A. brasiliana	Planície paleoestuarina	4015 ± 90	Souza et al 2001
Bah-1279	Radiocarbon	-26,955	-48,646667	0,6	Shells	Planície paleoestuarina	3480 ± 60	Souza et al 2001
UtC-5497	Accelerator mass spectrometry (AMS)	-25,993882	-48,656247	0,2	Soil	Sand ridge	3816 ± 36	Behling & Negrelle 2001
UtC-5498	Radiocarbon	-	-	-0,2	Wood	Sand ridge	3343 ± 38	

Laboratory ID	Method	S	W	Elevation (m)	Material	Environment	Age	Source
		25,993882	48,656247					Behling & Negrelle 2001
UtC-5499	Accelerator mass spectrometry (AMS)	-25,993882	-48,656247	-1,3	Soil	Sand ridge	6925 ± 44	Behling & Negrelle 2001
UtC-5500	Accelerator mass spectrometry (AMS)	-25,993882	-48,656247	-2,3	Soil	Sand ridge	7600 ± 60	Behling & Negrelle 2001
UtC-5501	Accelerator mass spectrometry (AMS)	-25,993882	-48,656247	-3,3	Soil	Sand ridge	7980 ± 50	Behling &

Laboratory ID	Method	S	W	Elevation (m)	Material	Environment	Age	Source
UtC-5502	Accelerator mass spectrometry (AMS)	-25,993882	-48,656247	-3,8	Soil	Sand ridge	7525 ± 44	Negrelle 2001 Behling & Negrelle 2001
UtC-5503	Accelerator mass spectrometry (AMS)	-25,993882	-48,656247	-4,3	Soil	Sand ridge	12330 ± 70	Behling & Negrelle 2001
UtC-5504	Accelerator mass spectrometry (AMS)	-25,993882	-48,656247	-4,8	Soil	Sand ridge	25650 ± 170	Behling & Negrelle

Laboratory ID	Method	S	W	Elevation (m)	Material	Environment	Age	Source
-	Thermoluminescence (TL)	-25,549167	-48,546944	7	Sediment	Coastal plain	105510 ± 2470	1999 Barreto et al
-	Thermoluminescence (TL)	-25,530556	-48,499722	8	Sediment	Coastal plain	106980 ± 9170	1999 Barreto et al
-	Thermoluminescence (TL)	-25,555278	-48,503056	4	Sediment	Coastal plain	122000 ± 4540	1999 Barreto et al
-	Thermoluminescence (TL)	-25,572222	-48,506111	2	Sediment	Coastal plain	100720 ± 2250	1999 Barreto et al
-	Thermoluminescence (TL)	-25,583889	-48,495278	2	Sediment	Coastal plain	85785 ± 9800	1999 Barreto et al
-	Thermoluminescence (TL)	-25,605	-48,48388	9	Sediment	Coastal plain	8540 ± 1330	1999 Barreto

Laboratory ID	Method	S	W	Elevation (m)	Material	Environment	Age	Source
			9					et al
			-					1999
-	Thermoluminescence (TL)	-25,605	48,483889	9	Sediment	Coastal plain	9150 ± 730	Barreto
								et al
		-	-					1999
-	Thermoluminescence (TL)	25,621667	48,480278	10	Sediment	Coastal plain	5845 ± 180	Barreto
								et al
		-	-		Wood			2008
CENA - 364	Radiocarbon	25,696276	48,504601	-0,5	fragment (trunk)	Sand barrier	2750 ± 60	Angulo
								et al
		-	-					2008
CENA - 370	Radiocarbon	25,695734	48,503917	-1	Vegetal debris	Sand barrier	3380 ± 60	Angulo
								et al
		-	-		Tivela foresti			2008
CENA - 300	Radiocarbon	25,696224	48,503488	-4,4	shell with periostracum	Sand barrier	3960 ± 80	Angulo
								et al
CENA - 363	Radiocarbon	-	-48,50268	-2,85	Vegetal debris	Sand barrier	7470 ± 80	2008

Laboratory ID	Method	S	W	Elevation (m)	Material	Environment	Age	Source
		25,695148						Angulo et al 2008
CENA - 473	Radiocarbon	-25,694358	-48,501853	-5	Tivela foresti shell; shell fragments	Sand barrier	3360 ± 70	Angulo et al 2008
CENA - 432	Radiocarbon	-25,69414	-48,502424	-3,2	Wood fragments	Sand barrier	5160 ± 70	Angulo et al 2008
CENA - 360	Radiocarbon	-25,697571	-48,502656	-3,5	Vegetal debris	Sand barrier	6410 ± 80	Angulo et al 2008
CENA - 380	Radiocarbon	-25,695647	-48,501853	-2,8	Vegetal debris	Sand barrier	3770 ± 70	Angulo et al 2008
CENA - 358	Radiocarbon	-25,69768	-48,502061	-2,2	Vegetal debris	Sand barrier	6860 ± 80	Angulo et al

Laboratory ID	Method	S	W	Elevation (m)	Material	Environment	Age	Source
GX - 30703	Radiocarbon	-25,694598	-48,50194	-7,67	Strigilla sp. Shell fragments	Sand barrier	4100 ± 40	2008 Angulo et al
CENA - 365	Radiocarbon	-25,696276	-48,504601	-1,2	Vegetal debris	Sand barrier	6750 ± 90	2008 Angulo et al
CENA - 380	Radiocarbon	-25,696276	-48,504601	-2,8	Young and adult shells	Sand barrier	3770 ± 70	2008 Angulo et al
CENA - 362	Radiocarbon	-25,695148	-48,50268	-2,85	Vegetal debris	Sand barrier	7580 ± 80	2008 Angulo et al
GX - 29115	Radiocarbon	-25,696276	-48,504601	-3,3	Vegetal debris	Sand barrier	4540 ± 40	2008 Angulo et al
CENA - 366	Radiocarbon	-25,69627	-48,50460	-4,3	Anomalocardia brasiliana	Sand barrier	3810 ± 70	2008 Angulo

Laboratory ID	Method	S	W	Elevation (m)	Material	Environment	Age	Source
		6	1		shells			et al
		-	-		Amiantis			2008
CENA - 385	Radiocarbon	25,696224	48,503488	-4	purpuratus	Sand barrier	3240 ± 70	Angulo
					shell			et al
		-						2008
CENA - 499	Radiocarbon	25,694598	-48,50194	-7,9	Organic mud	Sand barrier	6150 ± 80	Angulo
								et al
		-			Tellina sp.			2008
GX - 30704	Radiocarbon	25,694598	-48,50194	-8,3	Shell	Sand barrier	4190 ± 40	Angulo
					fragments			et al
		-						2008
CENA - 476	Radiocarbon	25,694598	-48,50194	-8,8	Organic mud	Sand barrier	30 400 ± 700	Angulo
								et al
		-	-					2008
CENA - 475	Radiocarbon	25,694381	48,502525	-8,2	Organic mud	Sand barrier	30 900 ± 900	Angulo
								et al
CENA - 368	Radiocarbon	-	-	-10,1	Organic mud,	Sand barrier	33 900 ± 90	2008

Laboratory ID	Method	S	W	Elevation (m)	Material	Environment	Age	Source
		25,696373	48,503116		vegetal debris, shell fragments		0	Angulo et al
CENA - 369	Radiocarbon	-25,695924	-48,502005	-9,8	Organic mud	Sand barrier	37 500 ± 2900	2008 Angulo et al
CENA#533/M	Radiocarbon	-25,881	-48,0264	-33	Sandstone	Inner shelf	25554,5 ± 851,5	2018 Simioni et al
CENA#531/	Radiocarbon	-25,8099	-48,0701	-29	Sandstone	Inner shelf	7223,5 ± 228,5	2018 Simioni et al
CENA#259/	Radiocarbon	-25,7056	-48,2887	-18	Sandstone	Inner shelf	7241 ± 224	2018 Simioni et al
GX-33475/	Radiocarbon	-25,5489	-48,3303	-6	Bioclastic limestones	Inner shelf	4343,5 ± 404,5	2018 Simioni

Laboratory ID	Method	S	W	Elevation (m)	Material	Environment	Age	Source
								et al
	Optically stimulated luminescence (OSL)	-25,625786	-48,507772	6,5	Sediment	Coastal plain (beach/foredune ridges)	132000 ± 11000	2020 Guedes et al
	Optically stimulated luminescence (OSL)	-25,582373	-48,490671	1	Sediment	Coastal plain (beach/foredune ridges)	151000 ± 20000	2020 Guedes et al
	Optically stimulated luminescence (OSL)	-25,529377	-48,582353	7,5	Sediment	Coastal plain (beach/foredune ridges)	Saturado	2020 Guedes et al
	Optically stimulated luminescence (OSL)	-25,543253	-48,497216	-1,5	Sediment	Coastal plain (beach/foredune ridges)	72000 ± 2000	2020 Guedes et al

Laboratory ID	Method	S	W	Elevation (m)	Material	Environment	Age	Source
	Optically stimulated luminescence (OSL)	-25,534559	-48,505504	3,5	Sediment	Coastal plain (beach/foredune ridges)	58000 ± 2000	2020 Guedes et al
	Optically stimulated luminescence (OSL)	-25,535918	-48,520685	6	Sediment	Coastal plain (beach/foredune ridges)	Saturado	2020 Guedes et al
	Optically stimulated luminescence (OSL)	-25,527691	-48,585192	7	Sediment	Coastal plain (beach/foredune ridges)	Saturado	2020 Guedes et al
	Optically stimulated luminescence (OSL)	-25,306669	-48,150837	5,2	Sediment	Coastal plain (beach/foredune ridges)	Saturado	2020 Guedes et al
CENA-135	Radiocarbon	-	-	-	Worm	Coastal plain	416,5 ± 61,5	2020

Laboratory ID	Method	S	W	Elevation (m)	Material	Environment	Age	Source
		25,157123	47,914315			(Beach)		Toniolo et al 2020
CENA-136	Radiocarbon	-25,157123	-47,914315	-	Worm	Coastal plain (Beach)	1166,5 ± 127,5	Toniolo et al 2020
Poz-75757	Radiocarbon	-23,804548	-45,547351	-	Worm	Coastal plain (Beach)	-122 ± 122	Toniolo et al 2020
Poz-75665	Radiocarbon	-25,157123	-47,914315	-	Worm	Coastal plain (Beach)	1086,5 ± 65,5	Toniolo et al 2020
CENA-137	Radiocarbon	-25,736949	-48,364946	-	Worm	Rocky coast (Ilha)	2586 ± 74	Toniolo et al 2020
CENA-138	Radiocarbon	-25,736949	-48,364946	-	Worm	Rocky coast (Ilha)	150 ± 126	Toniolo et al 2020

Laboratory ID	Method	S	W	Elevation (m)	Material	Environment	Age	Source
CENA-140	Radiocarbon	-25,846145	-48,536251	-	Worm	Coastal plain (Beach)	3074,5 ± 148,5	2020 Toniolo et al
CENA-141	Radiocarbon	-25,846145	-48,536251	-	Worm	Coastal plain (Beach)	0 ± 0	2020 Toniolo et al
CENA-142	Radiocarbon	-25,846145	-48,536251	-	Worm	Coastal plain (Beach)	1357,5 ± 102,5	2020 Toniolo et al
GSC-5251	Radiocarbon	-25,541263	-48,291148	-	Worm	Coastal plain (Beach)	1304,5 ± 92,5	2020 Toniolo et al
GSC-5255	Radiocarbon	-25,541263	-48,291148	-	Worm	Coastal plain (Beach)	837 ± 85	2020 Toniolo et al
Poz-75650	Radiocarbon	-25,56396	-48,30186	-	Worm	Coastal plain (Beach)	3742 ± 114	2020 Toniolo

Laboratory ID	Method	S	W	Elevation (m)	Material	Environment	Age	Source
		7	9					et al
		-	-					2020
Poz-75653	Radiocarbon	25,539957	48,290292	-	Worm	Coastal plain (Beach)	55,5 ± 81,5	Toniolo et al
		-	-					2020
Poz-75654	Radiocarbon	25,547543	48,293055	-	Worm	Coastal plain (Beach)	-120 ± 120	Toniolo et al
		-	-					2020
Poz-75655	Radiocarbon	25,563967	48,301869	-	Worm	Coastal plain (Beach)	568 ± 119	Toniolo et al
		-	-					2020
Poz-75990	Radiocarbon	25,541263	48,291148	-	Worm	Coastal plain (Beach)	4628 ± 198	Toniolo et al
		-	-					2020
Poz-75657	Radiocarbon	25,563967	48,301869	-	Worm	Coastal plain (Beach)	5347 ± 166	Toniolo et al
Poz-75659	Radiocarbon	-	-	-	Worm	Coastal plain	1761 ± 178	2020

Laboratory ID	Method	S	W	Elevation (m)	Material	Environment	Age	Source
		25,563967	48,301869			(Beach)		Toniolo et al 2020
Poz-62473	Radiocarbon	-26,176489	-48,524993	2,45	Worm	Coastal plain (Beach)	3290 ± 88	Toniolo et al 2020
Poz-62659	Radiocarbon	-26,176489	-48,524993	2,05	Worm	Coastal plain (Beach)	1223,5 ± 91,5	Toniolo et al 2020
Poz-62474	Radiocarbon	-26,176489	-48,524993	0,94	Worm	Coastal plain (Beach)	1453,5 ± 99,5	Toniolo et al 2020
Poz-62475	Radiocarbon	-26,176489	-48,524993	0,71	Worm	Coastal plain (Beach)	1212 ± 91	Toniolo et al 2020
Poz-62476	Radiocarbon	-26,176489	-48,524993	0,56	Worm	Coastal plain (Beach)	838 ± 79	Toniolo et al

Laboratory ID	Method	S	W	Elevation (m)	Material	Environment	Age	Source
Poz-62660	Radiocarbon	-26,176489	-48,524993	0,71	Worm	Coastal plain (Beach)	840,5 ± 89,5	2020 Toniolo et al
GX-14060	Radiocarbon	-26,221415	-48,497508	-	Worm	Coastal plain (Beach)	2207 ± 135	2020 Toniolo et al
Poz-62472	Radiocarbon	-26,229294	-48,4986	-	Worm	Coastal plain (Beach)	1700,5 ± 88,5	2020 Toniolo et al
Poz-62459	Radiocarbon	-26,233205	-48,499807	-	Worm	Coastal plain (Beach)	3503,5 ± 257,5	2020 Toniolo et al
Poz-62460	Radiocarbon	-26,233205	-48,499807	-	Worm	Coastal plain (Beach)	824 ± 72	2020 Toniolo et al
Poz-62461	Radiocarbon	-26,23320	-48,49980	-	Worm	Coastal plain (Beach)	679,5 ± 78,5	2020 Toniolo

Laboratory ID	Method	S	W	Elevation (m)	Material	Environment	Age	Source
		5	7					et al
		-	-					2020
Poz-62462	Radiocarbon	26,233205	48,499807	0,46	Worm	Coastal plain (Beach)	662,5 ± 93,5	Toniolo et al
		-	-					2020
Poz-62464	Radiocarbon	26,233205	48,499807	0,59	Worm	Coastal plain (Beach)	1375,5 ± 102,5	Toniolo et al
		-	-					2020
Poz-62465	Radiocarbon	26,233205	48,499807	2,64	Worm	Coastal plain (Beach)	3757,5 ± 105,5	Toniolo et al
		-	-					2020
Poz-62466	Radiocarbon	26,233205	48,499807	2,37	Worm	Coastal plain (Beach)	3624 ± 110	Toniolo et al
		-	-					2020
Poz-62468	Radiocarbon	26,233205	48,499807	1,47	Worm	Coastal plain (Beach)	2214 ± 83	Toniolo et al
Poz-62469	Radiocarbon	-	-	1,37	Worm	Coastal plain	2200,5 ±	2020

Laboratory ID	Method	S	W	Elevation (m)	Material	Environment	Age	Source
		26,233205 - 26,233205	48,499807 - 48,499807			(Beach)	130,5	Toniolo et al 2020
Poz-62470	Radiocarbon			1,13	Worm	Coastal plain (Beach)	2085 ± 104	Toniolo et al 2020
Poz-62471	Radiocarbon			0,94	Worm	Coastal plain (Beach)	1712 ± 113	Toniolo et al 2020
Poz-75660	Radiocarbon	26,221415 - 26,221415	48,497508 - 48,497508	0,81	Worm	Coastal plain (Beach)	1534,5 ± 99,5	Toniolo et al 2020
Poz-75661	Radiocarbon			0,62	Worm	Coastal plain (Beach)	1200,5 ± 61,5	Toniolo et al 2020
Poz-62661	Radiocarbon	-26,19497	48,527013 -	2,32	Worm	Coastal plain (Beach)	3392,5 ± 97,5	Toniolo et al

Laboratory ID	Method	S	W	Elevation (m)	Material	Environment	Age	Source
Poz-62479	Radiocarbon	-26,19497	-48,527013	0,63	Worm	Coastal plain (Beach)	1453,5 ± 99,5	2020 Toniolo et al
CENA-1005	Radiocarbon	-27,884494	-48,587848	-	Worm	Coastal plain (Beach)	2204 ± 122	2020 Toniolo et al
CENA-1006	Radiocarbon	-27,884494	-48,587848	-	Worm	Coastal plain (Beach)	390 ± 111	2020 Toniolo et al
CENA-1007	Radiocarbon	-27,884494	-48,587848	-	Worm	Coastal plain (Beach)	1573,5 ± 179,5	2020 Toniolo et al
CENA-1008	Radiocarbon	-27,884494	-48,587848	-	Worm	Coastal plain (Beach)	763 ± 151	2020 Toniolo et al
GX-14061	Radiocarbon	-27,74827	-48,49945	-	Worm	Coastal plain (Beach)	511 ± 129	2020 Toniolo

Laboratory ID	Method	S	W	Elevation (m)	Material	Environment	Age	Source
Poz-75649	Radiocarbon	-3 27,884494	-48,587848	-	Worm	Coastal plain (Beach)	3389,5 ± 221,5	et al 2020 Toniolo et al
Poz-75758	Radiocarbon	-27,146036	-48,480099	-	Worm	Coastal plain (Beach)	1077 ± 68	2020 Toniolo et al
Poz-75663	Radiocarbon	-27,884494	-48,587848	-	Worm	Coastal plain (Beach)	2211,5 ± 82,5	2020 Toniolo et al
Poz-75664	Radiocarbon	-27,884494	-48,587848	-	Worm	Coastal plain (Beach)	600 ± 90	2020 Toniolo et al
OS-157996	Radiocarbon	-26,342829	-48,715266	-1,8	*Felaniella candeana*	Bottom of Babitonga Bay	1770 ± 15	Bay Squeeze
OS-157997	Radiocarbon	-	-	-2,2	*Felaniella*	Bottom of	1900 ± 20	Bay

Laboratory ID	Method	S	W	Elevation (m)	Material	Environment	Age	Source
		26,342829	48,715266		*candeana*	Babitonga Bay		Squeeze Bay
OS-159598	Radiocarbon	-26,342829	-48,715266	-2,3	*Felaniella candeana*	Bottom of Babitonga Bay	1940 ± 20	Squeeze
OS-158007	Radiocarbon	-26,342829	-48,715266	-3	*Felaniella candeana*	Bottom of Babitonga Bay	2550 ± 20	Squeeze Bay
OS-159599	Radiocarbon	-26,342829	-48,715266	-3,52	*Diplodonta patagonica*	Bottom of Babitonga Bay	2530 ± 20	Squeeze Bay
OS-158008	Radiocarbon	-26,342829	-48,715266	-3,71	*Caryocorbula swiftiana*	Bottom of Babitonga Bay	2610 ± 25	Squeeze Bay
OS-158009	Radiocarbon	-26,284983	-48,71755	-3,365	*Caryocorbula swiftiana*	Bottom of Babitonga Bay	610 ± 15	Squeeze Bay

Laboratory ID	Method	S	W	Elevation (m)	Material	Environment	Age	Source
OS-158010	Radiocarbon	-26,284983	-48,71755	-3,925	*Juliacorbula aequivalvis*	Bottom of Babitonga Bay	1910 ± 20	Bay Squeeze
OS-158011	Radiocarbon	-26,200403	-48,642703	-1,21	*Coccodentalium carduus*	Bottom of Babitonga Bay	3030 ± 20	Bay Squeeze
OS-159600	Radiocarbon	-26,200403	-48,642703	-1,31	*Cyclinella tenuis*	Bottom of Babitonga Bay	3950 ± 30	Bay Squeeze
OS-158012	Radiocarbon	-26,200403	-48,642703	-1,61	*Coccodentalium carduus*	Bottom of Babitonga Bay	4430 ± 25	Bay Squeeze
OS-158013	Radiocarbon	-26,200403	-48,642703	-3,17	*Coccodentalium carduus*	Bottom of Babitonga Bay	6480 ± 30	Bay Squeeze
?	Radiocarbon	-26,27658	-48,80765	8,1	*Anomalocardia brasiliana*	Shell mound on alluvial	4170	2000 Oliveir

Laboratory ID	Method	S	W	Elevation (m)	Material	Environment	Age	Source
		7	6		(shell mound)	fan		a
		-	-		*Anomalocardi*	Shell mound		2000
?	Radiocarbon	26,27658	48,80765	7,3	*a brasiliana*	on alluvial	4490	Oliveir
		7	6		(shell mound)	fan		a
		-	-		*Anomalocardi*	Shell mound		2000
?	Radiocarbon	26,27658	48,80765	6,3	*a brasiliana*	on alluvial	4665	Oliveir
		7	6		(shell mound)	fan		a
		-	-		*Anomalocardi*	Shell mound		2000
?	Radiocarbon	26,27658	48,80765	2,4	*a brasiliana*	on alluvial	4815	Oliveir
		7	6		(shell mound)	fan		a
			-		*Anomalocardi*	Shell mound		2000
?	Radiocarbon	-26,28439	48,79326	9	*a brasiliana*	on alluvial	1160 ± 45	Oliveir
			2		(shell mound)	fan		a
			-		*Anomalocardi*	Shell mound		2000
?	Radiocarbon	-26,28439	48,79326	9	*a brasiliana*	on alluvial	1270 ± 60	Oliveir
			2		(shell mound)	fan		a
?	Radiocarbon	-26,28439	-	9	*Anomalocardi*	Shell mound	2970 ± 60	2000

Laboratory ID	Method	S	W	Elevation (m)	Material	Environment	Age	Source
			48,793262		*a brasiliana* (shell mound)	on alluvial fan		Oliveira
?	Radiocarbon	-26,29236	-48,778723	5	Coal (shell mound)	Shell mound on dune	1170 ± 200	2000 Oliveira
?	Radiocarbon	-26,29236	-48,778723	5	Coal (shell mound)	Shell mound on dune	2730 ± 80	2000 Oliveira
?	Radiocarbon	-26,29236	-48,778723	5	Coal (shell mound)	Shell mound on dune	3000 ± 95	2000 Oliveira
?	Radiocarbon	-26,29236	-48,778723	5	Coal (shell mound)	Shell mound on dune	3015 ± 130	2000 Oliveira
?	Radiocarbon	-26,316262	-48,92776	13	Human bone (shell mound)	Shell mound on rock	4030 ± 40	2000 Oliveira

Laboratory ID	Method	S	W	Elevation (m)	Material	Environment	Age	Source
?	Radiocarbon	-26,318437	-48,825977	1,5	Coal (shell mound)	Shell mound on alluvial fan	2350 ± 120	2000 Oliveira
Bah. 1393	Radiocarbon	-25,455	-48,755		Shells (shell mound)	Shell mound on rock	4890 ± 210	1988 Martin
Si. 1023	Radiocarbon	-25,455	-48,755		Shells (shell mound)	Shell mound on rock	4810 ± 100	1988 Martin
Si. 1022	Radiocarbon	-25,455	-48,755		Shells (shell mound)	Shell mound on rock	4960 ± 110	1988 Martin
Si. 1021	Radiocarbon	-25,455	-48,755		Shells (shell mound)	Shell mound on rock	4070 ± 100	1988 Martin
P. 588	Radiocarbon	-25,515	-48,691667		Shells (shell mound)	Shell mound on lagoon	4370 ± 70	1988 Martin
P. 587	Radiocarbon	-25,515	-48,691667		Shells (shell mound)	Shell mound on lagoon	4300 ± 70	1988 Martin

Laboratory ID	Method	S	W	Elevation (m)	Material	Environment	Age	Source
P. 586	Radiocarbon	-25,515	-48,691667		Shells (shell mound)	Shell mound on lagoon	3900 ± 70	1988 Martin
P. 536	Radiocarbon	-25,516667	-48,755		Shells (shell mound)	Shell mound on Pleistocene terrain	4050 ± 70	1988 Martin
P. 543	Radiocarbon	-25,516667	-48,755		Shells (shell mound)	Shell mound on Pleistocene terrain	4890 ± 70	1988 Martin
P. 542	Radiocarbon	-25,516667	-48,755		Shells (shell mound)	Shell mound on Pleistocene terrain	4870 ± 70	1988 Martin
P. 541	Radiocarbon	-25,51666	-48,755		Shells (shell mound)	Shell mound on	4490 ± 180	1988 Martin

Laboratory ID	Method	S	W	Elevation (m)	Material	Environment	Age	Source
		7				Pleistocene terrain		
P. 540	Radiocarbon	-25,516667	-48,755		Shells (shell mound)	Shell mound on Pleistocene terrain	4490 ± 140	1988 Martin
Bah.1392	Radiocarbon	-25,326667	-48,755		Shells (shell mound)	Shell mound on rock	5050 ± 220	1988 Martin
Si. 1029	Radiocarbon	-25,416667	-48,743333		Shells (shell mound)	Shell mound on rock	4740 ± 90	1988 Martin
SI. 1028 A	Radiocarbon	-25,416667	-48,743333		Shells (shell mound)	Shell mound on rock	3300 ± 90	1988 Martin
SI. 1028	Radiocarbon	-25,41666	-48,74333		Shells (shell mound)	Shell mound on rock	3360 ± 80	1988 Martin

Laboratory ID	Method	S	W	Elevation (m)	Material	Environment	Age	Source
Si. 1027	Radiocarbon	7 - 25,416667	3 - 48,743333		Shells (shell mound)	Shell mound on rock	3000 ± 90	1988 Martin
Si. 1026	Radiocarbon	7 - 25,416667	3 - 48,743333		Shells (shell mound)	Shell mound on rock	2980 ± 130	1988 Martin
SI. 508	Radiocarbon	7 - 25,521667	3 - 48,646667		Shells (shell mound)	Shell mound on rock	4760 ± 80	1988 Martin
SI. 507	Radiocarbon	7 - 25,521667	3 - 48,646667		Shells (shell mound)	Shell mound on rock	4540 ± 90	1988 Martin
SI. 506	Radiocarbon	7 - 25,521667	3 - 48,646667		Shells (shell mound)	Shell mound on rock	4740 ± 100	1988 Martin
Si. 505	Radiocarbon	-	-		Shells (shell	Shell mound	4620 ± 100	1988

Laboratory ID	Method	S	W	Elevation (m)	Material	Environment	Age	Source
		25,521667	48,646667		mound)	on rock		Martin
Si. 504	Radiocarbon	-25,521667	-48,646667		Shells (shell mound)	Shell mound on rock	4640 ± 80	1988 Martin
Bah. 1265	Radiocarbon	-25,55	-48,621667		Shells (shell mound)	Shell mound on lagoon	3670 ± 180	1988 Martin
P. 500	Radiocarbon	-25,55	-48,621667		Shells (shell mound)	Shell mound on lagoon	3500 ± 60	1988 Martin
P. 489	Radiocarbon	-25,55	-48,621667		Shells (shell mound)	Shell mound on lagoon	3420 ± 60	1988 Martin
P. 488	Radiocarbon	-25,55	-48,621667		Shells (shell mound)	Shell mound on lagoon	3360 ± 70	1988 Martin

Laboratory ID	Method	S	W	Elevation (m)	Material	Environment	Age	Source
P. 487	Radiocarbon	-25,55	-48,621667		Shells (shell mound)	Shell mound on lagoon	3280 ± 60	1988 Martin
P. 486	Radiocarbon	-25,55	-48,621667		Shells (shell mound)	Shell mound on lagoon	3370 ± 60	1988 Martin
P. 485	Radiocarbon	-25,55	-48,621667		Shells (shell mound)	Shell mound on lagoon	3270 ± 50	1988 Martin
P. 483	Radiocarbon	-25,55	-48,621667		Shells (shell mound)	Shell mound on lagoon	3240 ± 60	1988 Martin
P. 482	Radiocarbon	-25,55	-48,621667		Shells (shell mound)	Shell mound on lagoon	3310 ± 60	1988 Martin
Bah. 1390	Radiocarbon	-25,365	-48,42		Shells (shell mound)	Sambaqui sobre Terraço	3830 ± 190	1988 Martin

Laboratory ID	Method	S	W	Elevation (m)	Material	Environment	Age	Source
						holocênico		
Bah. 1391	Radiocarbon	-25,331667	-48,418333		Shells (shell mound)	Shell mound on Pleistocene terrain	3800 ± 190	1988 Martin
Bah. 1889	Radiocarbon	-25,373333	-48,315		Shells (shell mound)	Sambaqui sobre Terraço holocênico	1250 ± 150	1988 Martin
Gil. 1047	Radiocarbon	-25,416667	-48,66		Shells (shell mound)	Shell mound on rock	3150 ± 110	1988 Martin
Gil. 1046	Radiocarbon	-25,416667	-48,66		Shells (shell mound)	Shell mound on rock	2480 ± 110	1988 Martin
Bah. 1276	Radiocarbon	-25,845	-48,725		Shells (shell mound)	Shell mound on rock	2420 ± 170	1988 Martin
Bah.1275	Radiocarbon	-25,9	-		Shells (shell	Shell mound	4500 ± 190	1988

Laboratory ID	Method	S	W	Elevation (m)	Material	Environment	Age	Source
			48,703333		mound)	on Pleistocene terrain		Martin
Bah.1272	Radiocarbon	-25,917778	-48,638333		Shells (shell mound)	Shell mound on lagoon	3920 ± 190	1988 Martin
Bah.1273	Radiocarbon	-25,92	-48,62		Shells (shell mound)	Shell mound on lagoon	3290 ± 190	1988 Martin
Gif.	Radiocarbon	-25,861667	-48,571667		Shells (shell mound)	Shell mound on rock	1540 ± 150	1988 Martin
Bah.1280	Radiocarbon	-25,981667	-48,641667		Shells (shell mound)	Shell mound on Pleistocene terrain	5040 ± 210	1988 Martin
Bah.1282	Radiocarbon	-26,13833	-48,81333		Shells (shell mound)	Sambaqui sobre	5420 ± 230	1988 Martin

Laboratory ID	Method	S	W	Elevation (m)	Material	Environment	Age	Source
		3	3			Sedimento Continental		
Si.	Radiocarbon	-26,286667	-48,783333		Shells (shell mound)	Shell mound on Pleistocene terrain	2920 ± 100	1988 Martin
Si.	Radiocarbon	-26,286667	-48,783333		Shells (shell mound)	Shell mound on Pleistocene terrain	2870 ± 100	1988 Martin
Si.	Radiocarbon	-26,286667	-48,783333		Shells (shell mound)	Shell mound on Pleistocene terrain	2221 ± 210	1988 Martin
Bah.1279	Radiocarbon	-25,96626	-48,641184	> 0 m	Shells		5820 ± 220	1988 Martin

Laboratory ID	Method	S	W	Elevation (m)	Material	Environment	Age	Source
Bah.1271	Radiocarbon	-25,582927	-48,492853	> + 1,5 m	Shells		5040 ± 230	1988 Martin
	Radiocarbon	-25,844593	-48,539518	< 0	Shells		3830 ± 120	1988 Martin
Bah.1277	Radiocarbon	-25,947927	-48,602851	> + 1,0 m	Shells		3160 ± 170	1988 Martin
Bah.1278	Radiocarbon	-25,949594	-48,612851	> + 1,0 m	Shells		2970 ± 150	1988 Martin
Bah.1270	Radiocarbon	-25,552927	-48,46452	+ 1,0 (± 0,5) m	Shells		2680 ± 240	1988 Martin
Bah.1269	Radiocarbon	-25,54126	-48,52452	+1,0 (± 0,5) m	Shells		2650 ± 170	1988 Martin

Laboratory ID	Method	S	W	Elevation (m)	Material	Environment	Age	Source
Bah.1388	Radiocarbon	-25,372926	-48,314521	> 0 m	Wood		1100 ± 150	1988 Martin
Bah.1280	Radiocarbon	-26,17626	-48,61785	> 0 m	Shells		6080 ± 250	1988 Martin
Bah.1359	Radiocarbon	-27,232927	-48,716178	> 0 m	Wood		5870 ± 240	1988 Martin
Bah.1382	Radiocarbon	-28,724595	-49,177836	> 0 m	Shells		5710 ± 200	1988 Martin
Bah.1290	Radiocarbon	-26,864593	-48,687847	+ 1,0 (± 0,5) m	Shells		5580 ± 240	1988 Martin
Bah.1395	Radiocarbon	-28,21126	-48,72784	> 0 m	Shells		4490 ± 200	1988 Martin
Bah.1374	Radiocarbon	-	-	+ 1,5 (±	Shells		4240 ± 200	1988

Laboratory ID	Method	S	W	Elevation (m)	Material	Environment	Age	Source
		28,367925	48,294508	0,5) m				Martin
Bah.1369	Radiocarbon	-28,04626	-48,626175	> 0 m	Shells		4080 ± 200	1988 Martin
Bah.1368	Radiocarbon	-27,767926	-48,507843	> 0 m	Shells		4070 ± 190	1988 Martin
Bah.1370	Radiocarbon	-28,11626	-48,699508	> 0 m	Shells		3960 ± 200	1988 Martin
Bah.1286	Radiocarbon	-26,289593	-48,581183	> 0 m	Shells		3920 ± 190	1988 Martin
Bah.1381	Radiocarbon	-28,592928	-48,967838	> 0 m	Shells		3830 ± 180	1988 Martin

1

APÊNDICE C – RESUMOS DE TRABALHOS APRESENTADOS

Neste tópico são apresentados os resumos aceitos em eventos.

LAPECO 2019

Geophysical detection of shallow gas in a subtropical estuary: Babitonga Bay, Brazil*

Wilson Fabiano Leite Galvão[1], Antonio Henrique da Fontoura Klein[1], Maiara Werner Pinto[1], Michel Franco Volpato Prado[1], Luis Pedro Melo de Almeida[2]

*We appreciate the support given by CNPq to the project 441545 / 2017-3 were this work is included.
[1]Laboratório de Oceanografia Costeira, Universidade Federal de Santa Catarina, Brasil.
[2]Instituto de Oceanografia, Universidade Federal do Rio Grande, Brasil.

The aim of this work is to present the results from the seismic observations performed in Babitonga Bay, and report the occurrence of shallow gas. The Babitonga Bay (North of Santa Catarina State) is a 167 km² wide subtropical estuary, with high environmental and socioeconomic importance to the state. Sub-bottom high-resolution seismic investigation it is a very useful technic to produce geological evolutionary models. Besides that, it allows the observation of shallow gas features in the sedimentary layers, showing its importance in a scenario of increase of greenhouse gasses. Thus, a seismic survey dataset, collected using a CHIRP-type wave sub-surface profiler (SB-512-l, Edgetech®), was used in this study. Covering approximately 255 km, 113 survey lines were collected between 12 and 20 December 2018 in Babitonga, with high vertical resolution of 15 cm, with depth of penetration 30 m and a frequency of 2-9 kHz. Both seismic post-processing and manual digitalization of seismic features (e.g., shallow gas) were made using SonarWiz®. The shallow gas was identified based on their pattern features in the acoustic profiles such as the phase inversion of the seismic wave and the absence of reflectors below the gas, given by the high impedance difference of the seismic wave phase and the high reflection energy of the reflector. Distinct shallow gas features was observed, such as acoustic blanket (~39 km), acoustic turbidity (~13 km), black shadow (~203 m) and intra-sedimentary plumes (~530 m), of which the first two being the most frequent, summing up 98,04% of the gas occurrence, as well as gas seepage features: acoustic plumes (44 features) and pockmarks (just 3 of them). The acoustic plumes were the features that presents a pattern of occurrence, concentrating itself in the sheltered areas inside the estuary, as the others are randomly distributed.

PGGM – WORKSHOP EDIÇÃO AMAZONICA 2020

Investigação geológica da Baía da Babitonga, SC, no Pleistoceno Superior e Holoceno.

GALVÃO, WILSON [1]; KLEIN, ANTONIO [1]; MAHIQUES, MICHEL [2]; PINTO, MAIARA [2]; PRADO, MICHEL [1]; ALMEIDA, LUIS[3]; PANDOLPHO, BRUNA[1]; DIAS, RODOLFO[2]

Universidade Federal de Santa Catarina[1] (Wilson Fabiano Leite Galvão, galvao.wilson.1@gmail.com);
Universidade Federal de Santa Catarina[1] (Antonio Henrique da Fontoura Klein, antonio.klein@ufsc.br);
Universidade de São Paulo[2] (Michel Michaelovitch de Mahiques, mahiques@gmail.com);
Universidade Federal de Santa Catarina[1] Maiara Werner Pinto maiarawp@gmail.com);
Universidade Federal de Santa Catarina[1] Michel Franco Volpato Prado oc.francoprado@gmail.com);
Universidade Federal do Rio Grande[3] (Luis Pedro Melo De Almeida, melolp@gmail.com);
Universidade Federal de Santa Catarina[1] (Bruna Teixeira Pandolpho, b.pandolpho@gmail.com);
Universidade de São Paulo[2] (Rodolfo Jasão Soares Dias, jasaodias@hotmail.com)

O presente trabalho apresenta resultados preliminares da análise dos depósitos sedimentares presentes na Baía da Babitonga/SC com foco no Holoceno e Pleistoceno Superior, a fim de propor um modelo para a evolução geológica da baía. Para isso, foram analisados 283 km de dados sísmica rasa (CHIRP, de frequência entre 0,5 – 12,0 kHz) e de 5 testemunhos obtidos na baía, coletados em diferentes pontos selecionados a partir da análise prévia dos dados sísmicos. A Baía da Babitonga é composta pelo Canal do Palmital (CPa), Canal do Linguado (CL) e Canal Principal (CP). Separando a Ilha de São Francisco do Sul do continente, o CP e o CL se encontram com CPa, a montante. Dessa forma, o CPa e CL apresentam orientação NO-SE, encaixados sobre a Zona de Cisalhamento do Palmital (ZCP), e o CP, orientação de SO-NE. Até o presente momento, os dados sísmicos foram processados e previamente interpretados, onde feições acústicas de gás foram identificadas por toda baía. Também foram mapeadas as ocorrências do embasamento acústico, que por vezes aflora no assoalho da baía, sendo caracterizado como embasamento cristalino. O embasamento cristalino identificado faz parte do Complexo Paranaguá e se comporta como um alto estrutural em momentos de nível do mar baixo, separando a drenagem do CP do segmento da drenagem que era encaixado sobre a ZCP e conectava o CPa ao CL. Tal interpretação é feita a partir da relação entre as feições de paleocanais identificadas nos registros sísmicos com a presença do embasamento alçado no centro da baía. Para classificação do fundo da baía, agrupou-se os caráteres acústicos a partir da intensidade do sinal, de sua forma e da profundidade de penetração do sinal nas camadas sedimentares internas. Desta análise também se identificou marcas onduladas de fundo, na região da desembocadura do CP e em outras áreas no interior da baía, que indicam maior energia hidrodinâmica. Com as análises granulométricas feitas, observou-se que a intensidade do sinal sísmico é mais forte em áreas onde areias dominam e marcas de fundo ocorrem. Em contrapartida, o sinal é atenuado quando o sedimento é siltoso, contendo um alto teor de água, podendo apresentar ocorrência de gás no entorno. Por fim, a correlação de tais resultados mostra que o gás encontrado em menores profundidades está ligado à presença do embasamento cristalino alçado no interior da baía, enquanto paleocanais se relacionam às ocorrências de gás

em maiores profundidades no pacote sedimentar. Ainda, observa-se a relação da ocorrência de gás com um sedimento siltoso.

Palavras-chave: Baía da Babitonga. Sísmica de alta resolução. Gás no sedimento. Paleocanais.

17th INTERNATIONAL CONGRESS OF THE BRAZILIAN GEOPHYSICAL SOCIETY & EXPOGEF 2021

Seismic investigation of the mouth of Babitonga Bay, SC, and its adjacent Internal Platform

Wilson Fabiano Leite Galvão[1], Antonio Henrique da Fontoura Klein[1], Michel Michaelovitch de Mahiques[2], Christopher Hein[3], Luiz Antonio Pereira de Souza[4], [1] Universidade Federal de Santa Catarina, [2] Instituto Oceanográfico da Universidade de São Paulo, [3]Virginia Institute of Marine Science, [4]Instituto de Pesquisas Tecnológicas do Estado de São Paulo

Abstract

This study presents a model for the geological evolution of the mouth of Babitonga Bay (the northern coast of Santa Catarina) based on investigation of Holocene and Upper Pleistocene sedimentary deposits in the bay mouth and adjacent Internal Platform. The coastal plain adjacent to the surveyed area is composed of marine-beach sediments deposited during the Quaternary as a series of sandy ridges, coastal lagoons, and dunes. We collected and analyzed 106 km of high-frequency seismic data (CHIRP; frequency: 0.5 - 7.0 kHz) from the southern portion of the mouth of the main channel of the bay. From this, five seismostratigraphic units were identified, which reveal the succession of depositional environments from the end of the Pleistocene to the present. The first unit is ubiquitous, internally transparent, and characterized by an irregular upper surface. This acoustic basement is interpreted as igneous rocks, contiguous with those outcropping along the coast. Inside the bay and close to the headlands, the basement is close to the surface. Unit II, characterized by transparent seismic facies, represents Pleistocene sedimentary deposits, which were excavated by the local drainage system. These were subsequently capped by Unit III, consisting of continuous, high-amplitude reflectors and interpreted as middle Holocene transgressive deposits. Here, the morphostratigraphy of a barrier-lagoon system is observed along the Internal Platform, whereas inside the bay, Unit III deposits are predominantly channel fill. Characterized by internal parallel and/or subparallel reflectors, Unit IV is composed of characteristic sea-level highstand deposits (e.g., tidal flats and estuarine deposits) in the interior of the bay, and sandy barriers at the mouth. Finally, present throughout the survey area, Unit V consists of modern deposits characterized by high-intensity and continuous internal reflectors. Bedforms occur in this unit. Based on these findings, an evolutionary model of coastal change during the late Pleistocene to late Holocene regressive-transgressive episode is proposed. In this model, channels within the bay excavated earlier Pleistocene deposits as they flowed over the exposed platform. Then, with sea level at or near it's middle Holocene maximum, estuarine deposits were formed within the bay, capping the channels that were filled during the transgression. Meanwhile, the barrier-lagoon system on the Inner Platform was abandoned and overtopped with marine sediments. Finally, with sea level near its maximum or slowly falling over the last 5000 years, modern sedimentation patterns were established, with active seafloor bedforms marking locations with more intense flow.